University of Strathclyde

Department of Electronic and Electrical Engineering

Development of a Microfluidic Platform for Multicellular Tumour Spheroid Assays

Kay Seonaid McMillan

A thesis submitted in partial fulfilment of the requirements for the degree of Doctor of Philosophy

2016

Declaration of Authorship

This thesis is the result of the author's original research. It has been composed by the author and has not been previously submitted for examination which has led to the award of a degree.

Signed:

Date:

Abstract

Microfluidics is a valuable technology for a variety of different biomedical applications. In particular, within cancer research, it can be used to improve upon currently used *in vitro* screening assays by facilitating the use of 3D cell culture models. One of these models is the multicellular tumour spheroid (MCTS), which provides a more accurate reflection of the tumour microenvironment *in vivo* by reproducing the cell to cell contact, the development of a nutritional gradient and the formation of a heterogeneous population of cells. Therefore, the MCTS provides a more physiologically relevant *in vitro* model for testing the efficacy of treatments at the preclinical level. Currently, methods for the formation and culture of spheroids have several limitations, including being labour intensive, being low throughput, producing shear stress towards cells and the hanging drop system being unstable to physical shocks. Recently, microfluidics (especially droplet microfluidics) has been employed for the culture and screening of spheroids, providing a high-throughput methodology which only requires small volumes of fluids and small numbers of cells. However, current issues with droplet microfluidics include complicated droplet gelation procedures and short cell culture times.

In this thesis, the use of microfluidic technologies as an approach for spheroid formation and culture are investigated with the aim to create a platform for radiotherapeutic and chemotherapeutic treatment of spheroids using cell lines.

Initially, the use of emulsion technology at the macro scale was evaluated to determine the best conditions for spheroid culture. Once this was achieved the spheroids were compared to spheroids using a traditional method and radiotherapeutic treatment was conducted. Subsequently, avenues for miniaturising the developed emulsion-based methods were studied to provide a microfluidic technology. Finally, along with identifying the optimal culture conditions using hydrogels, a microfluidic system that integrated both droplet and single phase microfluidics features was developed for the formation and culture of spheroids. Using the latter, proof of principle experiments were conducted to demonstrate the suitability of the platform for both chemotherapeutic and radiotherapeutic assays within the same device.

Acknowledgements

Firstly I would like to express a massive thank you to my primary supervisor Dr Michele Zagnoni. From start to finish of my PhD journey he has provided an invaluable amount of guidance and support in an interesting and challenging multidisciplinary field.

Next I would like to thank my second supervisor Dr Marie Boyd for her enthusiasm and support with biological aspects of my project. I would also like to thank EPSRC for providing financial support for this PhD.

Special thanks also have to be given to Dr Anthony McCluskey for proof reading chapters of my thesis and to Dr Annette Sorenson for practical support within the lab. Thanks also have to be extended to Heather and Ralf for also proof reading chapters of my thesis.

My time in the Centre of Microsystems and Photonics has been very enjoyable which is thanks to the welcoming and fun environment created by people past and present who have made up this research group. In particular thanks has to go to Barbara and Anna for our tea breaks and chat about several back up plans, Ralf, Carlota, Theresa, Chris, Alan, Ian, G3 (aka Gordon Humphries), Graham (best/worst April Fools day prankster), Marjorie, Jonas, Craig, Mick, Gordon F, Dave, Li Li, Jessica, Jamie, Jo, Walter J, Deepak, George and Ran Li. Throughout there have been many unforgettable times created in and out with the office including fantastic pub trips, conference times, summer trips (Arran, Alton Towers and Orlando), Christmas lunches and many other moments which would fill a separate thesis. I would like to wish people who continue to work and study within CMP all the best for the future.

Thanks also has to be given to Rhona who was an amazing flat mate throughout my studies and offered brilliant advice along with hilarious random banter.

Finally I would like to thank my dad, mum, Ailsa, Zoe and Douglas for their encouragement, patience and loving support during my PhD.

Contents

Figures

Chapter 2 - Background

Chapter 3 – Materials and Methods

Chapter 4 – Formation and Culture of Spheroids within Emulsions

Chapter 5 – Development of a Droplet Microfluidic Device for Spheroid Culture

Chapter 6 - Characterisation of a Droplet Microfluidic Device for the Culture and Anticancer Treatment of Spheroids

Chapter 7 – Discussion

Tables

Chapter 2 – Background

Chapter 3 – Materials and Methods

Chapter 5 – Development of a Droplet Microfluidic Device for Spheroid Culture

Abbreviations

ATP	Adenosine triphosphate
BSA	Bovine serum albumin
DNA	Deoxyribonucleic acid
DSB	Double strand break
ECM	Extracellular matrix
EGFR	Epidermal growth factor
FBS	Foetal bovine serum
FDA	Fluorescein diacetate
IARC	International Agency for Research of Cancer
M/O	Medium in oil
MEM	Minimum essential medium
MCS	Multicellular spheroid
MCTS	Multicellular tumour spheroid
O/W	Oil in water
PEG	Polyethylglycol
PBS	Phosphate buffered saline
PGDF	Platelet derived growth factor
PDMS	Polydimethylsiloxane
Poly-HEMA	Poly-2-hydroxyethyl methacrylate
PI	Propidium iodide
PTFE	Polytetrafluoroethylene
UV	Ultraviolet
W/O	Water in oil

1. Introduction

In this chapter, the main motivations for carrying out this project are introduced and the aims and novelty of this work are provided. A brief outline of the thesis is given along with the project contributions and publications stemmed from this project.

1.1 Motivation

In the past decade, there has been a major increase in the discovery of potential anticancer treatments[1],[2]. However, less than 10% of novel anticancer compounds make it successfully through the clinical trial stages of the drug development process, mainly due to a lack of treatment efficacy observed *in vivo*[2],[3]. With regards to radiotherapy, further advancements are essential due to its lack of efficacy for certain types of cancer such as glioblastoma[4]. One of the major limitations in the development of anticancer treatments is the heavy reliance upon the use of two-dimensional (2D) cell culture models for preclinical studies[5]. 2D cell culture models such as monolayers provide a poor representation of the complex tumour environment and, as such, provide an inaccurate reflection of the efficacy of anticancer treatments *in vivo*[6], [7]. A better alternative to monolayers are three-dimensional (3D) cell culture models, such as the multicellular tumour spheroid (MCTS). Due to its 3D composition, MCTS has several of the features observed within a tumour *in vivo,* such as cell to cell contact and a heterogeneous population of cells[8], [9]. However, currently used methods for the culture of MCTSs (e.g. spinner flask or hanging drop plates) have several drawbacks, such as being labour intensive and low throughput. As a consequence, there has been a poor uptake of MCTS-based assays within the preclinical testing of anticancer treatments.[5]

Microfluidics has gained increased interest as a technology for potential use in biological applications[10], [11]. Microfluidics offers higher throughput solutions due to its miniaturised format whilst requiring only small amounts of cells and volumes of drugs or reagents[10], [11]. A particular microfluidic technology which is of interest in biological applications is droplet microfluidics, which offers high throughput methodologies to encapsulate cells within emulsions, creating multiple reactors for

single cell and cell population studies[11]–[14]. Droplet microfluidic studies involving the formation of MCTSs have mainly focussed on the use of alginate and/or matrix beads and microcapsules[15]–[20]. Overall, these studies have proven to be successful for the formation and culture of MCTSs with an example of a study producing over 1000 spheroids per device which, for example, highlights the high-throughput capabilities[21] of the technology. However, its compartmentalization properties suffers from the drawback of limiting the culture time for the encapsulated cells, often requiring the culture of spheroids off-chip in standard tissue culturing plates[19], [22] or the use of double emulsion droplets which are complicated to form[23]. Compartmentalisation, where each droplet acts as an environmentally isolated experiment[10], means that a finite amount of nutrients are available and a build-up of waste products is maintained, both of which can have a detrimental impact on cell viability. As a result, cell culturing duration times within droplets are short with the viability of cells reducing over days or even hours[19], [23], [24],[25], [26]. Thus, in order to carry out long term spheroid culture, useful for assessing long term treatment and spheroid responses within M/O droplets, an essential requirement is an investigation into the conditions to resolve the issue of compartmentalisation within a single, simplified microfluidic device. The ideal system would combine the high throughout characteristics of droplet microfluidics with the ease of medium perfusion of single-phase microfluidics. Both of these aspects have previously not been achieved and would be a positive advance in the use of microfluidic technology for spheroid culture and screening assays. More specifically, the development of a robust microfluidic assay for the culture and treatment of MCTSs has the potential to help in "bridging the gap" between *in vitro* cell culture models and *in vivo* models[27].

1.2 Aim and Objectives

The main aim of this thesis was to develop a microfluidic technology suitable for the formation, long term culture, and treatment (both radiotherapeutic and chemotherapeutic) of multicellular tumour spheroids (MCTSs).

The main objectives were as follows:

a) To characterise conditions for the formation and long term culture of MCTSs within macro medium in oil (M/O) droplets

b) Compare MCTSs formed and treated within M/O droplets with those formed and treated using traditional methods
c) Develop a microfluidic device suitable for the formation and storage of M/O droplets in a high-throughput format
d) Evaluate the suitability of the microfluidic device for the long term culture of MCTSs
e) Evaluate the suitability of the microfluidic device for carrying out radiotherapeutic and chemotherapeutic treatments on MCTSs

This work has produced the first comprehensive investigation of conducting long term culture of MCTSs within M/O droplets and developed an integrated platform for carrying out chemotherapeutic and radiotherapeutic screening on MCTSs within a single microfluidic device.

1.3 Thesis Outline

Chapter 2 provides an overview of why an improvement is still required in the development of anticancer treatments and how 3D cell culture models can help approach this issue. The current methods used for the formation of spheroids are evaluated and their limitations are discussed. The second part introduces the concept of using droplet microfluidics, providing a brief overview of this technology and how it is useful in biological applications. The use of droplet microfluidics in spheroid formation and culture will also be discussed and current literature will be evaluated.

Chapter 3 discusses the experimental methods and materials involved in the fabrication of microfluidic devices and protocols used to conduct droplet microfluidic experiments. This chapter also includes the methods required for the culturing of UVW glioma cells, radiotherapeutic and chemotherapeutic treatments and the analysis conducted on spheroids.

Chapter 4 introduces the concept of spheroid formation and culture within medium in oil droplets using macrodroplets within an open well device. Within this chapter, the conditions required for long term culture have been characterised and the spheroids formed within macrodroplets have been compared with those formed using a traditional method. Once this method was established, the ability to carry out radiation treatment on spheroids was evaluated. Several factors were tested such as spheroid size, radiation dose and the proliferative state of the spheroid. The radiotherapeutic

effects were also compared using spheroids formed in spinner flasks and non-adherent plates. The data within this chapter was published in a peer reviewed journal article which was featured on the front cover of the Analyst[28] and was included in a conference paper for Microtas 2014[29].

Chapter 5 describes the process involved in the development of a microfluidic device suitable for the formation and storage of droplets for the long term culture of spheroids. This chapter's aim was to develop a single device to reduce the complexity of the process whilst guaranteeing prolonged spheroid culture. Finally, a microfluidic device and protocols were developed to integrate droplet microfluidics with single phase microfluidics techniques.

Chapter 6 presents the assessment the microfluidic device and protocols developed for the formation and long term culture of spheroids. This system is tested for its suitability to carry out chemotherapeutic and radiotherapeutic assays. Finally, investigations were executed to determine if the device was suitable for spheroid formation and culture using hydrogels. Data from chapters 5 and 6 have been used for publishing a peer reviewed journal article in Lab on a Chip[30] and included in a conference paper which has been accepted for Microtas 2016.

Chapter 7 discusses the outcomes and limitations which are identified throughout this work. Additionally, a number of potential future applications are highlighted, and subsequent projects which have already arisen as a result of some of the findings in this thesis are discussed.

1.4. Project Contributions

In this project, all of the results and data analysed was conducted by the author unless stated otherwise. Training for cell culture was carried out by Dr Marie Boyd. Training to carry out photolithography and soft lithography was carried out by Dr Michele Zagnoni. Training to use the x-irradiator was conducted by Dr Anthony McCluskey. The dosimetry measurements reported in Chapter 6 and initial training to carry out tissue processing, sectioning and staining was conducted by Dr Annette Sorensen. The initial training of carrying out droplet microfluidic based experiments was conducted by Dr Michele Zagnoni and Bárbara Schlicht. The author independently optimised the experimental protocol for UVW glioma spheroid formation and culture within biocompatible M/O droplets and optimised a protocol for staining and sectioning

spheroids with haematoxylin and eosin (Chapter 4). Additionally, the author developed and tested different microfluidic device designs for droplet formation, cell encapsulation, spheroid culture and carried out radiotherapeutic and chemotherapeutic treatments (Chapters 5-6).

1.5. Publications

Aspects of this research have been published in the following journals and conference proceedings:

"Emulsion technologies for multicellular tumour spheroid radiation assays", K. S McMillan, A. G McCluskey, A Sorensen, M. Boyd & M Zagnoni (2016) Analyst, 141, 100 – featured on the journal front cover

"Transitioning from multi-phase to single-phase microfluidics for long-term culture and treatment of multicellular spheroids", K. S McMillan, M Boyd & M Zagnoni (2016) Lab on a Chip, doi:10.1039/C6LC00884D

"Development of a droplet microfluidic assay for radiotherapy treatment of multicellular spheroids", K McMillan, M Boyd & M Zagnoni, 18th International Conference on Miniaturized Systems for Chemistry and Life Sciences October 26-30, 2014, San Antonio, Texas, USA

"From emulsion to single-phase microfluidics: an integrated approach to culture and perfusion of multicellular spheroids", K. S McMillan, M Boyd & M Zagnoni, 20th International Conference on Miniaturized Systems for Chemistry and Life Sciences October 9-13 2016, Dublin, Ireland (accepted for poster presentation)

2. Background

2.1 Overview of Cancer

Cancer continues to be a serious problem worldwide with the International Agency for Research of Cancer (IARC) in 2012 predicting that the number of reported cases will increase by 75% in the next 20 years[31]. According to statistics from Cancer Research UK cancer is one of the leading causes of death with more than 1 in 4 deaths in the UK.

Cancer is defined as a disease which involves the uncontrolled proliferation and spread of cells throughout the body[32]. In order to understand the factors involved in the development of a normal cell into a cancerous cell it is important to understand the cell cycle. The cell cycle is a set of events which results in one cell dividing into two daughter cells and is made up of four main stages; G1 phase, S phase, G2 phase (known collectively as interphase) and mitosis[33]. A cell exits out of the resting phase, which is also known as the G0 phase, and enters the G1 phase once a growth factor binds to a specific receptor, resulting in stimulation of a signalling pathway[33], [34]. In the G1 phase the cell increases in size and gets ready for DNA replication. When the cell enters the S phase, DNA replication occurs and then moves into the G2 phase, where the cell further increases in size and produces proteins for mitosis. During the cell cycle, a cell has to pass through checkpoints in which the cell is checked to see if it has any abnormalities, such as DNA damage[33]. Checkpoints are located within G1, before a cell moves from G1 to S, before a cell moves from G2 to mitosis and in mitosis in metaphase before a cell enters anaphase. Here the daughter chromatids move to opposite ends of the cell before telophase, where the cell divides in two[33]. If at any of these checkpoints the cell is detected to have an abnormality (i.e. DNA damage), either the cell cycle is stopped and attempts are made to repair the cell or the cell undergoes programmed cell death, also known as apoptosis[33].

Hanahan and Weinberg suggested in 2000 that there are 6 physiological alterations (referred to as the hallmarks of cancer) involved during the development of cancer, which can be observed in the majority of cancer types[35], [36]. The first physiological alteration identified was “self-sufficiency in growth signals”, where a cell is able to produce its own growth signals. In a normal cell the growth signals, which stimulate a

cell to enter into the active phase of the cell cycle, are produced by the external microenvironment. However, in cancer cells they reduce their dependency upon other cells and the microenvironment by producing their own growth signals to which they can also respond. An example of this is glioblastoma, which has the ability to produce platelet derived growth factor (PDGF)[35].

Another physiological change linked to the control of cell proliferation is "insensitivity to anti-growth signals". Within a normal cell, anti-growth factors are released in order to maintain tissue homeostasis and prevent the unlimited proliferation of cells. Thus, cells are moved from an active phase of the cell cycle into the G0 stage until they are reactivated by growth factors. Cancer cells become insensitive to anti-growth factors and so the cells continue to proliferate even if no more cells are required or if an abnormality is detected within the cell.

The third hallmark is the ability of a cell to avoid apoptosis. In a normal cell, apoptosis is triggered if an abnormality such as DNA damage or hypoxia is detected. One of the best known mutations in cancer, which results in the evasion of apoptosis, is the tumour suppressor gene p53 which has been identified in over 50% of human cancers[37].

The fourth main alteration, which is a result of the previous three discussed, is "limitless replicative potential", allowing for the growth of tumours. Due to this physical alteration the replication of cancer cells is not regulated and, as such, uncontrolled proliferation of cells occurs.

The fifth main physiological capability is "sustained angiogenesis". Angiogenesis is the ability to produce new blood vessels from existing vasculature so that as the tumour increases in size there is an increased supply of nutrients and oxygen to allow cells to proliferate[38]. This is essential for a tumour to continue to grow, as tumour cells are estimated to be within 100 μm of a blood vessel in order for tumour cells to receive sufficient nutrition and oxygen[39].

The final hallmark of cancer and the main differential characteristic between benign and malignant tumours is its ability of malignant cells to invade and metastasise. The development of metastases from a primary tumour involves several steps: invasion of the primary tumour into the tissue surrounding it; migration into either blood vessels or the lymphatic system to allow transport to another site in the body; migration of the

primary tumour through the blood vessel wall into the new target organ; angiogenesis and then growth and metastases at the new site[40]. In the vast majority of cases the cause of death due to cancer is the development of the primary tumour into metastases which are difficult to cure with treatments currently available[40]. Death by metastases tends to be due to damage to the affected organ or complications in treatment of the metastases[40],[41]. Once cancer has metastasised it is difficult for it to be treated with surgery or conventional external beam therapy as there is the risk of there being too many lesions to remove or they are unable to be removed and the use of radiotherapy and chemotherapy is often used only to increase the time of survival of the patient.

2.2 Tumour Microenvironment

The tumour microenvironment (Figure 2.1) is composed of a heterogeneous mixture of cells and the extracellular matrix (ECM). There are several factors which contribute to the heterogeneity of a tumour, including the distance of cells from a blood supply, the presence of inflammatory cells and a sub-population of cells known as cancer stem cells[42], [43]. In a tumour, a blood supply is delivered to the cells by two main sources: the host's vasculature and blood vessels created through angiogenesis[38]. As a tumour grows, the host's vasculature does not increase at the same rate, resulting in an uneven supply of oxygen, nutrients and growth factors and removal of waste products, such as lactic acid[38]. In addition, some of the host's blood vessels within the tumour may become blocked or squeezed which further impacts upon the blood supply available[39]. Thus, angiogenesis acts to increase the vasculature available to the tumour to allow for nutrition and waste product removal. However, cells with different characteristics are still present within the tumour, some of which become hypoxic (defined as an area of cancer tumour with an oxygen tension (pO_2) of ≤ 2.5 mmHg)[44], necrotic (dead cells characterised by a breakdown of the plasma membrane and release of inflammatory markers)[45] or highly proliferating cells, depending upon their distance from the blood supply[43]. Furthermore, the vasculature created via angiogenesis tends to have an abnormal structure in comparison to normal blood vessels, resulting in lower flow rates and inadequate perfusion of nutrients and oxygen[46]. The ECM is composed of a mixture of proteins including collagen, laminin, elastin and fibronectin, which fill in the extracellular spaces between cells. The ECM has many functions which include acting as a scaffold and interacting with cells, which has an influence on tumour growth, angiogenesis, invasiveness and metastasis[6].

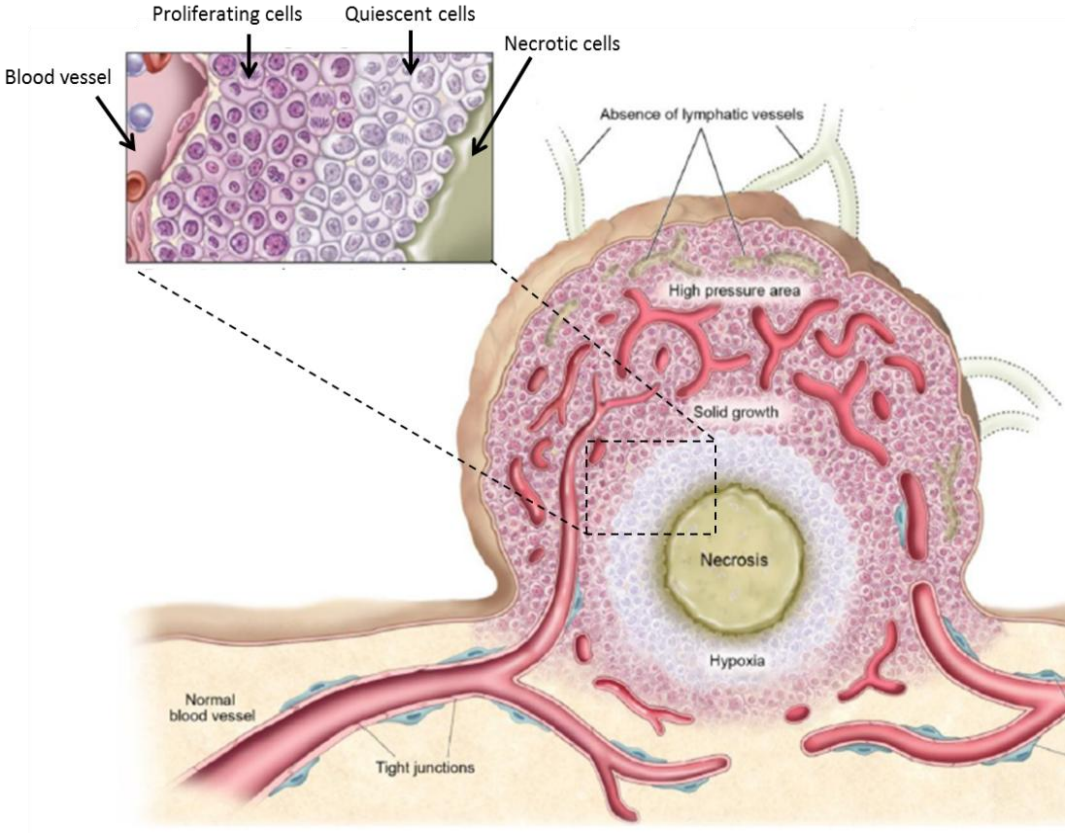

Figure 2.1: Schematic Diagram of Tumour Microenvironment. Diagram showing the different characteristics of cells in a tumour grown around blood vessels due to the distance from blood vessels. A magnified section of the tumour shows that the cells closest to the blood vessels are proliferative and then the further away they become quiescent and hypoxic, with cells in the core becoming necrotic. The figure has been adapted from Kobayashi et al..[47].

2.3. Treatment of Cancer

Current treatments for cancer include surgery, radiotherapy, chemotherapy and more recently biological or immunotherapies which may be given alone or in combination. It has been estimated that approximately 50% of all cancer patients receive radiotherapy at some point in their treatment[4], [48]. The main target for radiotherapy is deoxyribonucleic acid (DNA), which is damaged either directly or indirectly (via generation of reactive oxygen species) to result in single strand breaks and double strand breaks in the sugar phosphate backbone of DNA[49],[50]. Double strand breaks (DSBs) are difficult for a cell to repair and as a result the cell harbouring DNA DSBs undergoes apoptosis[51]. Although radiotherapy delivers high success rates, treatment

failure still remains high in certain types of cancer such as glioblastoma[4]. Glioblastoma is one of the most lethal forms of brain cancer with the vast majority of diagnosed cases surviving for only 1 year[52]. Glioblastoma is known for its intense invasiveness, impact on vital areas of the brain and complications with treatment[53]. The current treatment of glioblastoma initially involves surgery to either remove the whole tumour or to gain a biopsy depending upon the tumour size. Surgery is beneficial as it relieves the pressure within the brain, improves body functions and also helps in the penetration of chemotherapy into the brain by damaging the blood brain barrier. If the tumour cannot be removed completely and to target any residual cells which may have invaded into the normal margin, the next course of action is radiotherapy with or without chemotherapy. A major issue with glioblastoma is that it is highly radioresistant. Normal brain cells can only cope with up to 60 Gy of radiation, which is not a high enough dose to kill the glioblastoma cells[53]. Higher doses of radiation of up to 180 to 200 Gy are required to have any impact. As a result the higher doses used are associated with an increased risk of side effects due to the effect they have on normal brain tissue. In order to improve upon current treatment, research is currently investigating the development of radiosensitising treatments, which sensitise cancer cells to radiotherapy and thus lowering the dose required and reducing the damage caused to normal cells.

Although advances are constantly being made in treatments for cancer, they still suffer from drawbacks such as side effects, the development of resistance resulting in relapse and the issue that they tend to be discovered on a population basis rather than an individual one. Over the past decade there has been approximately a 140% increase in the number of anticancer drugs which are under development[1]. However, the success rate of a drug making it through clinical trials to being available for treatment in a patient is very low, at approximately 10%[3]. A strong reason for this poor success rate is due to *in vitro* cell culture models currently in use, which are physiologically inaccurate in comparison to tumours *in vivo*[54]. As a result the pharmacological activity and efficacy of the treatment *in vitro* may not be the same as observed in animal models and clinical trials. One of the issues with *in vitro* models is the routine use of 2D cell culture models such as monolayers[6]. Monolayers are a poor comparison to tumours *in vivo* as they do not contain cell to cell contact or a variation in the proliferative rate of cells as is witnessed in a 3D cancer tumour. Furthermore, the proliferation and differentiation of cells is artificially altered when they are plated as a

monolayer[7]. Therefore, there is a requirement for the development of new anticancer treatments to remove the use of 2D cell culture models and move onto the use of 3D cell culture models to "bridge the gap" between *in vitro* models and tumours.

2.4 Three-dimensional (3D) Cell Culture Models

The initial discovery of one of the best known 3D cell culture models is the multicellular spheroid (MCS) which was made by the Holtfreder (1944) and Moscona (1956) research groups[55],[56]. These groups observed that multicellular aggregates were able to form from malignant and embryonic cells within a non-adherent environment. The first application of this model for use in cancer research was in 1970 by Sutherland *et al..* as a model for radiosensitivity[57]. As a cancer model the name is changed to a multicellular tumour spheroid (MCTS). A MCTS is defined as a spherical cancer model which is produced by a single cell suspension[58]. A MCTS is a good *in vitro* cancer model for providing a more accurate reflection of the tumour physiology *in vivo* for several reasons.

First of all, in contrast to a 2D cell model, a MCTS has cell to cell contact resulting in cell to cell interactions which have been shown to have an impact on the efficacy of cancer treatments. A study by Bissell *et al..* (1998) demonstrated how the phenotype of breast cancer cells can be altered when grown as a multicellular spheroid when compared to a monolayer[59]. In this study they investigated the effect of β1 integrin blocking antibodies in spheroids and in monolayers to determine if there was an effect on the epidermal growth factor receptor (EGFR) signalling pathway. A reduction in the expression of EGFR was observed in the spheroid model, however this was not observed in cells grown in a 2D monolayer. Therefore, this shows that cell to cell contact can induce alterations to the phenotype of cells and thus on the potential efficacy of anticancer treatments. Close cell to cell contact also creates a barrier to drug penetration into the spheroid. In a study by Bryce *et al..* it was shown through confocal imaging that when colon cancer spheroids were treated with doxorubicin the concentration reduced to half within 20 μm and then 10% within 100 μm of the spheroid[60]. This is similar to what has been observed *in vivo,* where doxorubicin has been shown to only diffuse 40 to 100 μm from the blood vessels into a tumour mass[61].

Another factor which is similar to a tumour *in vivo* is the nutritional gradient which develops within a spheroid due to the close cell to cell contact (Figure 2.2)[8]. As a result, the outer layer of cells receives the highest amount of nutrients and oxygen whilst cells within the core receive the least[9]. In addition, a gradient of waste metabolites develops from the inside to the outside of a spheroid. Due to this, a heterogeneous population of cells develops within a spheroid, with cells on the outside being proliferative and the ones on the inside entering a dormant (quiescent) state[9].

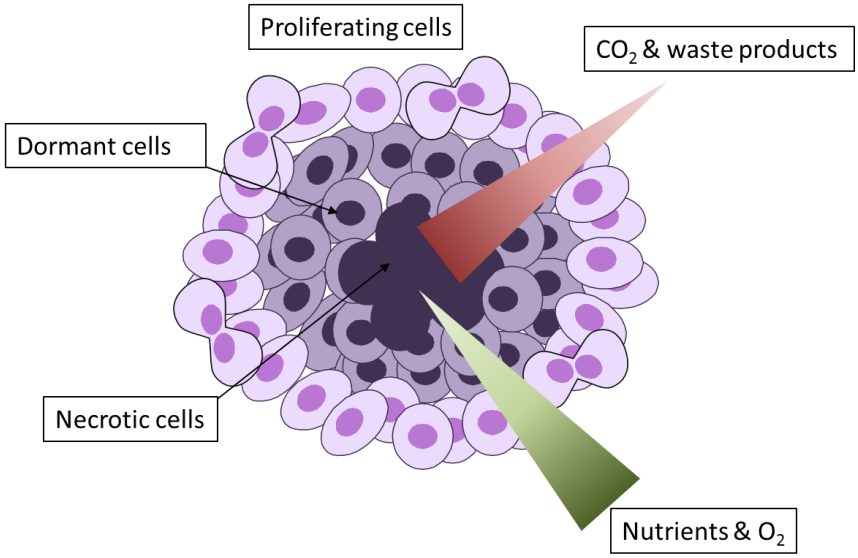

Figure 2.2: Schematic Diagram of a Multicellular Tumour Spheroid. The outer rim of cells represents proliferating cells, the middle cells quiescent cells and the dark centre represents necrotic cells. The triangles represent the concentration gradient of different substances within a spheroid, with the point of the triangle indicating a low concentration and the base a high concentration.

The development of different cell populations is determined by the size of the spheroid as it depends upon the diffusion limit of molecules such as oxygen, which has been shown to be around 150 to 200 μm[62]. Once spheroids grow to a diameter of 500 μm or more, apoptotic and necrotic cells begin to develop within the core. The development of a heterogeneous population of cells within a MCTS is similar to that observed within a tumour *in vivo,* which is due to the variation in distance of cells from the blood supply. It is important to consider the different populations of cells as it has been shown that quiescent cells have a greater resistance to chemotherapy and radiotherapy[63]. One of the reasons for quiescent cells having an increased resistance to radiation is due to the ability to repair potentially lethal damage such as DNA

damage[64]. This effect has been observed in glioblastoma, where a study compared the damage repair after radiation treatment between spheroids and monolayers, finding that there was a recovery of spheroid growth[65]. Another issue with quiescent cells is once the more sensitive proliferating cells have been killed by radiation, the more resistant quiescent cells are then able to proliferate when introduced to fresh nutrients (Figure 2.3)[63]. In terms of drug therapy, certain drugs are only effective against highly proliferating cells. Thus, they will have little if any effect on the quiescent cells within the spheroid. Examples of drugs which are only effective against proliferating cells are doxorubicin and 5-fluorouacil (5-FU). In a study by Tung *et al.*. they showed that when a 2D monolayer was treated with 5-FU, only 10% of cells were viable. However, with a spheroid, approximately 75% remained viable when compared to the control. The higher percentage of viability was thought to be due to the difficulty of the drug to penetrate into the spheroid, as well as the selective effect 5-FU has on proliferating cells. Therefore, quiescent cells are also resistant to certain chemotherapeutic drugs.

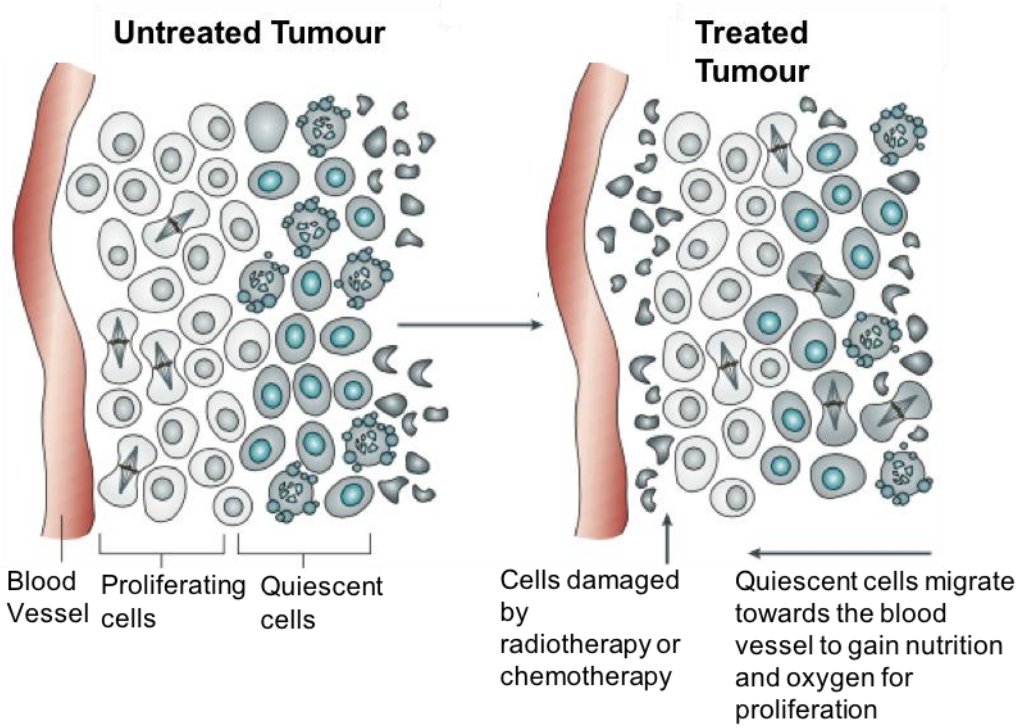

Figure 2.3: Schematic diagram of repopulation of quiescent cells in a tumour after treatment. Diagrams of a tumour before treatment and after treatment with either radiotherapy or chemotherapy showing the repopulation of quiescent cells due to better access to nutrition once the proliferating cells are selectively damaged. Figure has been amended by Kim and Tannock[66]

2.5 Three-dimensional (3D) Cell Culture Methods

In order to produce MCTSs, cell to cell contact is either promoted by seeding cells onto a culture surface which does not allow for adherence, or by incorporation of alginate or ECM. There are several *in vitro* methods currently used for the formation of 3D cell culture models such as MCTSs, which include agitation based methods, hanging drop, forced floating and the incorporation of alginates or matrices[5].

2.5.1 Agitation Based Methods

Agitation based methods can be split up into two main types which are the spinner flask and rotational culture methods. The main concept behind both approaches is that the cell suspension is kept in motion to prevent the adherence of cells to the culture vessel as well as to promote interactions between cells. The spinner flask approach was first developed by Sutherland *et al..* in 1970 and comprises of a flask with a stirring rod to keep the cell suspension in motion (Figure 2.4(A))[57]. The rotatory culture method was first developed in 1992 and involves keeping the cell suspension in motion via a rotating chamber (Figure 2.4(B))[67]. Overall the agitation based methods are fairly simple approaches and can produce a high number of spheroids. However, the range of spheroid sizes is heterogeneous and it can be laborious to pick out spheroids using a pipette for analysis. In addition, the high shear stress produced by the spinner flask method can have an impact on the physiology of cells. In a study by Song *et al..* they compared the characteristics of two different prostate cancer cell line spheroids (DU145 and LNCap) formed using a spinner flask or in non-adherent plates[68]. It was observed that there was a significant increase in the percentage of proliferative cells at the surface of the DU145 spheroids formed using a spinner flask in comparison to the use of non-adherent plates. In addition a significant decrease in the percentage of quiescent cells was observed in the same spheroid type in comparison to the liquid overlay method. However, no significant difference was observed in the percentage of proliferative and quiescent cells for the LNCap spheroids when comparing the two techniques used. A further disadvantage of the agitation based methods is the high volume of medium required per experiment, with approximately 100 to 300 ml being used per spinner flask depending on the size. Furthermore, agitation based methods cannot be used for the analysis of specific spheroids over time, thus only the initial

spheroid formation is carried out using this method and a secondary method has to be used for any long term experiments.

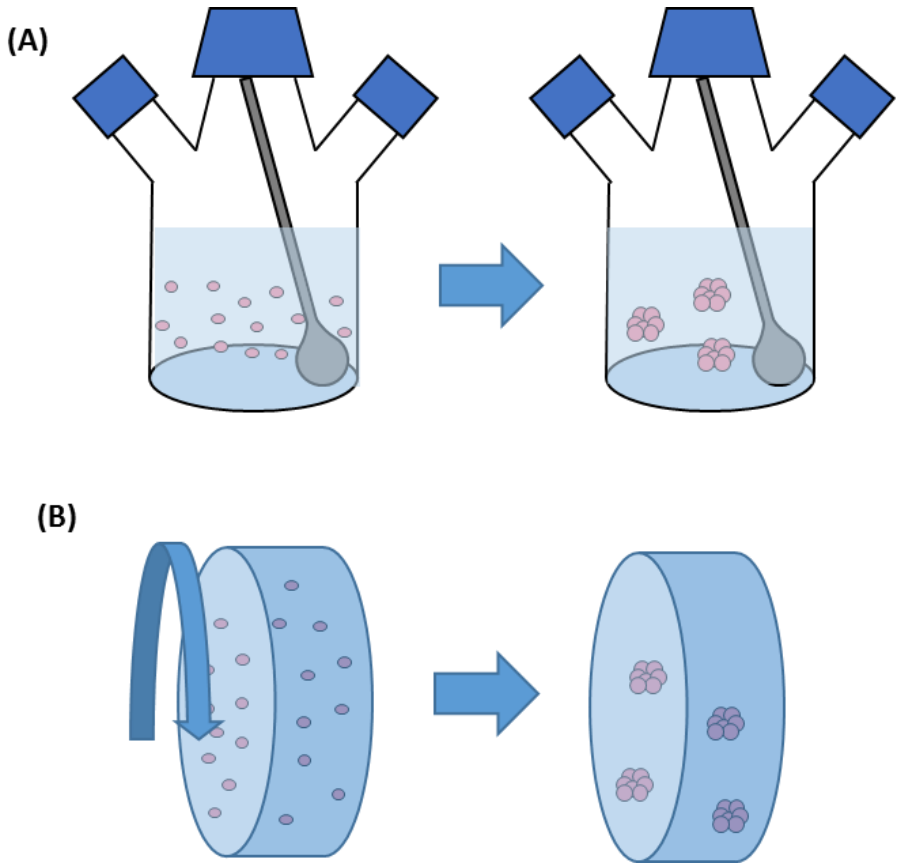

Figure 2.4: Agitation based methods for Spheroid Formation. Diagrams of spheroid formation via the spinner flask method, (A), and the rotary based method (with the arrow indicating the spinning of the rotary chamber) (B) showing a single cell suspension and then formed spheroids.

2.5.2. Hanging Drop Method

The hanging drop method was originally developed by Harrison *et al.*. for neuronal culture and was adapted for the formation and culture of spheroids by Kelm *et al.*.[69]. The method involves the pipetting of aliquots of cell suspension into a 96 well plate, which is then inverted to have the drops kept in place by surface tension (Figure 2.5). Cells gather at the bottom of the droplet resulting in proliferation and cell aggregation to form spheroids. Overall, the hanging drop system has been shown to be reproducible and can be used to form spheroids for a variety of different cell lines[69]. In recent

years there has been an increase in the number of studies aiming to produce a high throughput hanging drop system. Tung *et al..* managed to develop a 384 well plate suitable for the formation and culture of spheroids that also allowed for the drug testing of spheroids[70]. However, they found that the device still suffered from stability issues, with droplet spreading being an issue if there was any mechanical shock such as placing the plate on a table[70]. Furthermore, addition of medium to the drop can result in an increase in the size and spreading of drops, leading to increased risk of nearby drops coming into contact. It has also been shown that even slight tilting of a hanging drop plate, whilst moving from an incubator to a microscope for analysis, is enough to disrupt the droplets, resulting in the spheroid breaking up. In addition, the refreshment of medium can be problematic as aspiration of old medium can also disrupt the drop resulting in it falling. To resolve this issue, hanging drop plates have been developed by InSphero and 3D Biomatrix which sit above a non-adherent coated well tray. This allows if droplets do fall that the spheroid can be caught by the well below to allow for further culturing. Recently Hsaio *et al..* have attempted to resolve the stability issue of hanging drops by developing a device which incorporates the use of micro-ring structures[71]. The ring is located around the bottom of the droplet and acts to prevent the initial droplet spreading, which can result in droplet merging. However, the duration of spheroid culture was only increased to 22 days due to droplet spreading still occurring over time.

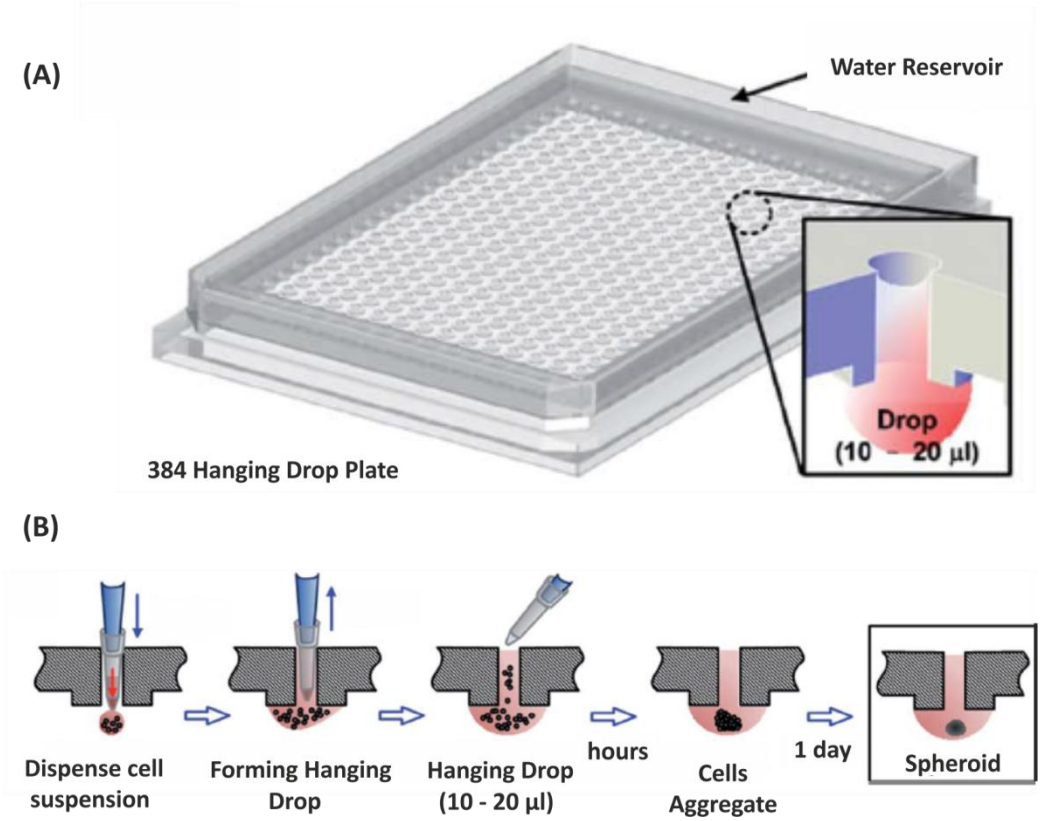

Figure 2.5: Hanging Drop System for the Formation of Spheroids. (A) A diagram showing a 384 hanging drop plate which has a water reservoir around the edge to reduce the rate of evaporation of droplets by creating a humidified environment, with a magnified section showing the hanging drop in place containing 10 to 20 µl. (B) A diagram showing the dispensing of a medium containing cell suspension from a pipette into a hanging drop well and the process of spheroid formation over time. The figure has been modified from figures by Tung et al..[70].

2.5.3. Forced Floating Method

The forced floating method (also known as the liquid overlay method) involves the seeding of cells into round bottomed 96 well plates which are coated to prevent the attachment of cells to the plate surface and so result in cell to cell contact[62]. To create a non-adherent surface, wells are coated with agarose or poly-2-hydroxyethyl methacrylate (poly-HEMA). The cell suspension is then added to the well, with the cell concentration used dependent upon the desired spheroid size. For some cell lines the use of poly-HEMA alone is not suitable for forming spheroids using the forced floating method. In a study by Ivascu and Kubbies they evaluated the suitability of this method

for eight different breast cancer cell lines[72]. Only half of the cell lines formed compact spheroids using this method, with the other four only forming cell aggregates. In order for the cell lines which formed aggregates to form spheroids, Matrigel (BD Biosciences) was added to the medium to create a matrix scaffold. Overall, the forced floating method is fairly simple and easy to replicate. In addition, it is easy to adjust the size of spheroids required by altering the cell number added to each well. However, the coating of the plates does add an extra step which, if poly-HEMA is used, can take up to 3 days for the coating to dry[5]. Thus this makes the use of poly-HEMA plates more time-consuming and laborious. Furthermore, even though pre-coated plates can be purchased they tend to be more expensive than the process of coating plates in-house.

2.5.4. Matrices and Scaffolds

A different type of method used for the formation of MCTSs involves the incorporation of a matrix with the aim to provide a better reflection of the cell to ECM interactions which occur *in vivo*. An example of a well-known commercially available extracellular matrix protein extract is Matrigel. Matrigel is a basement membrane preparation that contains a mixture of extracellular proteins which includes collagen IV, laminin and enactin as well as growth factors[73]. There are two main ways in which spheroids are formed using Matrigel within a 96 well plate; one is to embed cells within the gel while the second is to seed cells on top of the gel. One of the drawbacks of Matrigel is that it is expensive and thus not suitable for the large scale production of spheroids required for drug screening using current methods. Furthermore, the use of ECM can result in the formation of spheroids which are not uniform due to the uneven distribution of cells throughout the matrix. In addition, there can be variability between batches of Matrigel in terms of the mixture of protein extracts, which can have an influence on the reproducibility of results. However, it can be suggested that this is advantageous as it produces more realistic results similar to what would be observed *in vivo* with variation between tumours.

Scaffolds are a simpler idea to the incorporation of matrices: examples include alginate, laminin and collagen type 1[5]. As the name suggests, they act to provide support for the cells, with the cells migrating between them and attaching to them to form spheroids[5]. Scaffolds can be used to form spheroids of certain cell lines which are

anchorage dependent (for example the human melanoma cell line (M21)[74]) and as such are unable to form cell to cell contacts in non-adherent environments.

2.5.5. Limitations of Current Methods to Form 3D-Culture Models

Although there are a variety of different methods which have been used for the formation of spheroids they still suffer from several drawbacks, which are being low throughput, laborious and produce a heterogenous range of spheroid sizes. The hanging drop method is sensitive to shock such as the replacement of medium and the spinner flask method can result in physical stress resulting in physiological changes to cells[5]. As a result, the popularity of using spheroids within standard *in vitro* cancer treatment screening remains low. Therefore, the development of novel methodologies which are high-throughput, less laborious and allow for the formation of homogeneous spheroid sizes is essential.

In recent years there has been an increasing trend in the number of studies investigating the use of a technology known as microfluidics for cancer research, with one of these areas being in the culture of MCTSs[75], [76].

2.6 Overview of Microfluidics

Microfluidics involves the manipulation of fluid within the microlitre to picolitre range through sub-millimetre channel networks[20]. Microfluidics offers several advantages as a technology for biological applications, such as the use of reduced sample volumes, high-throughput capabilities and rapid prototyping. In order to develop microfluidic systems suitable for biological purposes, it is important to understand the physics of the fluid flow at the microscale which exhibits many differences in comparison to fluid flow at the macroscale. When a system decreases in size, its surface area to volume ratio increases, which results in an increased dependence on surface effects, such as surface tension and viscous forces[20]. A qualitative description of the behaviour of fluids at the microscale can be shown by a dimensionless number, known as the Reynolds number:

$$Re = \frac{\rho v L}{\mu} \qquad \text{(Equation 2.1)}$$

where ρ is the fluid density (g/cm^3); v is the velocity (cm/s); L is the diameter of the channel (cm) and μ is the dynamic viscosity of the fluid (g/s/cm)[77].[78]. The

Reynolds number gives a measure of the ratio of inertial forces to viscous forces in the flow of fluid. Inertia is the ability of an object to continue at constant velocity unless an external force acts upon it. The viscosity of a fluid is the measure of resistance to deformation by shear or tensile stress. In microfluidic systems the diameter of channels tends to range from 1 to 100 μm and fluid velocities do not typically reach more than a centimetre per second, thus resulting in small inertial forces. As the inertial forces are small, the Reynolds number in a microfluidic system typically equals no more than 10^{-1}. When the Reynolds number is less than 1 the flow of fluid becomes laminar[78]. The reason for laminar flow being observed is due to the presence of low inertial forces meaning that the flow of fluid can be controlled easily. This characteristic of the flow is particularly desirable in developing biological assays as it enables the controlled transport of particles and reagents within microchannels. Microfluidic devices (also referred to as "lab-on-a-chip devices") are typically fabricated using photo- and soft-lithography. One of the most popular polymers used to fabricate microfluidic devices is polydimethylsiloxane (PDMS). PDMS has several attractive qualities, such as being biocompatible, allowing for the exchange of gases, flexible, optically transparent and inexpensive[79].

2.7 Droplet Microfluidics

In the past decade there has been an increased interest in the use of droplet microfluidics as a method for the formation and culture of spheroids. Droplet microfluidics involves the formation of a micron-sized emulsion (a mixture of two immiscible fluids consisting of a continuous phase and a dispersed phase, i.e. water droplets in oil) [80],[81].

2.7.1 Droplet Formation

The two most well established geometries used to form droplets are the T-junction (Figure 2.6 (A)) and the flow focussing junction (Figure 2.6(B)). The T-junction was first proposed as a suitable geometry for droplet generation in 2001 by Thorsen *et al.*[81]. A T-junction involves at least one channel containing an aqueous phase which sits perpendicular to the main channel containing a continuous phase. The two phases meet at the junction to form an interface and, as the flow of the two phases continues, the tip of the aqueous phase then enters the continuous phase stream[82]. As the flow continues the aqueous phase blocks the channel resulting in a restriction in the flow of

the continuous phase around the droplet. Due to the obstruction of the channel the pressure of the continuous phase upstream from the droplet increases, causing the neck of the droplet to thin and then break off to form a droplet if the capillary number is above a critical number. The Capillary number is a dimensionless number which can be calculated by the following equation:

$$Ca = \frac{\mu v}{\gamma} \qquad \text{(Equation 2.2)}$$

where μ is the dynamic viscosity of the continuous phase (g/s/cm); v equals the velocity of the continuous phase (cm/s) and γ equals the interfacial tension (g-force/cm) between the two phases. The capillary number has an influence on the size of droplets generated, as this is directly related to the deformability of the droplet interface. The flow focusing junction was first proposed by Anna *et al..* in 2003[83]. In a flow focusing junction (figure 2.6 (B)) the aqueous phase enters through a middle channel whilst the continuous phase flows through two outer channels. The two phases then meet through an aperture resulting in breakup of the aqueous stream into droplets. The formation of either water in oil (W/O) or oil in water (O/W) droplets is dependent upon the hydrophobicity of the channel walls[80]. In order to form W/O droplets the channel walls have to be treated to become hydrophobic so that the discrete aqueous phase does not adhere to the walls.

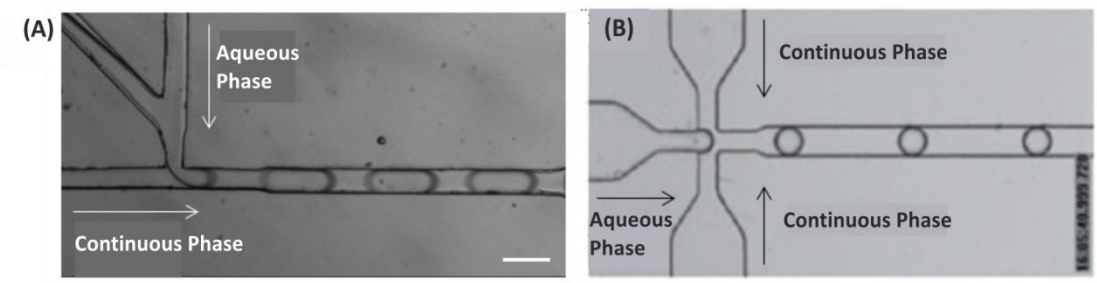

Figure 2.6: Droplet Formation via different geometries. Brightfield images of droplet formation using T junction (A) and a flow focusing junction (B). The flow focusing image has been modified from Theberge et al..[10]

In addition to the geometry of the microfluidic device and surface functionalisation, other factors are important in droplet generation which include the size of the aperture

at the junction; the ratio of flow rates and the viscosities and ratio of channel widths[82]. The flow rate ratio also has an impact on the size of droplets formed:

$$Q = \frac{Q_o}{Q_w} \qquad \text{(Equation 2.3)}$$

where Q_o equals the flow rate of the continuous phase and Q_w the flow rate of the aqueous phase.

2.7.2 Encapsulation of Cells within Droplets

During droplet formation, cells can be encapsulated within droplets by using a cell suspension as the aqueous phase. The distribution of cells within droplets follows a Poisson distribution:

$$k = \frac{\lambda^k \exp(-\lambda)}{k!} \qquad \text{(Equation 2.4)}$$

where λ is the average number of cells per droplet. Therefore, the number of cells within droplets increases with increasing the cell concentration used. The use of cell encapsulation within droplets was initially used for single cell studies. Various different cells have been encapsulated within droplets, which include bacteria, yeast, hybridoma cells and human cells[11], [12]. Furthermore, organisms have been encapsulated within droplets, such as *C. elegans*[84], [85]. More recently, there has been a focus on the encapsulation of multiple cells in order to create MCTSs which will be discussed in more detail in section 2.8.

2.7.3 Droplet Storage

In order to analyse droplets and/or carry out cell based experiments over a long time period the storage of droplets is essential. There are two main options for storing droplets once they are formed: either off-chip or within a microfluidic device. Droplets can be stored off-chip within a syringe or within a standard 96 well plate, petri dish or flask. One of the first microfluidic designs used for the storage of droplets on-chip was developed by Frenz *et al.*. and involved the use of a long serpentine channel for storage after the droplet formation junction (Figure 2.7)[86]. The serpentine channel had an initial entrance and outlet which was 25 μm in depth and the main part being 75 μm in depth to allow for the storage of droplets on top of each other. This device is only

suitable for short storage times as there is a risk of coalescence due to the droplets remaining in contact with each other. Since the development of simple serpentine microchannel geometries, more sophisticated designs involving the separation of droplets have been proposed[87], [88]. Several different types of storage chambers have been developed: from traps to specific channel geometry, allowing for the trapping and separation of droplets (Figure 2.8). The separation of droplets aids with tracking single droplets over a longer period of time.

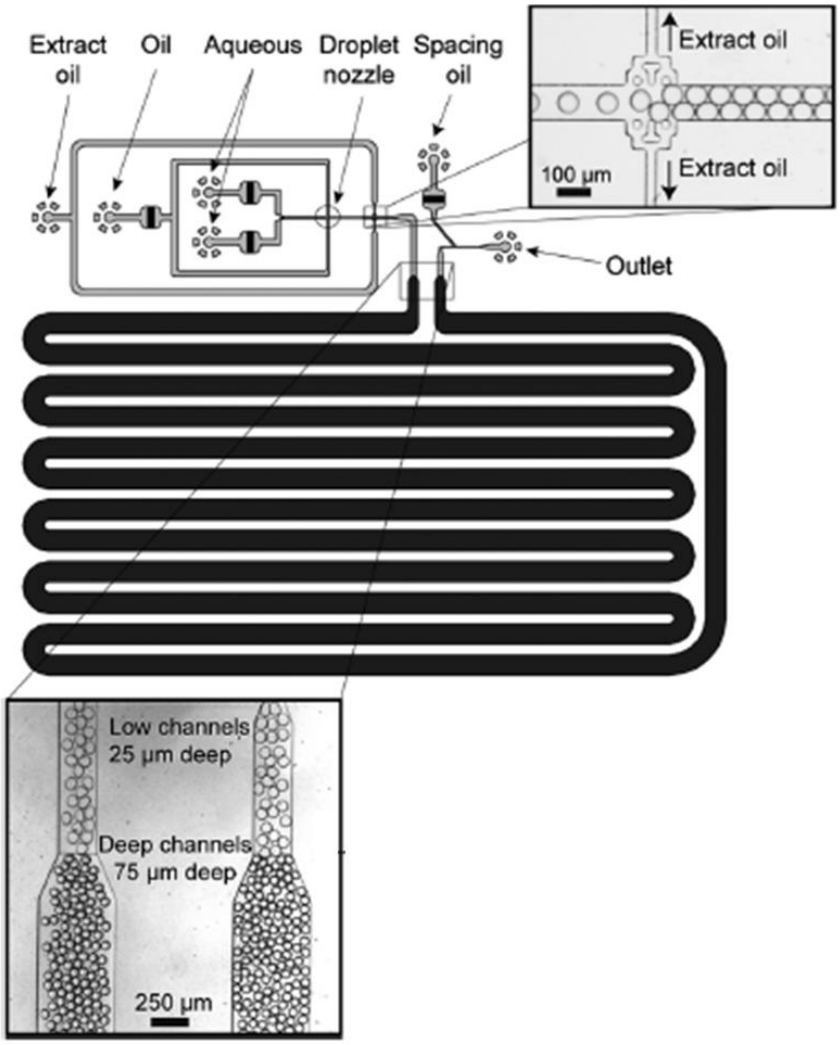

Figure 2.7: Droplet Storage within a serpentine storage channel. A diagram showing a droplet microfluidic device for the formation of droplets via a flow focusing junction and a long serpentine channel for storage of droplets. The brightfield images show the channels used for the extraction of oil prior to the droplets entering the channel and the droplets within the channel. The figure has been taken from Frenz et al.[86].

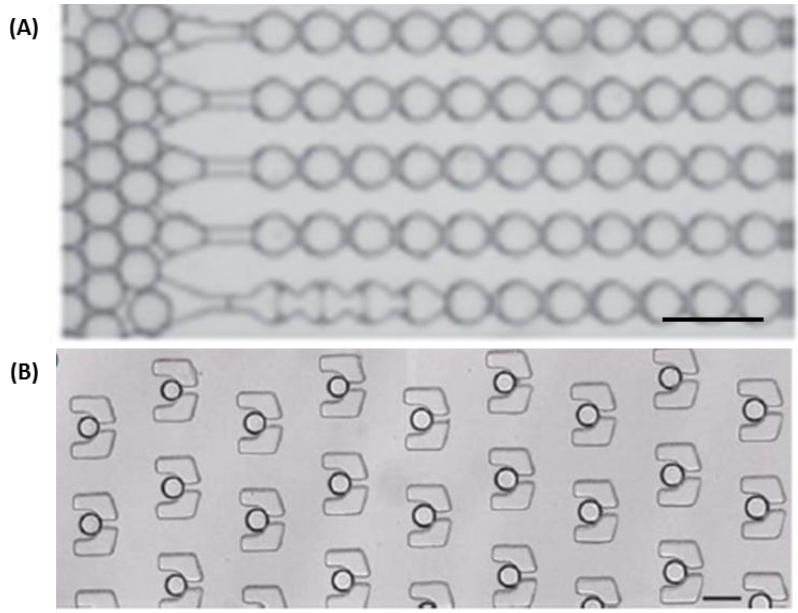

Figure 2.8: Examples of Droplet Storage Arrays which Separate Droplets. (A) A brightfield image of droplets stored within the storage array of the "Dropspot" device developed by Schmitz et al..[88]*. (B) A brightfield image of droplets stored within microfluidic traps which was developed by Huebner et al..*[89]*. The scale bar for (A) is 500 µm and for (B) is 75 µm. Figure (A) has been adapted from Schmitz et al..*[88] *and figure (B) has been adapted from Huebner et al..*[89]*.*

2.7.4 Droplet Stability

Emulsions are thermodynamically unstable mixtures, as increases to the surface area also increases the interfacial free energy. Therefore, to lower the interfacial free energy the emulsion acts to increase the size of the droplets, resulting in a separation of the two phases into separate layers (coalescence). In order to prevent the coalescence of droplets upon contact, surfactants have to be used. Surfactants are amphiphillic molecules which have a hydrophilic head and a hydrophobic tail and are used to stabilise emulsions[90]. Surfactants reduce the interfacial free energy via several different methods, which include reducing the interfacial tension; forming either a mechanical barrier or an electrostatic barrier around the droplets[90]. In addition to preventing coalescence, surfactants used in emulsions for biological applications have to be biocompatible[91] (i.e. not toxic or harmful to living cells or tissues). In order for a surfactant to be biocompatible it should not contain an ionic head which could interact with oppositely charged biomolecules such as DNA or proteins.

However, the coalescence of droplets has been shown in several studies to be useful for the addition of reagents for biological assays. Coalescence of droplets can be carried out either passively or actively. Passive methods require the lowering of surfactant concentrations and/or use of different channel geometries to control the movement of droplets to allow for close contact[92]. Active methods, including thermocapillary methods[93] and electrocoalescence[94], [95] do not require a change in the surfactant concentration. The thermocapillary method involves localised heating of droplet interfaces via the use of a laser to result in the removal of surfactants from an area of the interface to induce coalescence (Figure 2.9A)[93]. Electrocoalescence occurs when the conductivity of the droplets is greater than the conductivity of the surrounding phase and they are subjected to an electric field [95], [96]. The electric field is applied to the microfluidic device by applying electrodes to an area of it and applying a set voltage. The difference in conductivity between the two phases is created due to the high salt content of the buffer or cell medium used as the aqueous phase. As two droplets enter the area of microfluidic channel were the electrodes are located the interfaces of the droplets deform due to the difference in the conductivity between the two phases and thus when they come into contact the droplets coalesce (Figure 2.9B). An example of a biological application where coalescence was proven useful has been shown recently by Wen *et al.* with *C. elegans* cultured within droplets (Figure 2.10)[85]. The design used in this study allowed the refreshment of trapped droplets by coalescence with medium droplets. This was possible due to the low surfactant concentration used.

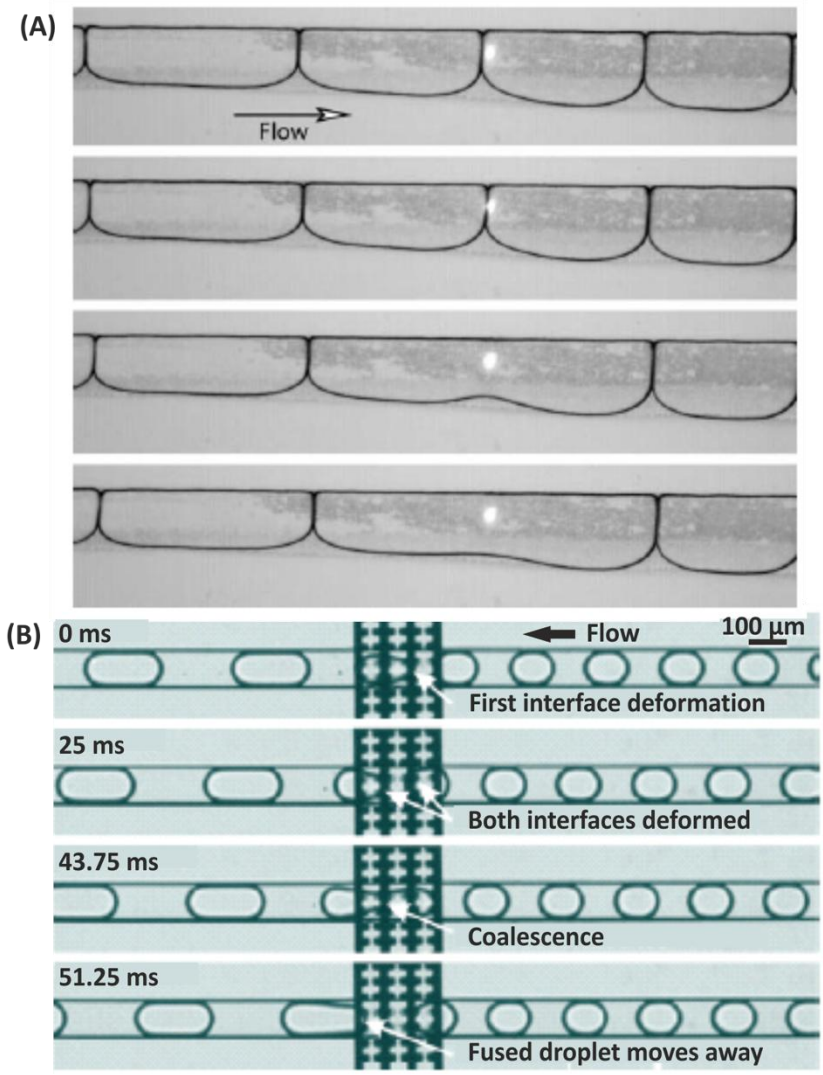

Figure 2.9: Active Coalescence Methods. (A) Brightfield images showing a timelapse of droplets passing through a channel with the interfaces coalescing once the interface passes the laser (shown by the white dot). (B) Brightfield images showing a timelapse of droplets passing through a channel with electrodes with the interfaces deforming and droplets coalescing once the droplets pass the electrodes within the channel. In both (A) and (B) the direction of flow of the droplets is indicated by the arrow. (A) is a figure taken from Baroud et al.[93] *and (B) is a figure adapted from Zagnoni et al.*[95]

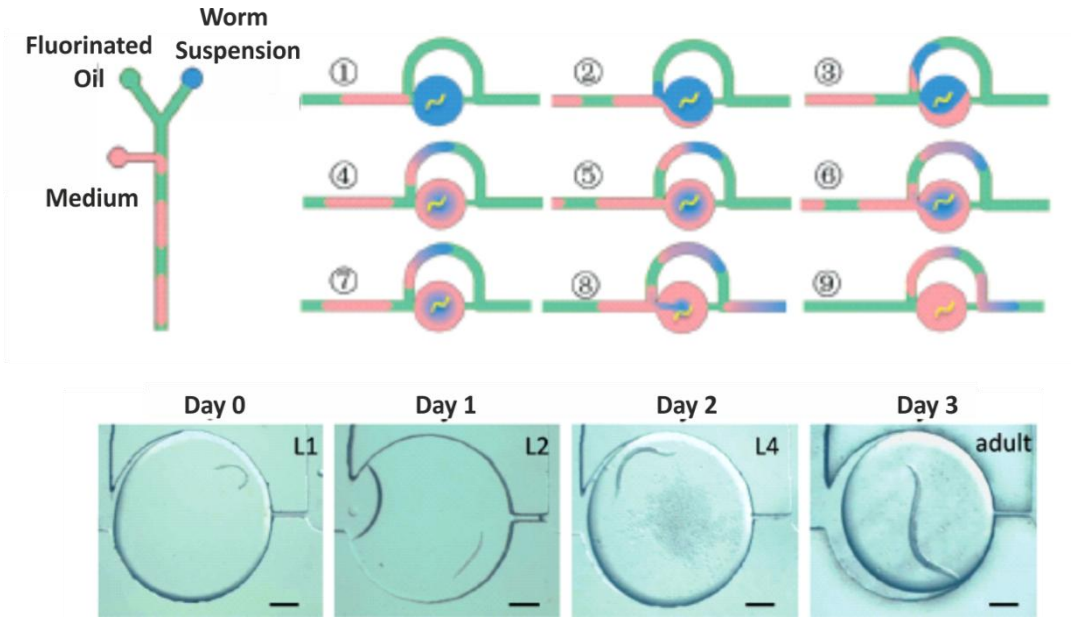

Figure 2.10: Droplet Coalescence for Medium Exchange of C. elegans. A schematic diagram of the microfluidic device with the junction for droplet formation shown on the left, and on the right the trap used for the trapping of droplets containing C. elegans and the coalescence of medium droplets for medium exchange until full exchange has occured. The bottom brightfield images show a timelapse of C. elegans culture over 3 days. The scale bar is 200 µm. The figure has been adapted from Wen et al.[85].

2.8 Droplet Microfluidic Applications for Spheroid Culture

In the past decade there has been an increased interest in the use of droplet microfluidics as a technology for the culture of 3D cell culture models. The main concept is that cells are encapsulated within droplets which are either aqueous or composed of alginate and/or a matrix, resulting in the aggregation of cells over time to form spheroids. The time taken for the formation of spheroids depends upon the properties of the droplets and the cell number per droplet. In comparison to traditional methods, droplet microfluidics offers several advantages such as the potential to be high throughput, the formation of uniform spheroid sizes and the use of low volumes of liquids and cell numbers[21], [28]. Another attractive feature is the concept of compartmentalisation, which is where each droplet acts as an environmentally isolated experiment[10]. In comparison to the spinner flask method cells are not exposed to the same shear stress which can have a negative impact on the physiology of cells and thus the spheroid cultured[62]. In contrast to the hanging drop method, droplet microfluidic based methods are more stable to mechanical shocks[70], [71]. By culturing spheroids

using this method it opens up the potential for high throughput *in vitro* screening, as well as the possible use of biopsy samples for the development of personalised medicine.

2.8.1 Alginate Beads and Microcapsules

A commonly used material for the encapsulation of cells within droplets is alginate. Alginate is a family of naturally occurring polysaccharides, extracted from seaweed, which are made up of two main types of monomer blocks of (1,4)-linked β- D-mannuronate (M) and α-L-guluronate (G) residues[97]. Alginate forms a hydrogel in the presence of divalent cations, such as calcium ions, which bind to the free carboxyl groups within the G unit monomers. For spheroid culture, alginate hydrogels offer several beneficial properties such as providing a scaffold, a suitable surface for cell to cell aggregation and creating cell to matrix contacts. Prior to the use of microfluidics, the technologies used for the formation of alginate beads and microcapsules suffered from an inability to control bead size, leading to their coagulation into large aggregates of beads[98]. The use of microfluidic devices for the formation and gelation of alginate beads was first shown in 2006 by Huang *et al.*[98]. The device simply involved a flow focusing junction geometry for the formation of alginate beads, which were then gelated off chip in a calcium chloride bath. The main advantages of using microfluidics was the ability to produce beads less than 100 μm in diameter and the formation of uniform sized beads. Furthermore, it opened up the opportunity of encapsulating cells within alginate beads. One of the first studies carried out to investigate the potential of droplet microfluidics for cancer spheroid culture was by Yu *et al.* in 2010, where they encapsulated LCC/Her2 breast cancer cells within alginate beads (Figure 2.11)[15]. Once the beads were formed in one device they were transferred to a calcium chloride ($CaCl_2$) bath to allow for the gelation of the beads. After the gelation step, the beads were transferred to a second device with traps to allow for storage and perfusion with medium. Spheroids were formed within four days, however the spheroids were only viable for a further two days after formation. Spheroids were treated with doxorubicin on day four for two days and viability staining confirmed a reduction in viability on day six. A more complicated alginate bead formation process was developed by Yoon *et al.*, where they incorporated magnetic nanoparticles within the alginate with HeLa cells to allow for the transfer of beads from the oil phase to medium (Figure 2.12)[16]. The rationale behind this design was that the magnetic transfer allowed for a simpler

method to remove beads from the toxic oleic acid. Spheroids were only cultured within beads off chip for up to five days and an experiment was carried out with Paclitaxel which showed a reduction in spheroid viability. A different method of forming hydrogels from alginate beads is through the incorporation of calcium carbonate ($CaCO_3$) particles, which are slowly release into the alginate upon lowering the pH of the solution with which the beads are in contact[17]. Lowering the pH results in the breakdown of $CaCO_3$ to release water, CO_2 and calcium ions. This process then promotes the gelation of alginate.

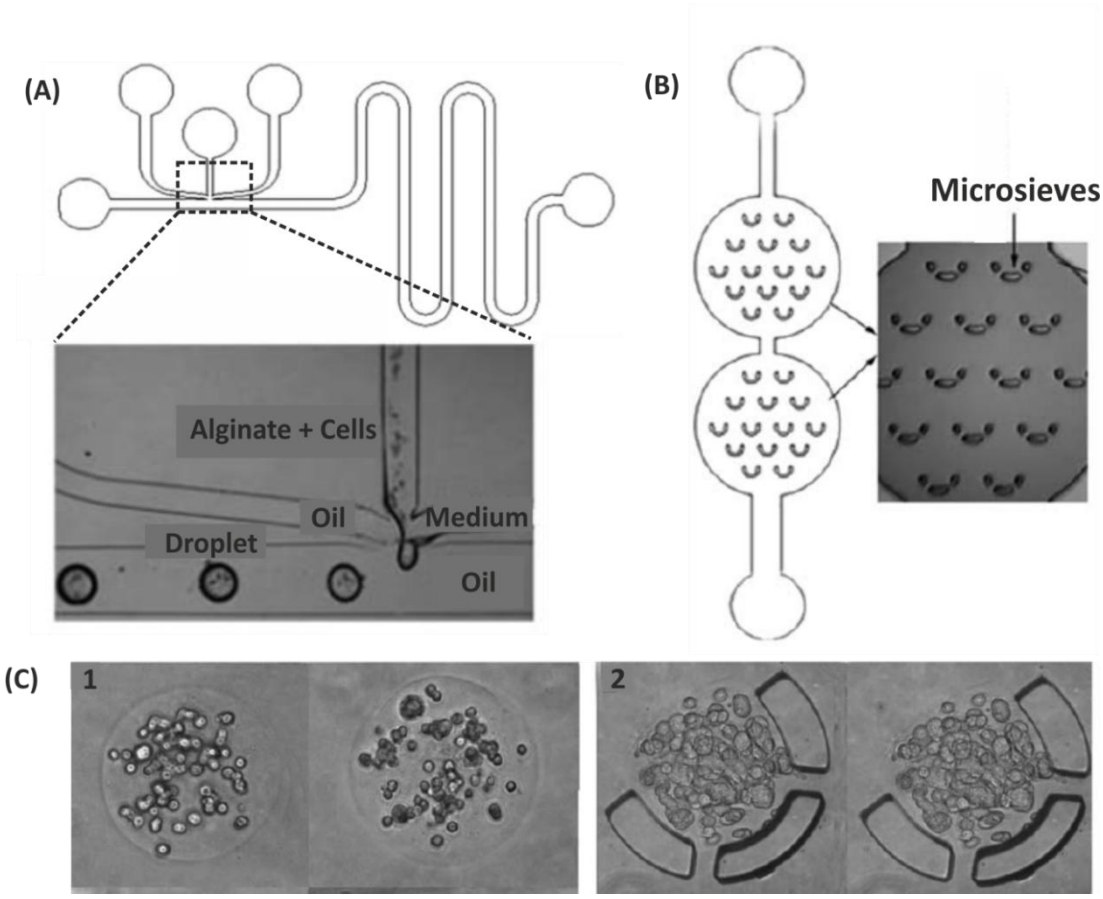

Figure 2.11: Formation and Culture of Spheroids within Alginate Beads using Two Devices. (A) Design of the droplet formation device with a brightfield image showing the formation of droplets containing alginate with cell. (B) Design of the culture device containing microsieves for the trapping of alginate droplets for the perfusion with calcium chloride solution and medium. (C) Brightfield images showing cells encapsulated within alginate droplets (1) and droplets with spheroids trapped within the microsieves on day 3 of culture (2). Figure has been amended from Yu et al.[22].

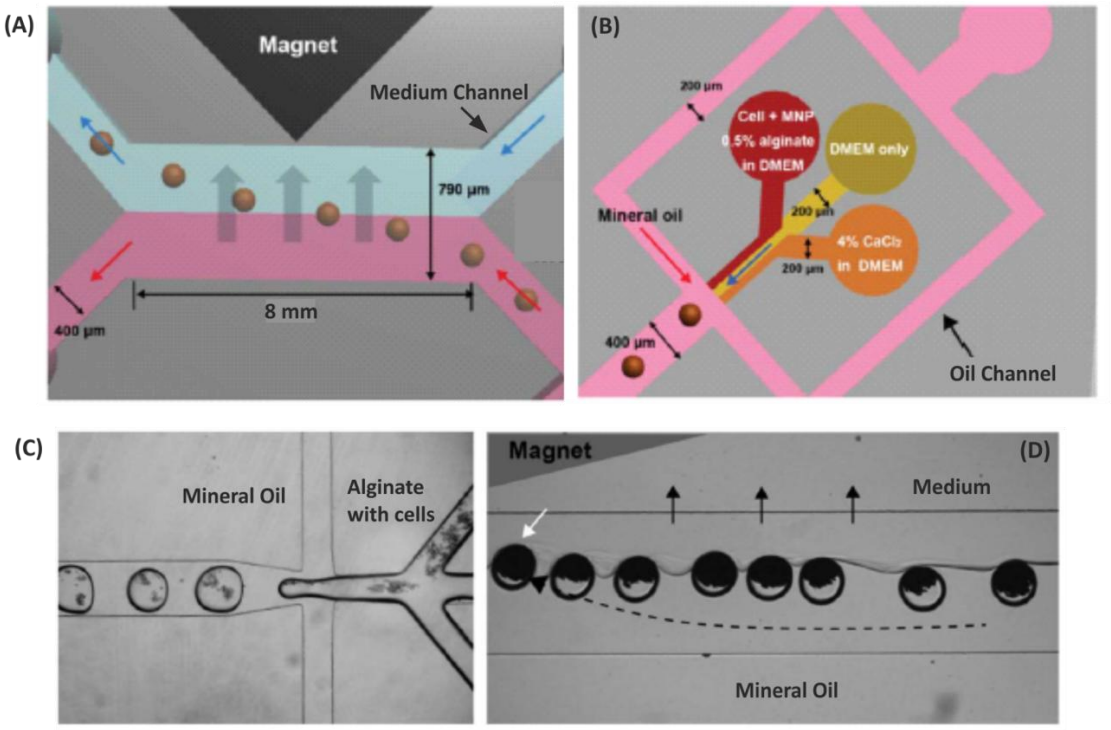

Figure 2.12: Formation of Alginate Beads and Transfer into Medium using Magnetic Nanoparticles. Schematic diagrams of the microfluidic device including the junction for the formation of alginate beads containing cells (B) and the main channel which the alginate beads are transferred to from the oil into the medium due to the presence of a magnetic field to move the beads containing magnetic nanoparticles (A). Brightfield images showing alginate bead with cells formation (C) and transfer of the beads into the medium from the mineral oil (D). Figure has been adapted by Yoon et al.[16]

Studies have also investigated the use of alginate microcapsules for the formation and culture of spheroids. One of the first studies involving the use of microcapsules was by Kim *et al.* (2011), where they compared the formation of embryonic carcinoma cell spheroids using this method with alginate microbeads[18]. The microcapsules were formed using multiple flow focusing junctions (Figure 2.13) with the first junction containing cells with medium in the middle channel and alginate in the two outer channels to create alginate on the outside and medium in the centre. The second junction then created microcapsules with a medium core by splitting the long capsule with oleic acid containing $CaCl_2$ in order to cause gelation of the alginate shell. In comparison to the formation of spheroids in microbeads, the spheroids formed were more compact and smooth in the microcapsules. As well as demonstrating the ability to grow size controlled spheroids, Nassoy *et al.* (2013) have shown that microcapsules

could be used to measure the pressure exerted by a spheroid (composed of mouse colon carcinoma cells) as it increased in size[19]. This was done to simulate the pressure exerted onto surrounding tissues by a growing tumour, a phenomenon which has been suggested to have a role in the regulation of growth. A drawback of their device was that it was only composed of a feature for the formation of the microcapsules. After the microcapsules were formed they had to be placed into a petri dish containing a calcium bath for the gelation of the microcapsules and then the encapsulated spheroids were cultured using standard culture conditions. The majority of studies which have formed and cultured spheroids within alginate beads or microcapsules have required the use of two or more devices. Only recently (2015) a study was carried out with one device for the formation and culture of spheroids within alginate beads[21]. The device used was based on the "dropspot" design by Schmitz *et al.* (Figure 2.8A), which allowed for the trapping of the alginate beads containing breast cancer cells (MCF-7) for spheroid formation and long term storage for culturing[88]. Once the beads were trapped they could be perfused with a $CaCl_2$ solution to allow for gelation of the beads and then refreshment of the spheroids with medium. However, in this study, the spheroids were only cultured within the device for up to four days, with drug treatment carried out on day two of spheroid culture (with day one being the day of spheroid formation).

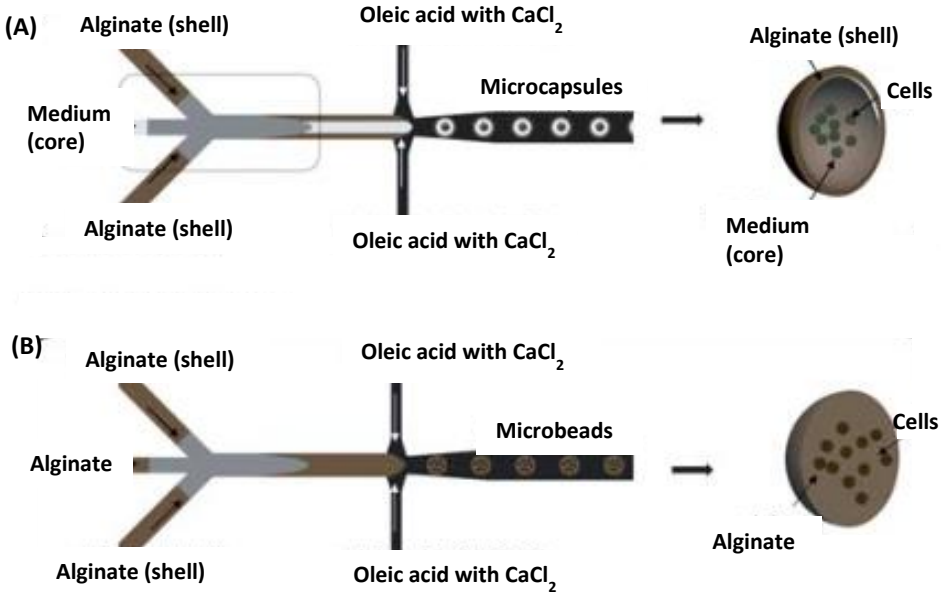

Figure 2.13: Formation of Alginate Beads and Microcapsules. Schematic diagrams showing the geometry of the microfluidic flow focusing junction and how it is used for the formation of microcapsules (A) and microbeads (B). The figure has been adapted from Kim et al.[18]

2.8.2 Alginate and Matrigel Beads and Microcapsules

Cells have also been encapsulated in beads or microcapsules composed of a mixture of alginate and Matrigel in order to provide a better imitation of a tumour microenvironment. In one study by Wang *et al.* they compared the formation and culture of HeLa cell spheroids within alginate beads and alginate with Matrigel beads[20]. It was found that those formed within the alginate with Matrigel mixture formed the most compact spheroids (Figure 2.14). A similar result was shown in a study by Yu *et al.* Breast cancer spheroids were formed within microcapsules with an alginate shell and a core made up of a combination of Matrigel, alginate and collagen I[99]. A comparison was carried out with spheroids formed with a core composed of only alginate and a combination of alginate and collagen I. The geometry of the device used to form the microcapsules is shown in Figure 2.15. The alginate contained $CaCO_3$ particles that will diffuse into the alginate upon contact of the acidic mineral oil with acetic acid and cause gelation. To make sure that the Matrigel did not gelate within the

tubing it had to be kept at a temperature below 22°C. This was achieved by storing the Matrigel mixture within an ice bath and cooling the tubing with ice cold water. Overall, it was observed that cells encapsulated within a core with a mixture of Matrigel, collagen I and alginate produced spheroids which were the most compact, with a core of only alginate creating the least compact spheroids. In this study they only had a device for the formation of the microcapsules, with culturing taking place off chip in tissue culture flasks. An advantage of using microfluidics to form and culture spheroids within Matrigel is that only small quantities are required which reduces costs. However, a major drawback with forming microcapsules or beads composed of a mixture of alginate and Matrigel is the complexity in the gelation process.

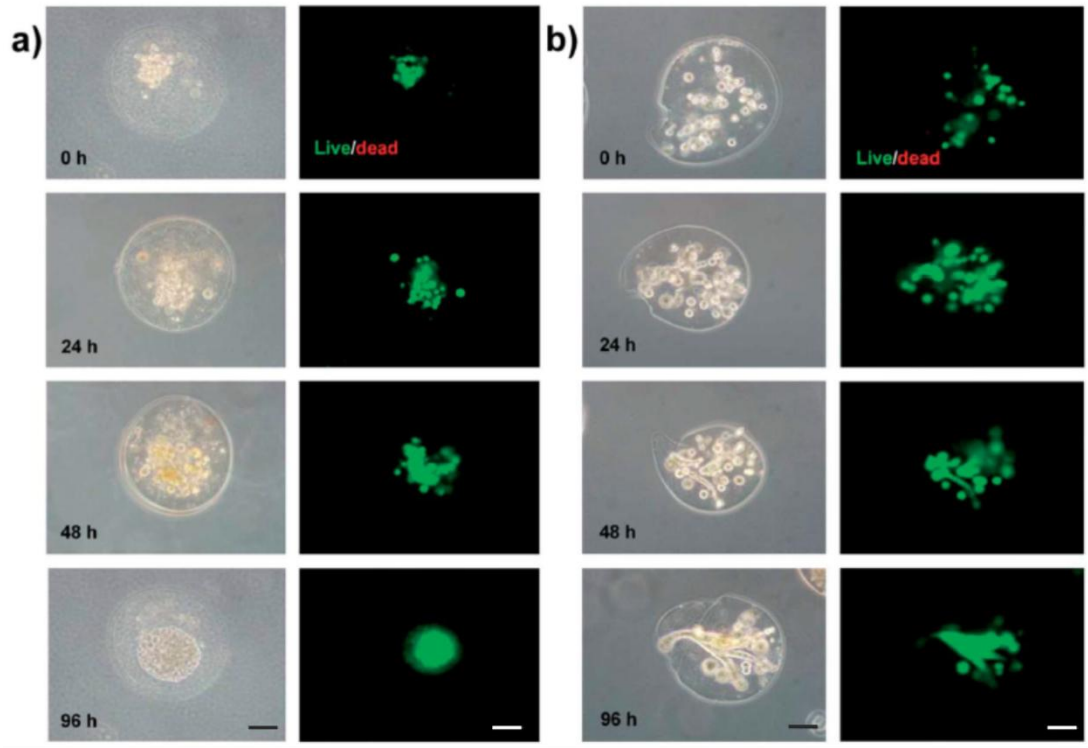

Figure 2.14: Comparison of Spheroid Formation and Culture within Alginate only and Alginate with Matrigel Beads. Brightfield and fluorescent images of spheroids cultured over 96 hours within alginate mixed with Matrigel beads (A) and alginate only beads (B). The scale bar is 75 µm. The figure has been adapted from Wang et al.[20].

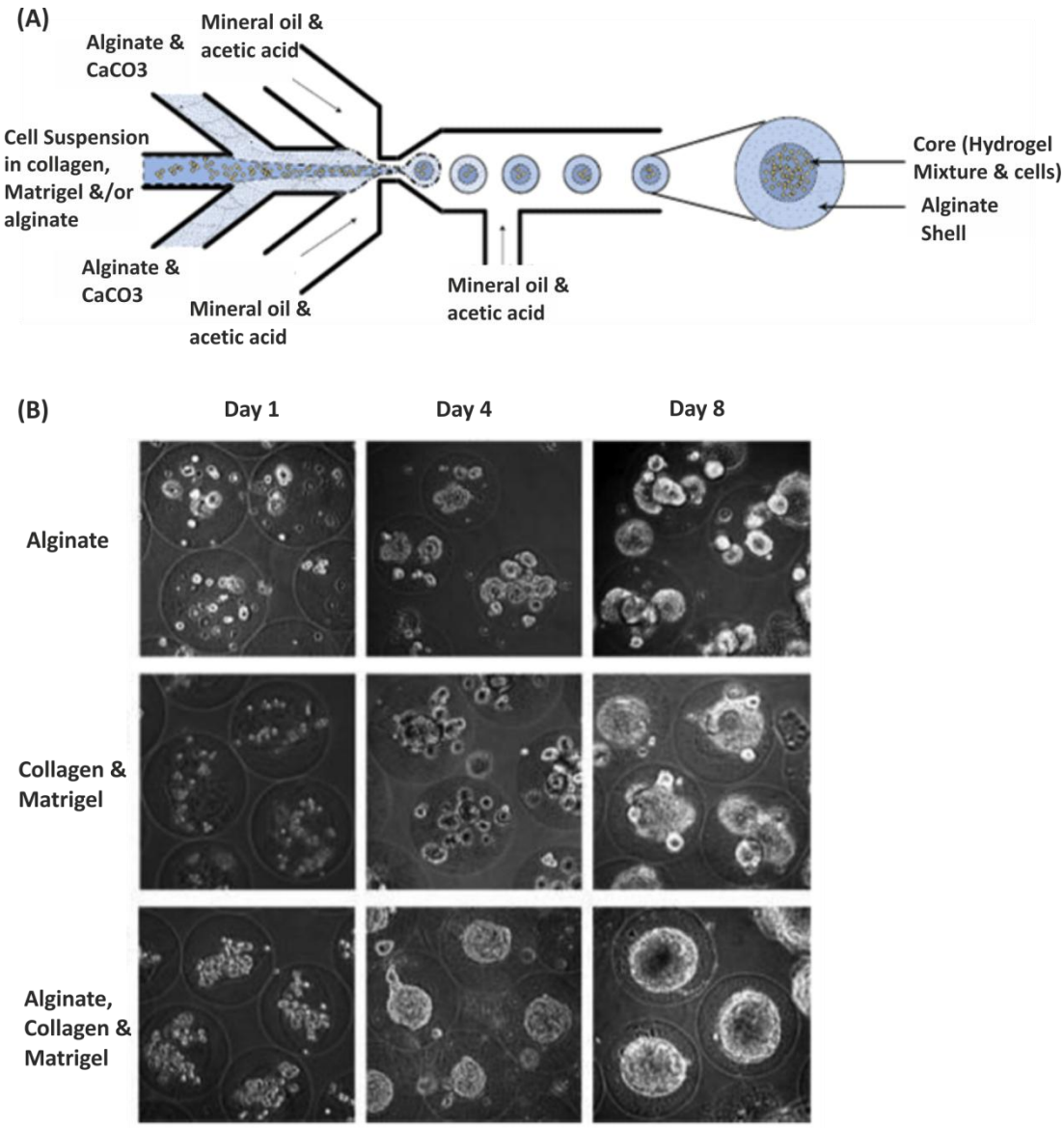

Figure 2.15: Alginate Microcapsules with a Core of Matrigel, Alginate and Collagen for Spheroid Culture. (A) A diagram showing the design of the flow focusing junction used by Yu et al.[99] *for the formation of microcapsules. The shell contains alginate and calcium carbonate ($CaCO_3$) particles for the gelation of the alginate shell upon contact with the oil with acetic acid and the core contains cells with Matrigel, collagen and alginate. (B) Brightfield images of spheroids on days one, four and eight formed within microcapsules containing a core of alginate only; collagen and Matrigel or alginate, Matrigel and collagen. The figure has been adapted from Yu et al.*[99].

2.8.3 Aqueous Droplets

Cells can also be encapsulated within droplets which do not contain a hydrogel or matrix and only medium. The majority of studies involving the encapsulation of cells within aqueous droplets have involved the analysis of single cells or organisms. One of the only studies which identified the potential of forming spheroids in aqueous droplets was by Chan *et al.* in 2013[23]. In this study the authors formed double emulsion droplets using a continuous phase of fluorinated oil with a PEG-PFEF surfactant. It was observed in previous studies that the polyethylglycol (PEG) head group produced a non-adherent surface for cells[100]. Due to the non-adherent interface, the cells preferably aggregated together to form MCSs within 150 minutes. This was a significant improvement upon existing formation techniques within alginates or matrices, which can take from 1 to 4 days[16], [70], [101]. They found that several types of cells could form spheroids within the double emulsion droplets, which were human mesenchymal stem cells (hMSC), human liver cancer cells (HepG2), primary mouse embryonic fibroblast (PMEF) cells and human colon epithelial cancer (CaCO-2) cells. The droplet formation process required the use of two devices; one for the formation of single emulsion droplets and a second to form double emulsion droplets. The double emulsion droplets were then cultured off chip using standard cell culture flasks. Double emulsion droplets were used within this study in order to create a controlled environment for spheroids, with the outer layer containing medium and the nutrients being able to diffuse across the oil interface into the droplet containing a spheroid[102]. However, spheroid culture was only supported in this device for a maximum of four days, which they attributed to the fact that large molecules such as growth factors were unable to diffuse through the droplet interface.

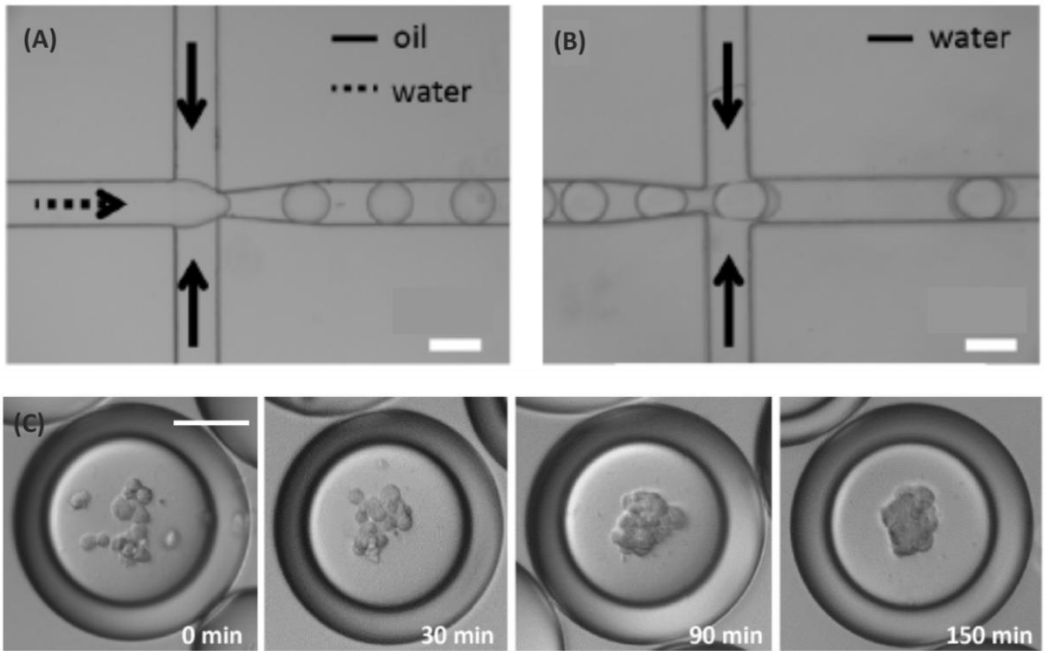

Figure 2.16: Spheroid formation within Double Emulsion Droplets. (A) Brightfield images of the first device used for single emulsion droplet formation and (B) the second device used for the formation of double emulsion droplets. (C) A timelapse sequence of brightfield images showing the formation of spheroids within double emulsion droplets over time. The scale bars equal 100 μm for all images. Figure has been amended from figures from the paper by Chan et al.[23]

2.8.4. Current Limitations with Droplet Microfluidics for Spheroid Culture

While it has been shown that droplet microfluidics can be used for the formation, culture and drug testing of spheroids, there are several issues which can be improved upon as summarised in table 2.1. One of these issues is the duration of time which spheroids can be cultured for. Studies involving the encapsulation of cells within droplets have been limited to a maximum of fourteen days[16], [18], [20], [22], [23] with cell viability reduced over hours or days[12], [24], [103]. The ideal duration of time to conduct a cancer drug screening assay so that it would reflect *in vivo* studies would be up to four weeks to determine if the drug has a cytotoxic or cytostatic effect[104], [105]. Therefore investigations need to be carried out on the conditions required for spheroid culture within droplets in order to design better microfluidic devices.

Another drawback with alginate and matrix based methods is the complicated gelation process involved in the formation of beads or microcapsules. In the case of alginates, ionic gelation has to take place for them to form hydrogels. For Matrigel it needs to be kept at a low temperature so that it does not gel before entering the device. Additionally, the majority of studies have involved the use of more than one device for droplet formation, gelation and/or droplet storage. In some cases the culture of alginate beads and microcapsules has taken place off-chip using standard tissue culture plates.

For aqueous droplets, the only method that has been used for spheroid culture involves the formation of double emulsion droplets that requires the use of two devices, thus complicating the formation process[23]. Another issue for aqueous droplets for spheroid culture is that, currently, it is not possible to use a device which allows for substance exchange, thus limiting the ability for long term culture, drug screening and/or the use of live/dead stains[28].

Table 2.1: Current Droplet Microfluidic Methods for Spheroid Formation and Culture. Table showing a summary of the strengths and limitations of different droplet microfluidics methods used for the formation and culture of spheroids along with references for each method.

Type of Method	**Strengths**	**Limitations**	**References**
Alginate Beads	- Alginate is porous so allows for medium refreshment and drug treatment	- Limited spheroid culture duration up to 10 days - Spheroids formed are not compact - Gelation procedure can be complex - Usually involve use of 2 or more microfluidic devices or a device and standard spheroid culturing plates	15,16, 17,21
Alginate Microcapsules	- Alginate is porous so allows for medium refreshment and drug treatment - Compact spheroids can be formed - Can be used as a method to measure the pressure exerted by growing spheroids	- Microcapsules are complicated to form - Involve use of a device and standard cell culturing plates - Spheroid culture limited to 4 to 14 days	18,19, 101
Alginate and ECM (e.g. Matrigel) Beads	- Formation of compact spheroids - Only requires small quantities of ECM	- Complex gelation process with alginate and ECM - Spheroids only cultured for 4 days	20
Alginate and ECM Microcapsules	- Formation of compact spheroids - Only requires small quantities of ECM	- Microcapsules are complicated to form - Complex gelation process with alginate and ECM - Spheroid culture only lasts for 11 days	99

Double Emulsion Aqueous Droplets	- Cells aggregate quickly to form spheroids - Allows for cells to form spheroids which are unable to in alginate	- Use of 2 devices and cell culturing plates - Spheroid viability reduced over time – maximum of 4 days culture	23

Therefore, there are still improvements which need to be implemented in order for droplet microfluidics to be considered as a suitable method for spheroid culture. If these issues are addressed, then droplet microfluidics opens up the potential of a high throughput *in vitro* anticancer treatment screening method. Additionally, the low cell numbers required would allow the use of biopsy samples in future studies, which would increase the potential of this approach in the development of personalised medicine.

2.9. Objectives

From this analysis, it is clear that the development of a droplet microfluidic based assay for the formation and long term culture of MCTSs would prove to be of major benefit in the *in vitro* screening of anticancer treatments.

To achieve this, several main objectives were identified for this work. Firstly, the characterisation of a medium in oil system for the formation and long term culture of spheroids will be conducted to determine the culturing conditions required in aqueous droplets. Secondly, I will discuss the development and associated challenges involved in testing a droplet microfluidic device suitable for spheroid formation and culture. From this device development process a decision will be made as to whether droplet microfluidics can be used alone or bridged with single phase microfluidics for long term culture and treatment of spheroids. As a result of the previous objectives, a microfluidic device will be evaluated for its suitability in conducting long term spheroid culture and anticancer treatment.

3. Materials and Methods

3.1 Materials

3.1.1 Equipment

Equipment	Supplier
Microscope: Axiovert A1	Zeiss
CMOS Genie HM1024 camera	Teledyne Dalsa
Microscope: Axioimager	Zeiss
AxioCam Mrm camera	Zeiss
GXCam-3 camera	GT Vision Ltd, UK
Millex syringe-driven filter unit (0.22 μm)	Millipore, UK
Glass slides	Fisher Scientific, UK
Stylus profiler	Alpha-Step IQ, KLA-Tencor Corporation, CA
Oxygen plasma asher	Pico A, Diener Electronic, Germany
Plastic syringes	Fisher Scientific, UK
Glass syringes	Hamilton Company, USA
Haemocytometer	Fisher Scientific, UK
96 well ultra-low attachment plate	VWR, UK
Syringe pump: Aladdin 1000	World Precision Instruments, UK
PTFE tubing	Cole Palmer
Capillary silica tubing	Composite Metal Services
Onstage incubator	Tokai Hit, Japan

Microtome (Leica RM2125RTE)	Leica Biosystems, UK
Acetate photomask	JD Photo-Tools, UK
Biopsy punches	Stiefel, SmithKleine Beecham Ltd, UK
PXI X-Rad 225C X-irradiator	RPS Services, Surrey, UK
UNIDOS® E universal dosimeter with a CC04 ionisation chamber	PTW, Germany

3.1.2 Chemicals

Chemical	Supplier
Acetone	Fisher Scientific, UK
Methanol	Fisher Scientific, UK
Isopropanol	Fisher Scientific, UK
Ethanol	Fisher Scientific, UK
Clearing agent (Histoclear)	National Diagnostics
Hydrochloric acid	Sigma Aldrich, UK
Haematoxylin	Thermo Scientific, UK
Eosin	Thermo Scientific, UK
Magnesium sulphate	Sigma Aldrich, UK
Sodium bicarbonate	Sigma Aldrich, UK
Fluorescein diacetate	Sigma Aldrich, UK
Propidium iodide	Sigma Aldrich, UK
Cis-diammineplatinum (II) dichloride (cisplatin)	Sigma Aldrich, UK
Doxorubicin	Sigma Aldrich, UK
Sodium chloride	Sigma Aldrich, UK
SU8 3035 photoresist	MicroChem, Newton, MA

MicroPosit EC solvent	MicroChem, Newton, MA
1H, 1H, 2H, 2H-perfluorooctyl-trichlorosilane	Sigma Aldrich, UK
Aquapel	PGG Industries Inc, Pittsburgh
Foetal bovine serum	Life Technologies, UK
L-glutamine	Life Technologies, UK
Minimum essential medium	Life Technologies, UK
Penicillin/streptomycin	Life Technologies, UK
Fungizone (Amphotercin)	Life Technologies, UK
Phosphate buffered saline tablets	Fisher Scientific, UK
Trypsin-EDTA	Life Technologies, UK
Fluorinated oil (FC-40)	Sigma Aldrich, UK
Block copolymer fluorosurfactants	designed by the Weitz Group at Harvard and supplied by RAN Biotechnologies, catalogue# 008-FluoroSurfactant, Beverly, MA, USA
Calcein	Sigma Aldrich, UK
Alginic acid sodium salt from brown algae (sodium alginate)	Sigma Aldrich, UK
Calcium chloride	Sigma Aldrich, UK
Mounting media (Histomount)	National Diagnostics

3.2 Device Fabrication

The microfluidic devices used for experiments were fabricated using standard photolithography and soft-lithography techniques, as shown in figure 2.2.

3.2.1 Design of Photomasks

Microfluidic devices were designed using CorelDRAW X5 and acetate photomasks were printed by JD photo tools, UK. The exact measurements of the x and y axes of the features of the design were determined by the mask, while the depth was created through the thickness of the photoresist. An example of a photomask design is shown in figure 3.1.

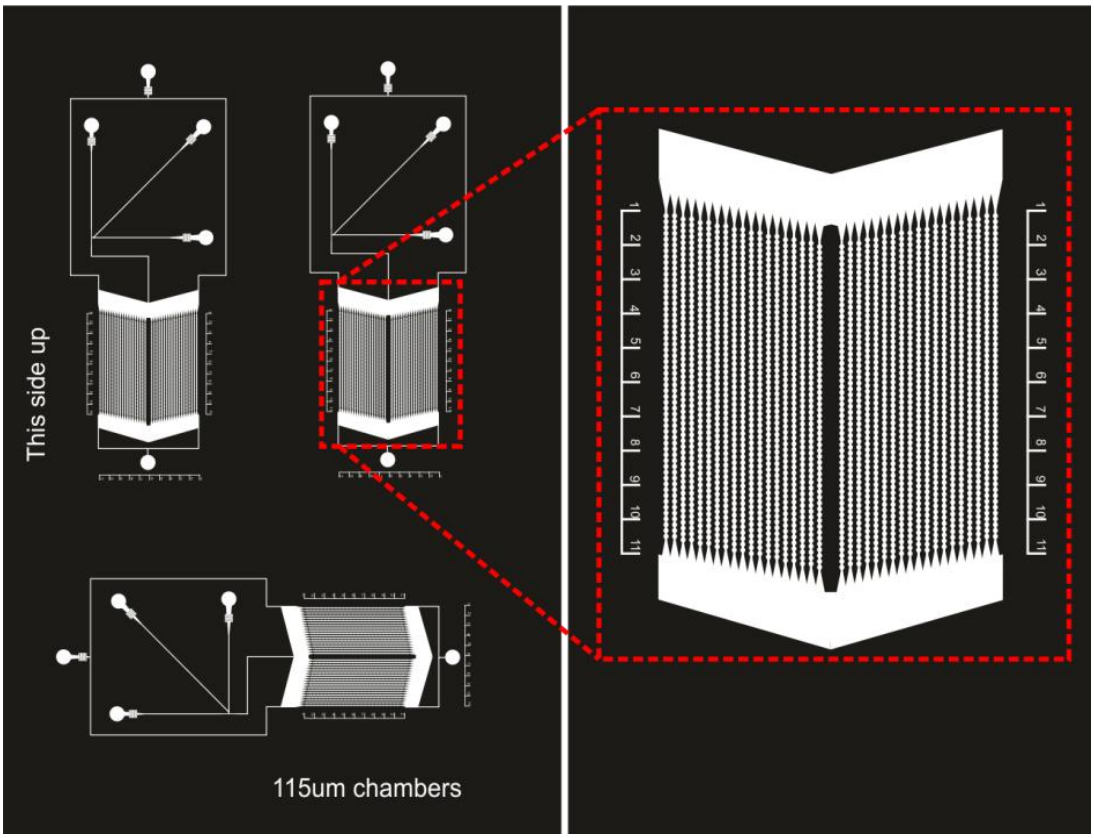

Figure 3.1: Example of a Microfluidic Photomask created using CorelDRAW. A photomask with microfluidic patterns in white over black background with a magnified section of the mask showing the details of a droplet chamber array.

3.2.2 Fabrication of a Microfluidic Master using Photolithography

Microfluidic masters were made via photolithography (steps 1 to 4 in figure 3.2)[106], [107]. First, a silicon wafer as cleaned with acetone, methanol and isopropanol to remove particles and then dried with nitrogen gas. Next the wafer was dehydrated on a hot plate at 180^{o}C for at least one hour to evaporate solvents which remained and remove moisture, then left to cool to room temperature. SU8 3035 photoresist (MicroChem, Newton, MA) was spin coated on a silicon wafer to produce an even coating layer, with the spin rate selected to obtain the desired thickness of SU8 and according to manufacturer data sheet. For wafers which had a photoresist layer of 100 µm or more the wafer was left to relax for approximately 15 minutes. Next, the wafer was soft baked on a hot plate to produce an even thickness of SU8 at a maximum of 95^{o}C with the time dependent on the thickness of the SU8 layer required and then left to cool to room temperature. For wafers with a 100 µm thickness or more the wafer was left to relax after cooling to room temperature. An acetate photomask was then placed on top of the wafer and exposed to UV light (150 – 250 mJ/cm^{2}) for 40 to 135 seconds (exact timing was dependent on the thickness of SU8). After exposure the wafer was placed on a hot plate at 85^{o}C – 99^{o}C and allowed to cool to room temperature before immersing the wafer in MicroPosit EC solvent (MicroChem, Newton, MA). After development, the wafer was washed with isopropanol to check if all the features on the wafer had fully developed. The appearance of a milky colour within the isopropanol whilst washing the wafer would indicate that the resist had not fully developed. In this situation, the wafer was placed back into the developer for an extra 5 to 10 minutes before checking with isopropanol again. After washing with isopropanol the wafer was dried with nitrogen and then hard baked on a hot plate at an initial temperature of 95^{o}C which increased in increments to a maximum temperature of 210^{o}C over approximately 30 mins. For designs which required a feature thickness of approximately 200 µm, two layers of 100 µm of SU8 3035 photoresist had to be spun. This was carried out using the same method previously described, with the exception that, after the soft bake had been carried out for the first layer. Once the soft bake had been carried out for the first layer, the wafer was left to cool to room temperature before spin coating the second layer of photoresist onto the wafer. The protocol was then the same as before after the soft baking step. Table 3.1 shows the spin rates, baking times and exposure times used for different photoresist thicknesses. The table

also shows variations in the soft baking step, e.g. the use of a single hot plate, or two hotplates with one set at 65°C and another at 95°C. To determine the exact thickness of the features on the final wafer a stylus profiler was used (Alpha-Step IQ).

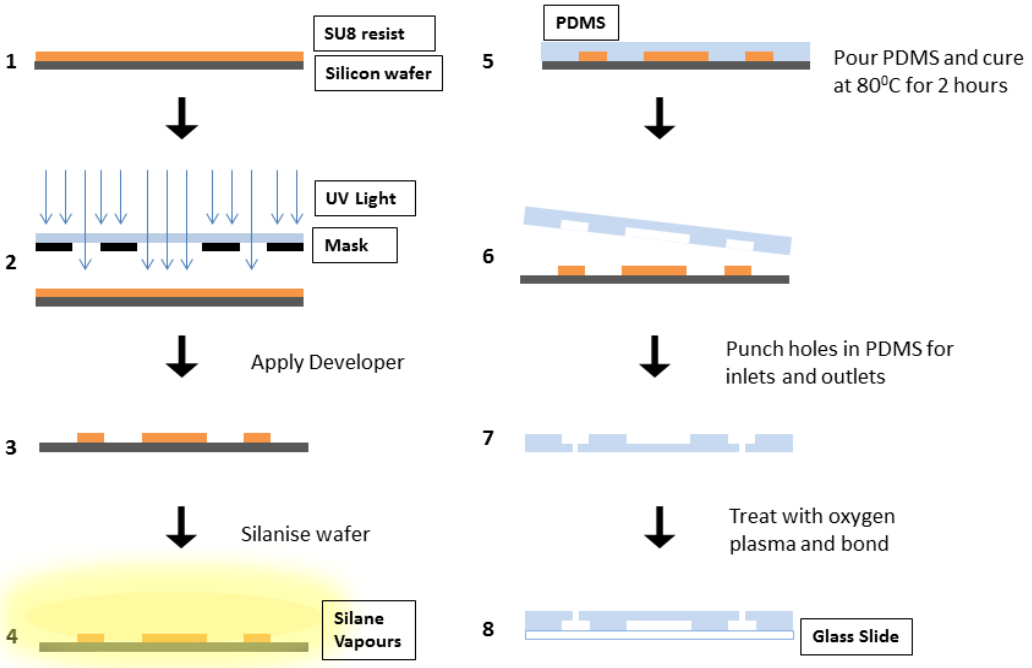

Figure 3.2: Schematic Diagram of Device Fabrication. Steps 1 to 4 show the photolithography process of achieving a patterned wafer and steps 5 to 8 show the soft lithography process carried out to achieve a microfluidic device. The full process is described in more detail in section 3.1 of the material and methods.

Table 3.1: Photolithography Protocols for Different SU8 3035 Thicknesses. Table showing the different spin rates (rpm); soft baking times (min); UV exposure times (sec); post-exposure baking times (min); development times (min) and hard baking times used to create SU8 thicknesses of 40 µm, 100 µm and 180 µm.

SU8 3035 Thickness (µm)	**Spin Rate (rpm)**	**Soft Baking**	**Exposure (sec)**	**Post-Exposure Baking**	**Development (min)**
40	2000	Heated from 80°C to 95°C for 15 mins	40	65°C for 1 min and 95°C for 3 mins	6
100	900 - 1000	One hot plate: heated from 80°C to 95°C for 25 mins Two hot plates: 65°C for 7 mins and 95°C for 27 mins	85	65°C for 1 min and 95°C for 5 mins	15 - 20
170 – 180 (Aiming for 200)	2 layers of 100µm	Same as for 100µm thickness but soft bake is carried out after each layer is spun	120 - 135	65°C for 1 min and 95°C for 5 mins	30 - 35

3.2.3 Silanisation of Master

In order to prevent adhesion of PDMS to the master, the wafer was silanised (Figure 3.2 step 4). Prior to silanisation the master was exposed to oxygen plasma for 2 minutes. The master was salinized in a vacuum by adding 50 µl of 1H, 1H, 2H, 2H-perfluorooctyl-trichlorosilane (Sigma Aldrich, UK) to a weighing boat which was placed on the bottom of a dessicator, with the wafer raised above and left for 55 minutes.

3.2.4 Soft Lithography

The master was placed in a glass petri dish coated with tin foil to act as a mould for the PDMS. PDMS (Dow Corning Sylgard 184) was mixed with curing agent at a 10:1 ratio and then poured onto the master. The master was then degassed in a dessicator to remove air bubbles from the PDMS before placing it in the oven to cure at 70°C - 80°C for a minimum of 2 hours. The cured PDMS was then cut out of the master using a scalpel and the slab was divided into individual device sections. For microfluidic devices to be used with syringe pumps, holes were punched using a sharp, tapered 22G needle to create inlet and outlet ports. For open well PDMS devices, the wells were created by punching a piece of approximately 7 mm thick PDMS with 8 mm biopsy punches to create approximately 20 wells.

3.2.5 Bonding of PDMS to Glass Slides

Prior to bonding the PDMS devices to glass slides (size dependent on device design), surfaces were cleaned in a sonic bath (with acetone, methanol and isopropanol for the glass slides and only methanol for the PDMS). The wafer was then dried with nitrogen gas and dehydrated at 70°C - 80 °C for 1 hour.

An alternative cleaning method, which was used at a later stage of this study, involved the use of Scotch tape[108]. In this method, tape was applied firmly to the surface of the PDMS or glass slide and then removed, in order to remove any dust or particles from the surface. This process was repeated until the surfaces remained clean.

Bonding of microfluidic devices was carried out by treatment of PDMS and glass slides within an oxygen plasma chamber (Pico A, Diener Electronic, Germany). Exposure of PDMS to oxygen plasma creates a change to the repeating $–O\text{-}Si(CH_3)_2\text{-}$ resulting in the replacement of methyl groups with polar silanol (SiOH) groups[79]. When the treated PDMS comes in contact with glass it forms irreversible covalent Si-O-Si bonds. After exposure to oxygen plasma the PDMS was placed onto the glass slides and were pressed to ensure no air was visible within the two layers.

After bonding, the devices were flushed with Aquapel (PPG Industries Inc., Pittsburgh) to create a hydrophobic surface coating within the channels so that to promote wetting

of the channel walls to fluorinated oil. An example of a microfluidic device is shown in figure 3.3.

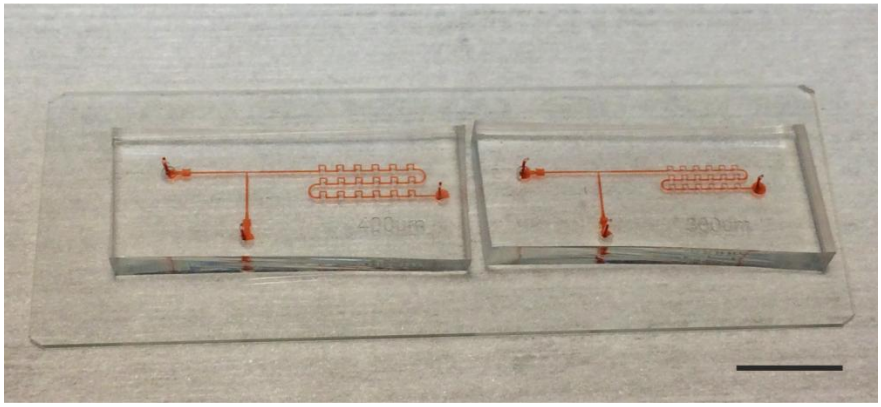

Figure 3.3. Example of a microfluidic device. A photograph of two microfluidic devices bound to a single glass slide with red dye flown through the microchannels. The scale bar is 10 mm.

For open well PDMS devices (figure 3.4), the bonding was carried out by spin coating PDMS on a glass slide (76 mm x 52 mm) at a rate of 1000 rpm to which the PDMS well layer is to be bonded. The two layers were then bound to each other and cured for 2 hours at 70°C – 80°C.

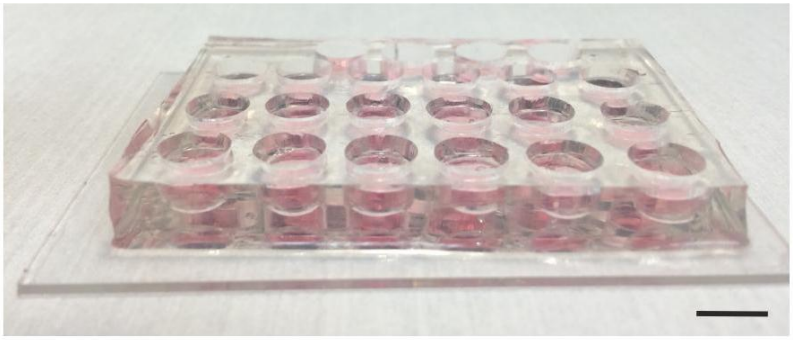

Figure 3.4. Open well Device. Photograph of a PDMS well device bound to a glass slide with each well containing a medium in oil (M/O) droplet. The scale bar is 8mm

3.3 Cell Culture

The human glioblastoma cell line (UVW) which was developed in house was used in this investigation[109]. UVW cells were maintained in medium composed of minimum essential medium (MEM), 10% (v/v) of foetal bovine serum (FBS), L-glutamine (200

mmol), penicillin/streptomycin (100 U/ml) and Fungizone (2 μg/ml) which was kept at an atmosphere of 5% CO_2 and incubated at 37°C. All of the medium and additional supplements were purchased from Invitrogen, Paisley, UK. After the incubation period the medium was removed from each of the flasks and cells was washed with 10 ml of phosphate buffered saline (PBS). 4ml of 0.05% trypsin-EDTA (Invitrogen) was added for 2 -3 minutes in order to detach the cells from the bottom of the flasks,. Once detached, the cells were suspended in fresh medium and the cell concentration was determined using a haemocytometer. The cells were then washed twice by centrifugation and the required cell concentration was obtained.

3.4 Spheroid Culture within Macrodroplets

To form spheroids within medium in oil (M/O) droplets in open-well devices, 60 μl of FC-40 (3M) fluorinated oil with 2% wt block copolymer fluorosurfactants (designed by the Weitz Group at Harvard and supplied by RAN Biotechnologies, catalogue# 008-FluoroSurfactant, Beverly, MA, USA) was added to each well. Subsequently, a cell suspension ranging from 40 to 10^4 cells/ml was manually pipetted into the wells in droplet volumes of 25-100 μl of medium depending on the experimental purpose. The exact volumes of droplets, cell concentrations used and frequency of medium refreshment used for different experiments are detailed within chapter 4.

3.5 Spheroid Culture within Spinner Flask and Non-adherent Plates

Spheroids were formed using a spinner flask method by seeding 1 x 10^6 cells into 75 ml of medium into a spinner flask (Sigma Aldrich) and then incubating, on a magnetic stirrer, at an atmosphere of 5% CO_2 at 37°C for 3 days. Spheroids were then manually selected and individually transferred into wells of a 96 well ultra-low attachment plate (VWR) using a Gilson pipette and incubated for up to 28 days. Each well contained a final volume of 200 μl medium, which was refreshed every 2 days.

3.6. Operation of Droplet Microfluidic Devices

Droplets were formed using devices with a T-junction geometry. The continuous phase which was used for all experiments was FC-40 (3M) fluorinated oil which contained 2% wt block copolymer fluorosurfactants to stabilise droplets. All liquids were loaded into either 1 ml (0.48 mm diameter) syringes or 250 μm (0.12 mm diameter) glass syringes

and were injected via PTFE tubing (0.255 mm diameter) by syringe pumps (Aladdin 1000, World Precision Instruments, Hertfordshire). An example of the experimental set up used for the operation of the microfluidic devices is shown in figure 3.5.

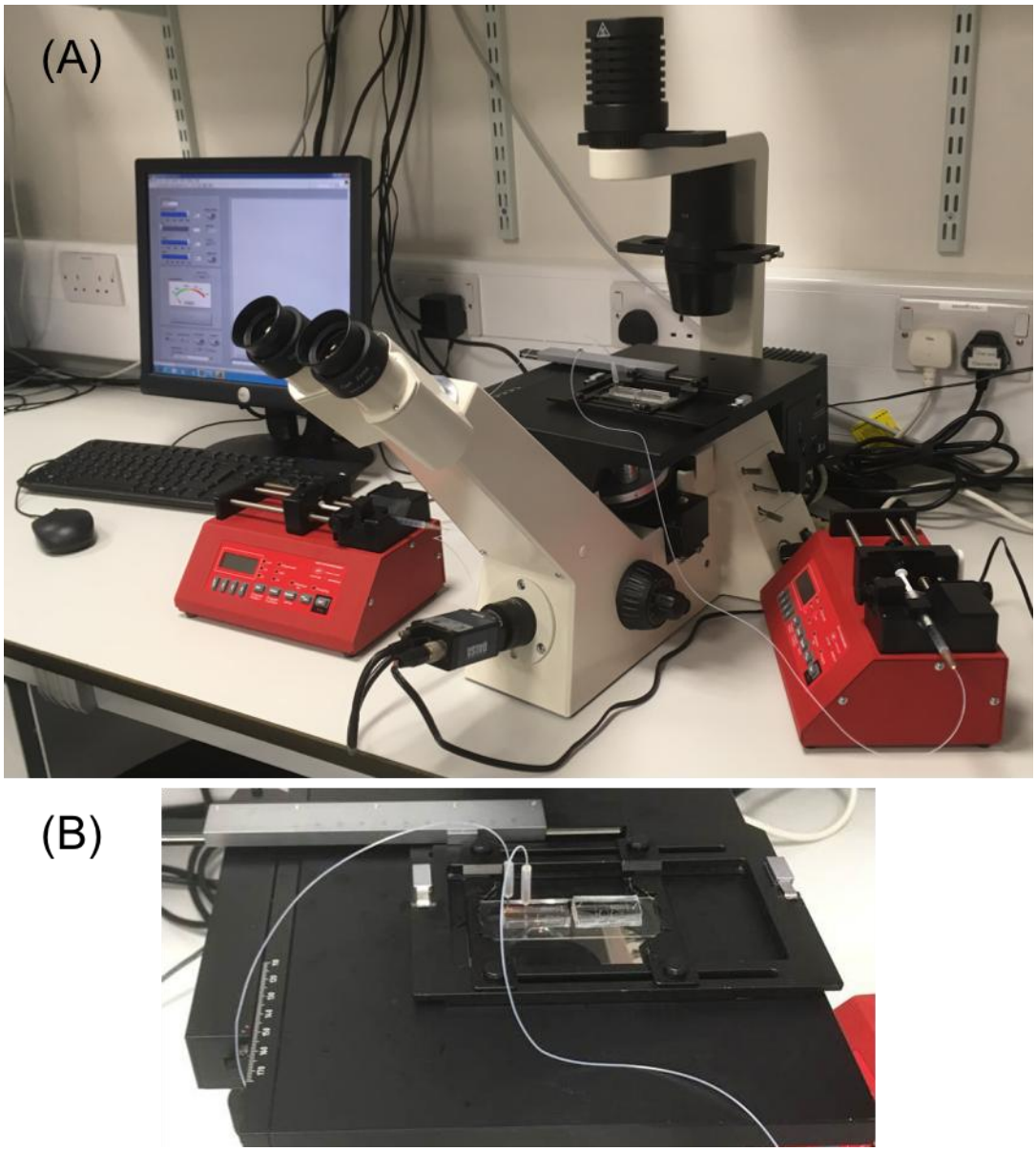

Figure 3.5: Example of an Experimental Set Up for Operation of a Droplet Microfluidic Device. Photographs of (A) a microfluidic device on a microscope connected to syringes which are driven by syringe pumps and (B) an image of the microfluidic device on the microscope stage with tubing connected to the inlets.

During the initial part of this study, capillary silica tubing (Composite Metal Services) was used to connect PTFE tubing to a device. To do this the capillary silica tubing (0.32 mm inner diameter, 0.435 mm outer diameter) was cut into sections using a scalpel and was connected to tubing connected to a syringe with water to wash out any debris. The sections were then inserted into the inlets and outlets of the device and sealed with silicone glue and left over night to dry. The PTFE tubing could then be connected to the capillary silica sections. However, during these investigations there were issues with the fragility of the silica tubing and upon connection of the PTFE tubing debris would enter the device resulting in blockage of channels. Therefore, an improved method was developed which involved the use of tapered 25 gauge needles as connections, which were inserted into Tygon tubing before connecting to the PTFE tubing. For the continuous phase and aqueous phase, inlets liquids were manually loaded into the syringes. Air bubbles were removed from syringes before connecting to the PTFE tubing. The liquids were pushed into the PTFE tubing to remove air before attaching to the device. For all microfluidic experiments the continuous phase was initially flown through the device to remove air from the device. Once the device was filled with the continuous phase, the aqueous phase would then be dispensed into the device and the flow rates would be changed depending upon the size of droplets required for the device. The exact designs and dimensions of the microfluidic devices and flow rates used are detailed within chapter 5.

3.6.1 Operation of Droplet Coalescence Device

Syringes were loaded and droplets were formed as discussed in the preceding section Once the droplets were trapped within the device the flow of the aqueous phase was stopped and the tubing was removed to remove the medium from the channel. The tubing was reconnected and the continuous phase flow remained on to remove droplets which were not trapped from the chamber array. After the initial loading the flow of the continuous phase was stopped and followed by the dispensing of an aqueous phase of water or medium to form a long droplet. For proof of principle experiments to visualise whether the long droplet coalesced with trapped droplets the aqueous phase contained 100 μM of calcein. Detailed information regarding the device design, flow rates and experiments involving cells to form spheroids for specific devices can be found within chapter 5.

3.6.2 Encapsulation of Cells within Droplets

In experiments involving the encapsulation of cells within droplets in microfluidic devices the same initial set up was used for the continuous phase and PTFE connections. For the aqueous phase including cells, initially only cell medium was withdrawn into a syringe and then connected to PTFE tubing with a needle connector with the medium dispensed to remove air. Next a cell suspension of 3-6 x 10^6 cells per ml (depending upon the required number of cells per droplet) was withdrawn into PTFE tubing using the withdrawal function of a syringe pump. Prior to withdrawing the cell suspension into the tubing it was disaggregated using a syringe and 21 G needle. Once the cells were withdrawn into the tubing, the cell suspension was dispensed into a microfluidic device. The flow rates of the syringe pumps varied due to trapped air and blockages caused by cells. Once devices contained a sufficient number of cell-containing droplets, the flow of the fluids was stopped and the connected tubing was slowly removed from the device. All devices containing droplets with cells were kept at an atmosphere of 5% CO_2 and incubated at 37^{o}C. For videos and images showing spheroid formation recorded overnight, the device was kept in an onstage incubator (Tokai Hit, Japan) and a Zen controlled Zeiss AxioCam Mrm camera was used to take time-lapse images (Figure 3.6). All devices placed in an incubator were stored in a petri dish containing PBS to maintain humidity. The exact flow rates used for the microfluidic devices varied depending upon the design and are specified in chapter 5.

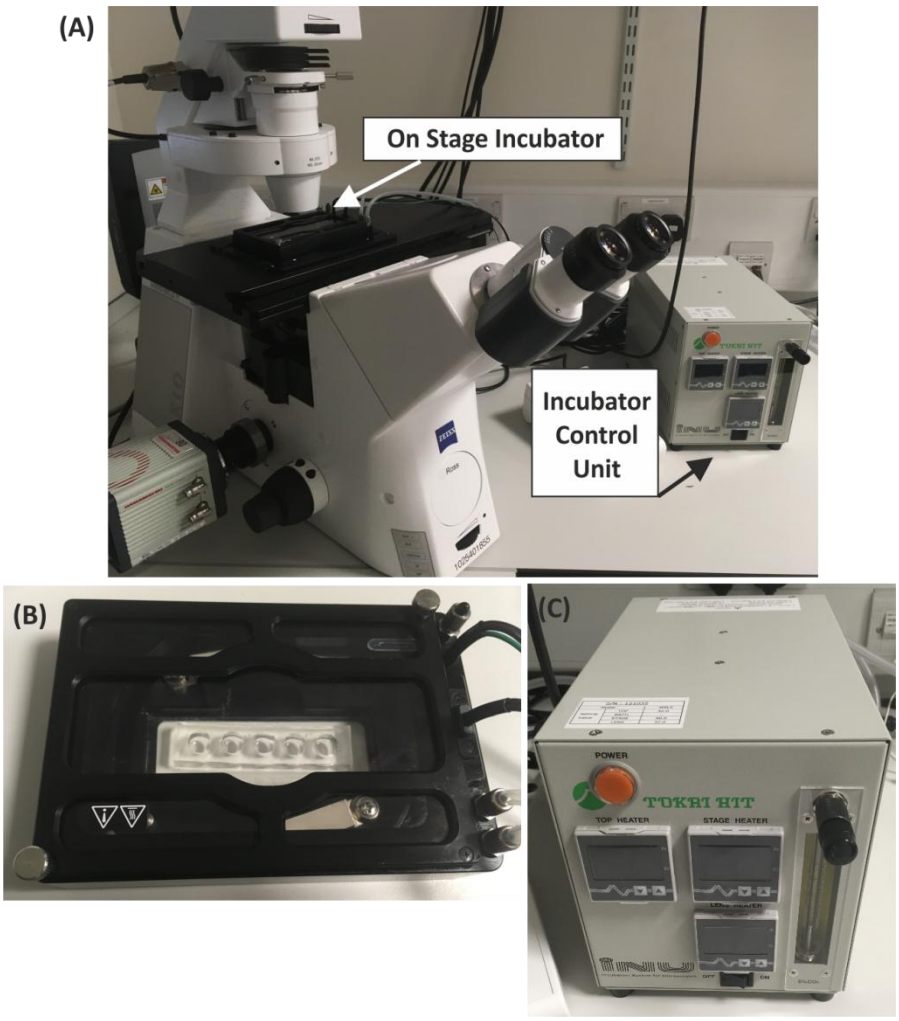

Figure 3.6: Example of an Experimental Set-up using an on-stage incubator. Photographs of (A) the on-stage incubator set up on the microscope, (B) the on-stage incubator with an example of a device inside and (C) the control unit for the on-stage incubator used to change the temperature and CO_2 settings.

3.6.3 Alginate Bead Formation

Alginic acid sodium salt from brown algae (sodium alginate, Sigma Aldrich, UK) was dissolved into medium at a concentration of 2% (w/v) and heated to 50°C for 2 hours before storing at 4°C prior to use. Before using for cell culture the sodium alginate solution was filtered through a 0.2 μm filter to remove any particulates. Cells were cultured and detached using the normal protocol and made up to a concentration of 3 x 10^6 cells/ml before resuspending in the sodium alginate mixture. Droplets were formed and stored using the same method as previously described for the droplet perfusion device (section 2.5.1). To carry out gelation of the alginate beads, a 4% (w/v) calcium

chloride (Sigma Aldrich, UK) in medium solution was filtered through a 0.2 μm filter to remove any particulates. The calcium chloride solution was perfused through the device in a similar way to the medium plug, to coalesce the droplets. Once the calcium chloride solution had been perfused through the device the spheroids were refreshed every 2 days with medium. The flow rates for droplet formation, calcium chloride perfusion and medium perfusion are specified in chapter 6.

3.7. Spheroid Sectioning and Staining

Spheroid sectioning and staining was only carried out using spheroids formed from spinner flasks, non-adherent plates and open well PDMS devices. Spheroids to be sectioned were retrieved from their devices and fixed in 10% formalin for a minimum of 12 hours. Once fixed, the spheroids were wrapped in biowrap paper (Leica Biosystems) and transferred into a biopsy casette for tissue processing. The spheroids were tissue-processed by dehydrating them in successive immersions of 50% (v/v) ethanol, 70% (v/v) ethanol, 90% (v/v) ethanol, 100% (v/v) ethanol, 50% (v/v) histoclear in ethanol, histoclear and then wax. The spheroids were then transferred from the paper into a casette and wax was then poured in and allowed to cool to form a wax block containing spheroids. Blocks containing spheroids were then sectioned using a microtome (Leica RM2125RTE) to form 4 μm thick sections which were mounted on polysine coated slides using a water bath and allowed to dry before being ready for staining.

Sections were stained with haematoxylin which stains for nuclei and eosin which stains for proteins in the cytoplasm. For staining, the sections were first de-waxed in histoclear (National Diagnostics) and re-hydrated by successive immersions in 100% (v/v) ethanol, 70% (v/v) ethanol and water. The staining procedure involved immersions in haematoxylin for 7 mins, 1% (v/v) acid alcohol, Scotts tap water and eosin with intermediate washes in water. The formula for the Scotts tap water was 10g of magnesium sulphate, 0.67g of sodium bicarbonate which was made up to 1 l with distilled water. The stained sections were then dehydrated in 70% (v/v) and 100% (v/v) ethanol and immersed in histoclear before applying mounting media (Histomount, National Diagnostics) and a coverslip. An example of a spheroid stained for haematoxylin and eosin is shown in figure 3.7.

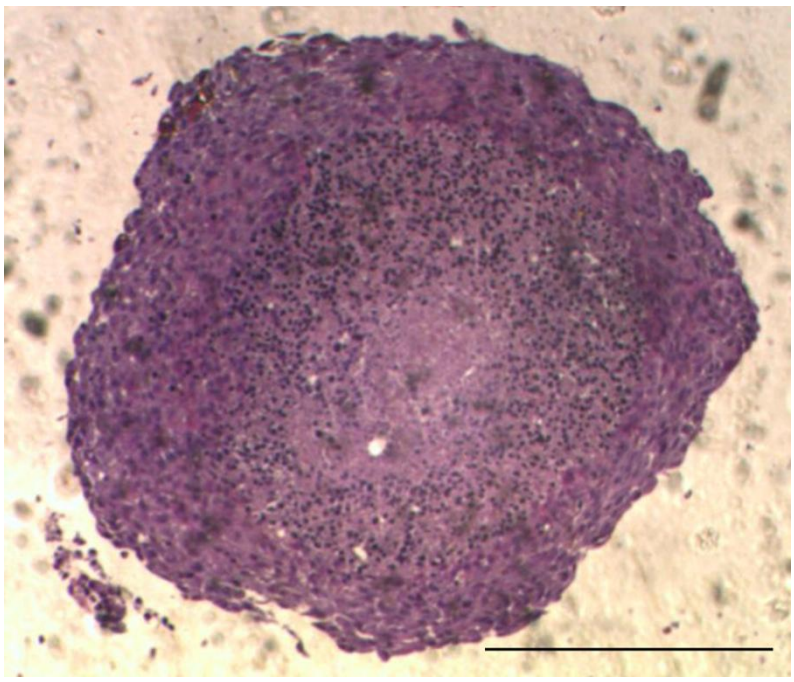

Figure 3.7: Haematoxylin and eosin stain. An example of a section taken from a multicellular tumour spheroid which was stained for haematoxylin and eosin. The scale bar is 350 μm.

3.8. Viability Staining of Spheroids

Live spheroids were stained for viability using fluorescein diacetate (FDA) and propidium iodide (PI) (Sigma Aldrich, UK). FDA is a cell-permeable esterase substrate which acts as a live stain as it becomes fluorescent upon cleavage with intracellular esterases. PI is not permeable to live cells and only fluoresces upon binding to DNA so acts as a stain for dead cells. For the open well experiments spheroids were extracted from the droplets and washed with PBS. Spheroids were then incubated with staining solution containing 20 μg ml^{-1} of PI and 8 μg ml^{-1} of FDA for approximately 20 minutes. The staining solution was then washed off and replaced with PBS before imaging to remove any excess dye within the medium. For the microfluidic experiments the staining solution was flowed through the device for 20 minutes before being incubated for about 15 minutes. The staining solution was then washed out of the device using PBS for 20 minutes before imaging. An example of a spheroid stained for FDA and PI is shown in figure 3.8.

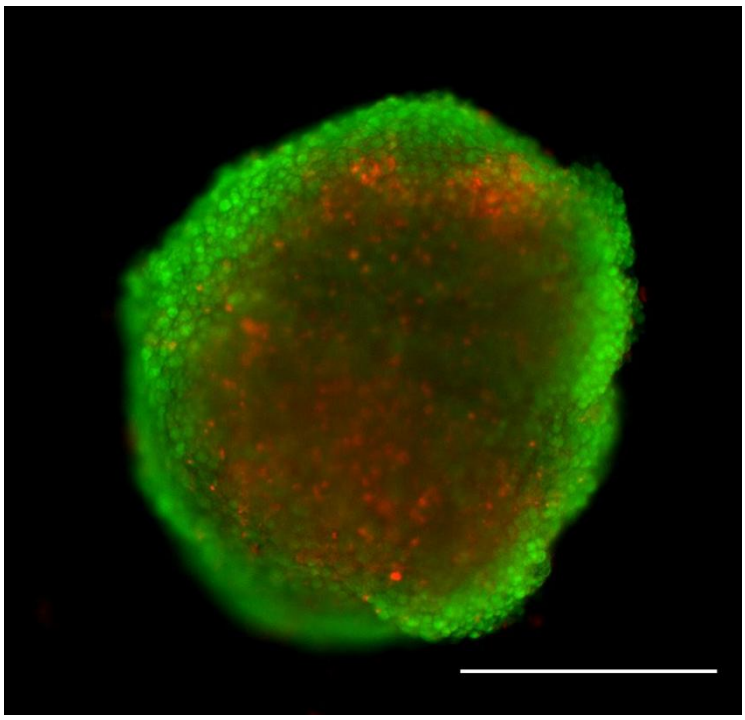

Figure 3.8: Viability stain of spheroid. An example of a fluorescent image of a spheroid stained for fluorescein diacetate(FDA) (green) and propidium iodide(PI) (red). The scale bar is 400 μm.

3.9. Radiation Treatment of Spheroids

Spheroids were formed and cultured in either emulsions in open wells or in microfluidic devices for up to 7 days before treatment with radiation unless a quiescent spheroid experiment was being conducted (details within chapter 4 and 6). Spheroids were treated with a single dose of either 4 Gy or 8 Gy on chip using a PXI X-Rad 225C X-irradiator with a dose rate per min equating to 2.2 Gy per min (RPS Services, Surrey, UK).

3.10. Dosimetry Measurements

A UNIDOS® E universal dosimeter with a CC04 ionisation chamber (PTW, Germany) was used to measure if radiation was absorbed by a PDMS device, a glass slide and PDMS alone.

3.11. Cisplatin Treatment of Spheroids

Cis-Diammineplatinum(II) dichloride (Cisplatin, Sigma Aldrich, UK) was dissolved in 0.9% sodium chloride solution to initially make a stock solution of 1 mM. For treatments, the stock solution was diluted with medium to make a 50 μM solution and loaded into a glass syringe for dispensing into the device. Spheroids were formed and cultured in droplet perfusion microfluidic devices for 7 days before treatment with cisplatin. The spheroids were incubated for 24 hours with cisplatin before washing off with medium.

3.12. Doxorubicin Treatment of Spheroids

Doxorubicin (Sigma Aldrich, UK) was dissolved in deionised water to initially make a stock solution of 5 mM. For treatment the stock solution was diluted with medium to make a 4 μM solution and loaded into a glass syringe for dispensing into the device. Spheroids were formed and cultured in droplet perfusion microfluidic devices for 7 days before treatment with doxorubicin. The spheroids were incubated for 24 hours with cisplatin before washing off with medium.

3.13. Imaging

A Zeiss transmission microscope was used to image the microfluidic devices and imaging was acquired using a Labview controlled Dalsa Genie CMOS HM1024 camera for still images on set days. For taking time-lapse images a Zen controlled Zeiss AxioCam MRm camera was used. Images were analysed using Image J. For taking images of stained sections a GXCam-3 camera and GX Capture software (GT Vision Ltd) was used.

3.14. Spheroid Growth Measurement

Spheroid growth was monitored by measuring the increase of the multicellular spheroid diameter over time from brightfield images, acquired using a Zeiss inverted microscope (Axiovert A1) with a Labview controlled Dalsa Genie CMOS HM1024 camera. Spheroid dimensions were estimated using ImageJ by measuring the longest and shortest diameters (D1 and D2, respectively).

These values were then used to calculate the approximated volume (V) of each spheroid, estimated as:

$$V = \frac{4}{3}\pi\frac{D1}{2}\left(\frac{D2}{2}\right)^2 \qquad \text{(Equation 3.1)}$$

The Mann Whitney and Kruskal Wallis tests were used to evaluate the statistical difference between experiments (significant difference between groups obtained for p value ≤0.05).

4. Formation and Culture of Spheroids within Emulsions

4.1. Introduction

The formation and culture of multicellular tumour spheroids (MCTSs) within emulsions offers several advantages in comparison to traditionally used methods. Advantages include enhanced mechanically stability in comparison to the hanging drop method and a lower amount of shear stress to spheroids with respect to spinner flasks[5]. There is also the potential to create high throughput platforms through the use of droplet microfluidics with the potential to store 1000 droplets per device[21], [88]. In recent years there has been an increase in the usage of droplet microfluidics for spheroid culture which have mainly involved the use of alginate and hydrogel materials rather than medium in oil (M/O) droplets. However, one of the drawbacks of the use of droplets is their intrinsic compartmentalised nature which limits the availability of nutrients and causes a build-up of toxic metabolites resulting in a detrimental impact to cell viability[10]. Studies involving cells encapsulated within droplets or beads have experienced varied culture times from 2 to 12 days[15]–[17], [20], [23] with viability of cells reducing over hours or days[12]. Therefore, the identification of conditions required for long term culture of spheroids within droplets is essential for the development of droplet microfluidic devices.

In this chapter, the concept of using medium in oil droplets as a method for the formation and culture of MCTSs will be introduced. Due to the compartmentalised nature of the droplets, the volume of medium to number of cell ratio and the maximum amount of time that spheroids can be cultured within droplets when its encapsulated medium is not refreshed has been investigated. Furthermore, the influence of medium refreshment on spheroid growth was examined. In addition, spheroids formed using the emulsion method were compared to those formed using a spinner flask and then non-adherent plate. As MCTSs were first introduced as *in vitro* models for testing the radiosensitivity of cancer cells[57], the potential of this technology for carrying out radiotherapeutic assays was also investigated. Throughout this thesis, the UVW glioma cell line has been used as it is known that it can form compact MCTSs within non-

adherent conditions and is a robust cell line, thus suitable for carrying out proof of principle experiments[109].

4.2 Principle of Spheroid Formation within Emulsion Droplets

The investigation of spheroid formation in M/O droplets was initially carried out in macrodroplets in a PDMS open well device (Figure 4.1). The advantages of using an open well device is that it allowed for the exchange of medium and the altering of droplet volumes so that the parameters required for spheroid formation and culture using M/O droplets could be investigated by using a pipettor. The fabrication process to form open well PDMS devices is described within chapter 3. Cells were seeded at a specific concentration in suspension (100 µl of medium) in a well previously filled with 60 µl of FC-40 oil with 2% (w/w) fluorosurfactants to investigate the spheroid formation process. As the oil-surfactant phase was denser than the medium, the droplet containing the cells floated to the top of the well. Immediately after dispensing the cell suspension into the well, the cells sedimented to the bottom of the droplet at the medium to oil with surfactant interface. As is shown in figure 4.1, cells were observed to aggregate within 12 to 24 hours to form a flat layer of cells at the bottom of the droplet. From day 2 onwards the cells began to cluster on top of each other and, over time, the cellular aggregate became more tightly packed creating a spherical structure. The time that took to form a spherical spheroid depended upon the cell concentration used, with the lower the cell number taking less time to form a spheroid. The curvature of the bottom of the droplet, due to interfacial tension between the phases, facilitated cell aggregation. One of the drawbacks of the open well device was the potential to introduce contaminants (e.g. fibres) into wells through the pipetting of cells or medium into the emulsions. This was an issue as the cells would prefer to aggregate around the fibre resulting in loss of the spheroid shape and creating difficulty when assessing the growth of the spheroid via imaging techniques.

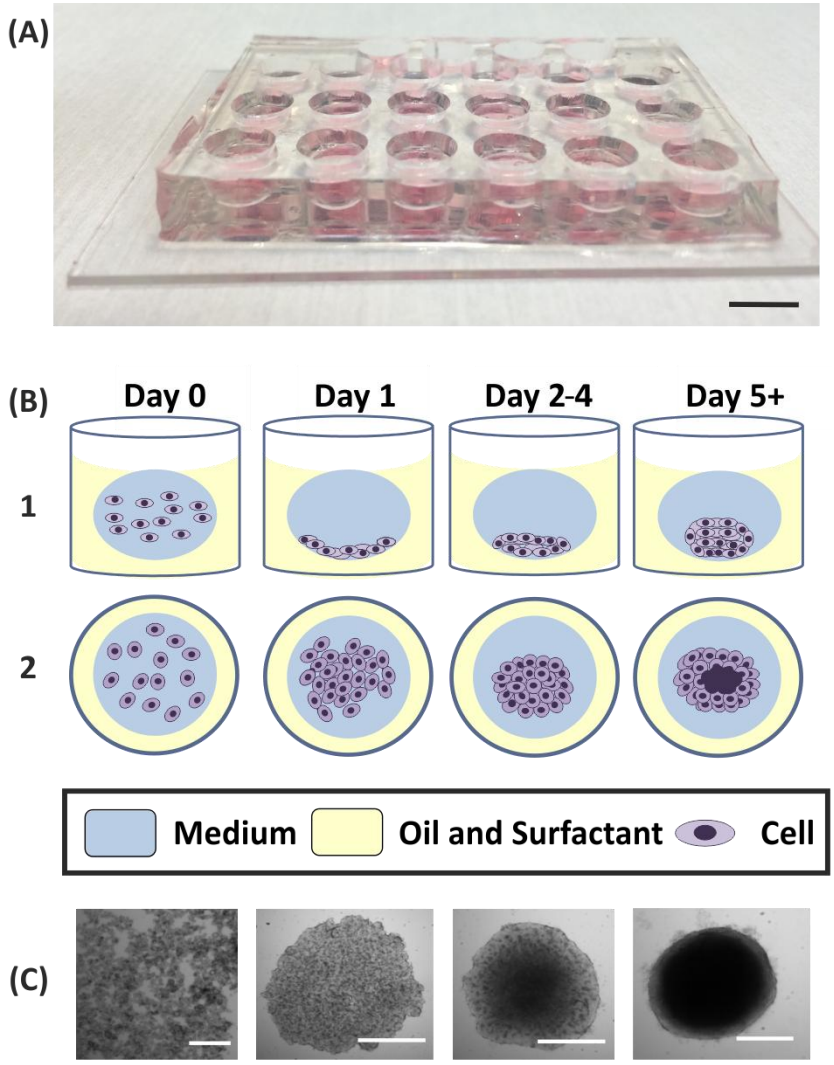

Figure 4.1: Formation of multicellular spheroids within medium in oil (M/O) droplets. (A) A photograph of an example of a PDMS well device containing medium and oil within each well. (B) Schematic diagrams showing the formation of a multicellular spheroid over time (1 side view, 2 top view). (C) Representative time lapse sequence of brightfield images (top view) during spheroid formation within a 100 µL M/O droplet. Scale bar is 8 mm for (A) and 300 µm for (C) (scale bar is relative to image size after cropping). Figure adapted from McMillan et al.[28]

4.3 Investigations of the Parameters for Spheroid Growth

4.3.1 Volume of Medium to Cell Number Ratio

An important consideration to be made with an emulsion based system for the culture of MCTSs is that there is a finite volume of medium within a droplet. As a result, there is

a limited amount of nutrients available to cells in addition to an accumulation of waste products. Both of these factors have a detrimental impact on the viability of cells. Therefore, the first investigation was to identify the maximum amount of time in which the spheroids can remain viable within a minimum volume of medium. To determine this, a range of droplet volumes (25 – 100 µl) encapsulating different cell concentrations (24 – 3700 cells per µl) were tested. The growth of spheroids and detrimental signs to spheroid health such as the disaggregation of cells from the intact spheroid were monitored. The last day at which no signs of cell disaggregation from the compact spheroid occurred was considered the end of spheroid culture and was the time-point plotted in figure 4.2. To further confirm the health of the spheroids, these were stained with fluorescein diacetate (live) and propidium iodide (dead). Fluorescein diacetate is a cell permeable esterase substrate which is cleaved by esterases within the cell to create a fluorescent substance so indicates live cells[110]. Propidium iodide is a cell impermeable substrate which fluoresces once bound to DNA so can only do this once the plasma membrane has broken down and thus is a marker of cell death[110], [111]. As shown in figure 4.2 (B) the cells which had disaggregated from the spheroid stained for propidium iodide while the compact spheroid stained for fluorescein diacetate. Thus, this confirmed that the cells that had disaggregated from the spheroid were dead. As expected in the condition where there was a larger volume of medium to cell ratio the spheroids remained intact for a longer period of time. A maximum of 14 days for spheroid culture without cell disaggregation was achieved with a cell concentration of approximately 200 cells per µl. During this investigation there was no increase in spheroid size suggesting they had entered a dormant state. The only change in spheroid size was an initial decrease in size from the cells aggregating together to be a flat aggregate to gathering together on top of each other to form a compact spheroid. Even though the devices were incubated within a humidified environment, a reduction in the volume of medium was observed over time resulting in a difference in the concentration of salts and pH within the medium.

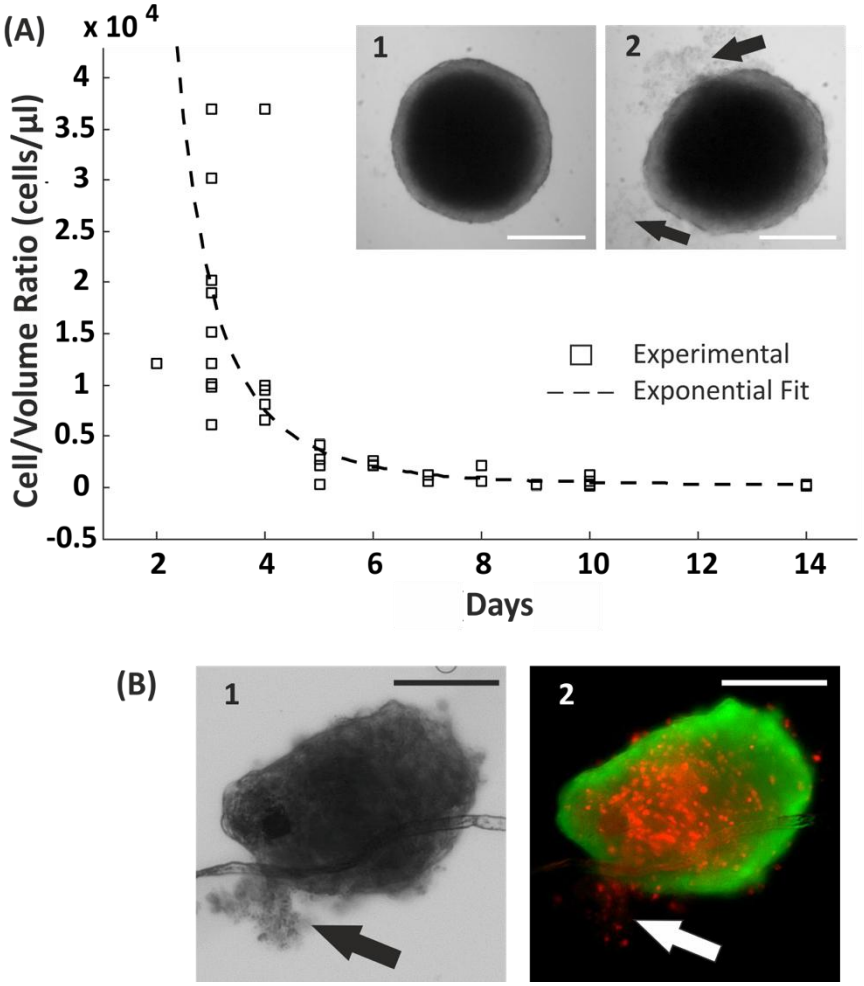

Figure 4.2: Assessment of the minimum volume of medium required for spheroid culture. (A) The scatter plot shows the cell number to volume of medium ratio over the number of days at which the spheroids remained intact with no visible sign of cell disaggregation. Each square box refers to the last day a spheroid remained intact at that cell number to volume of medium ratio. The brightfield images show (1) an intact spheroid and (2) a spheroid with visible cell disaggregation (as indicated by the arrows). (B) A brightfield (1) and a fluorescent image with fluorescein diacetate (green) and propidium iodide (red) staining (2) of spheroids showing cell disaggregation (as indicated by the arrows). The scale bar for (A) equals 450 µm and for (B) equals 150 µm. Figure adapted from McMillan et al.[28].

4.3.2 Influence of Medium Refreshment

The next parameter investigated for its influence on spheroid culture was medium refreshment. In the previous section it was shown that when medium was not refreshed spheroids could only remain intact for a limited period of time before cell

disaggregation occurred. Therefore, experiments were conducted to determine if it was possible for spheroids to recover from this deprived state if medium was exchanged once the initial signs of cell disaggregation occurred (figure 4.3). This was of interest to identify whether with a restricted volume of medium the spheroids enter a reversible dormant state which could be used to investigate the efficacy of radiotherapeutic and chemotherapeutic treatments towards quiescent cells. Spheroids were formed using a cell concentration of 500 cells per μl (100 μl of medium) with this concentration producing spheroids which remained viable for approximately 10 days (figure 4.2(A)). For the first 7 days of spheroid formation the size decreased suggesting that the cells were still aggregating together to form a compact spheroid (figure 4.3). After day 7 no significant increase in spheroid growth was observed and, on day 9, the first signs of cell debris within the droplet appeared. On day 14, a significant number of cells were observed to have disaggregated from the compact spheroid. From day 15, some spheroids continued to not have their medium exchanged (control) and medium exchange was carried out with a sample of the spheroids to determine whether they could be recovered from the induced deprived state. For the spheroids which had medium exchanged, 50% of the total volume of medium was removed and replaced with 50% of fresh medium. Due to the size of the spheroids (typically 700 μm at the cell number per μl used), these could be easily seen by eye within the droplet, making it easy not to withdraw the spheroids by mistake when using a pipettor. As the medium floated to the top of the oil it was easy to withdraw medium without withdrawing the oil, although this could also be checked by monitoring the liquid withdrawn in the pipette tip. For spheroids which had no medium exchanged, these decreased in size due to the disaggregation of cells. In contrast for the spheroids which had their medium exchanged, it was observed that from day 18 onwards the spheroids increased in size by 6% from day 14. A significant difference in size of 17% was observed from day 20 with a p value of less than 0.001 ($p = 1.62 \times 10^{-4}$). On day 28 spheroids which had been refreshed had increased in size by 34% to approximately 1 mm in diameter.

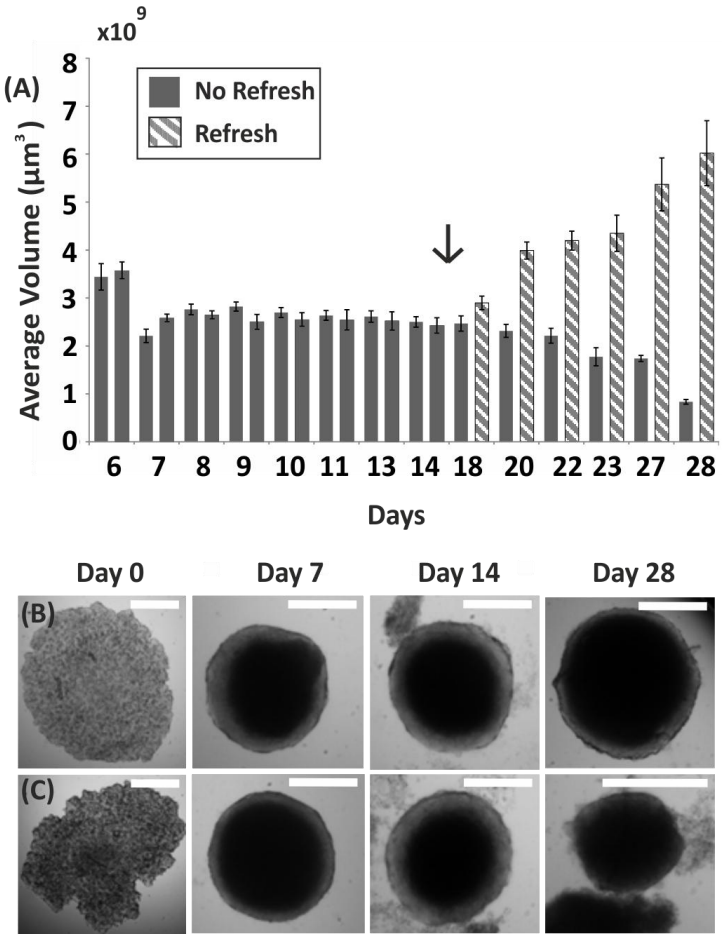

Figure 4.3: Effect of Medium Refreshment on Spheroid Culture. (A) Bar chart showing the average volume of spheroids over 28 days with the error bars representing the standard error of the mean. The patterned bars are the spheroids which were refreshed from day 15 (as indicated by the arrow). (B) and (C) are a timelapse of brightfield images of spheroid formation with the top row showing spheroids refreshed from day 15 and the bottom row showing spheroids which were not refreshed. The number of spheroids till day 14 was 17 and from day 18 the n number for non-refreshed spheroids was 11 and for refreshed spheroids was 6. Scale bar is 500 µm. Figure taken from McMillan et al.[28]

A further investigation was carried out to determine if there was a significant difference in the growth rate of spheroids which had been refreshed throughout the culture versus spheroids that were only refreshed after they stopped growing. For spheroids which were refreshed throughout the culture (medium refreshed from the start), refreshment of 50% of medium occurred every second day. In the case of the non-refreshed spheroids, refreshment was carried out from day 16 (defined as refresh

from day 16 in figure 4.4). Day 16 was chosen as it was observed from day 15 that spheroid growth had stopped and there were signs of cell disaggregation thus suggesting that the spheroids had entered a non-proliferative state. The difference in spheroid growth was calculated as the percentage increase in spheroid volume in comparison to spheroid volume at the start of medium refreshment (S_0). For the refreshed spheroids, S_0 was day 6, as this was when the spheroid was considered to be formed, and for the non-refreshed spheroids, S_0 was day 15. Thus it was considered that the non-refreshed spheroids had entered a dormant/non-proliferative state. For spheroids which were refreshed every two days there was a steady percentage increase in growth over time compared to S_0 (figure 4.4). In contrast, for non-refreshed spheroids refreshed only from day 16 there was a significant percentage increase in volume in comparison to S_0.

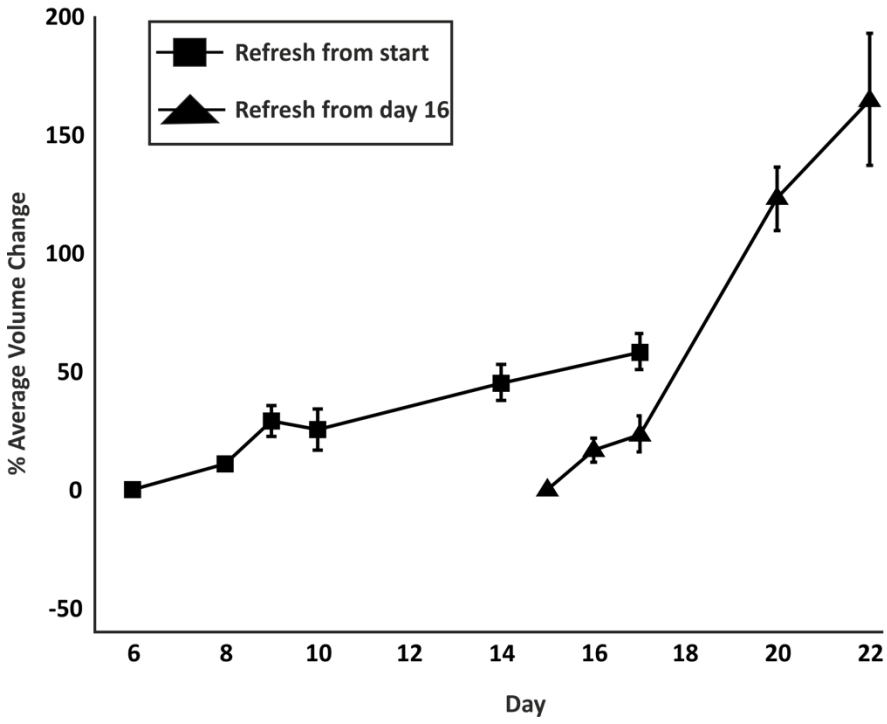

Figure 4.4: Influence of Different Medium Refreshment on Spheroid Growth. Growth curves showing the percentage volume change ± standard error of the mean (error bars) in spheroids refreshed from the start of culture every 2 days and in spheroids which were not refreshed until day 16. The number of spheroids per experiment (n) were n=15 for the refreshed spheroids and n=7 for the spheroids refreshed from day 16.

Viability staining was carried out on spheroids which had been refreshed from the start of culture and compared to spheroids which had no medium exchanged till spheroid growth had stopped (figure 4.5). Spheroids which were in day 3 of culture and had been refreshed every two days had no visible dead cells and the whole spheroid stained for fluorescein diacetate (figure 4.5(A)). In contrast, in refreshed spheroids on day 20 of culture, a visible core of cells staining for propidium iodide was visible (figure 4.5(B)). In spheroids which were not refreshed, cell death was observed at the outer rim of the spheroid at day 15 (or at S_0), indicating that dead cells started disaggregating from the spheroids (figure 4.5(C)). In contrast, in 20 day old spheroids, which were refreshed from day 16 after being starved for 15 days, there was a visible core of dead cells and the outer rim stained for fluorescein diacetate (figure 4.5(D)). Therefore, this suggests that the dead cells which were observed on the outer layers had disaggregated after refreshment and confirms spheroid viability after medium refreshment. Furthermore, the spheroid in figure 4.5 (D) is in a similar state to a spheroid which was refreshed from the start (figure 4.5 (B)), suggesting even after a period of no medium exchange there was not a detrimental impact on viability of cells and instead remained in a dormant state.

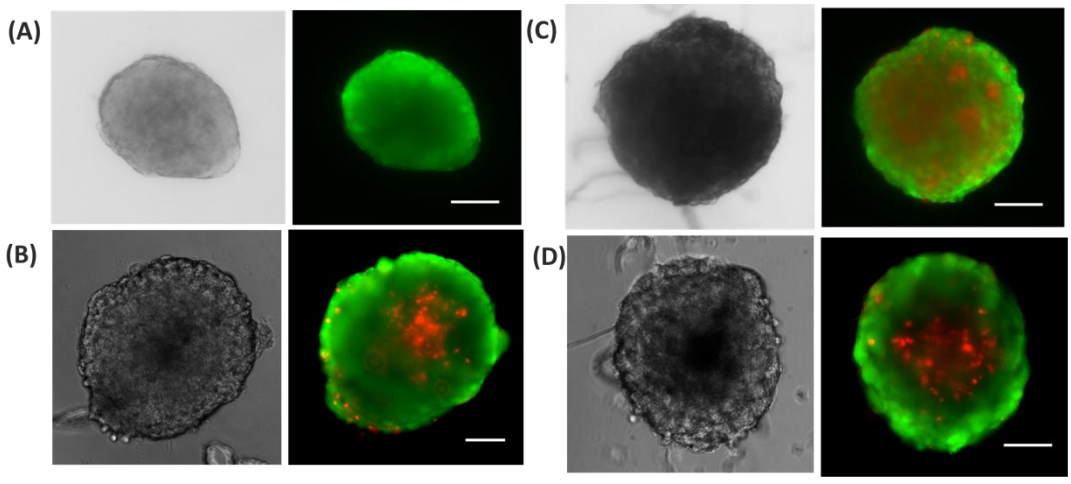

Figure 4.5: Influence of Refreshment on Spheroid Viability. Brightfield and fluorescent images of spheroids stained with fluorescein diacetate (green) and propidium iodide (red). Images are representative of spheroids which were 3 days old and refreshed (A); 20 day old spheroids which were refreshed (B); 15 day old spheroids which had not been refreshed from the start of culture (C) and 20 day old spheroids which were only refreshed from day 16 (D). The scale bars are 100 µm.

4.4 Control of Spheroid Size

Once the conditions had been identified for the formation and culture of spheroids, experiments were carried out to produce spheroids of a uniform size range (Figure 4.6). A uniform size range of spheroids is desirable for conducting radiotherapeutic and chemotherapeutic assays in order to obtain repeats to determine if the treatment had a significant effect as size can have an influence on efficacy. The size of spheroids was controlled by seeding different initial cell numbers which were approximately 500 or 1500 cells in a droplet of 100 μl. In these experiments 50% of medium was refreshed every two days from the start of culture to allow spheroids to grow and not remain in a dormant state. The first spheroid measurement was made once the minimum spheroid size had been achieved before an increase in size occurred. At this point it was considered that the cells had gathered together to form a compact spheroid. Spheroid growth for both spheroid sizes was monitored over 17 to 18 days. For an approximate estimated number of 500 cells, an initial average spheroid diameter was achieved of around 275 to 350 μm (termed 'small spheroids'). For the initial cell number of 500 the cells had gathered to form spheroids on day 3. In contrast an approximate cell number of 1500 did not achieve a compact spheroid until day 5 with the initial diameters ranging from around 530 to 600 μm (termed 'large spheroids'). As can be observed in figure 3.5, a similar growth curve was observed in experiments which used a cell number of 500 showing the reproducibility of controlling the spheroid size through cell number. A similarity in growth curves was also observed for the experiments which used a cell number of 1500. The main difference between the two different size ranges was that the small spheroids were observed to have a quicker initial increase in spheroid size in comparison to the large spheroids.

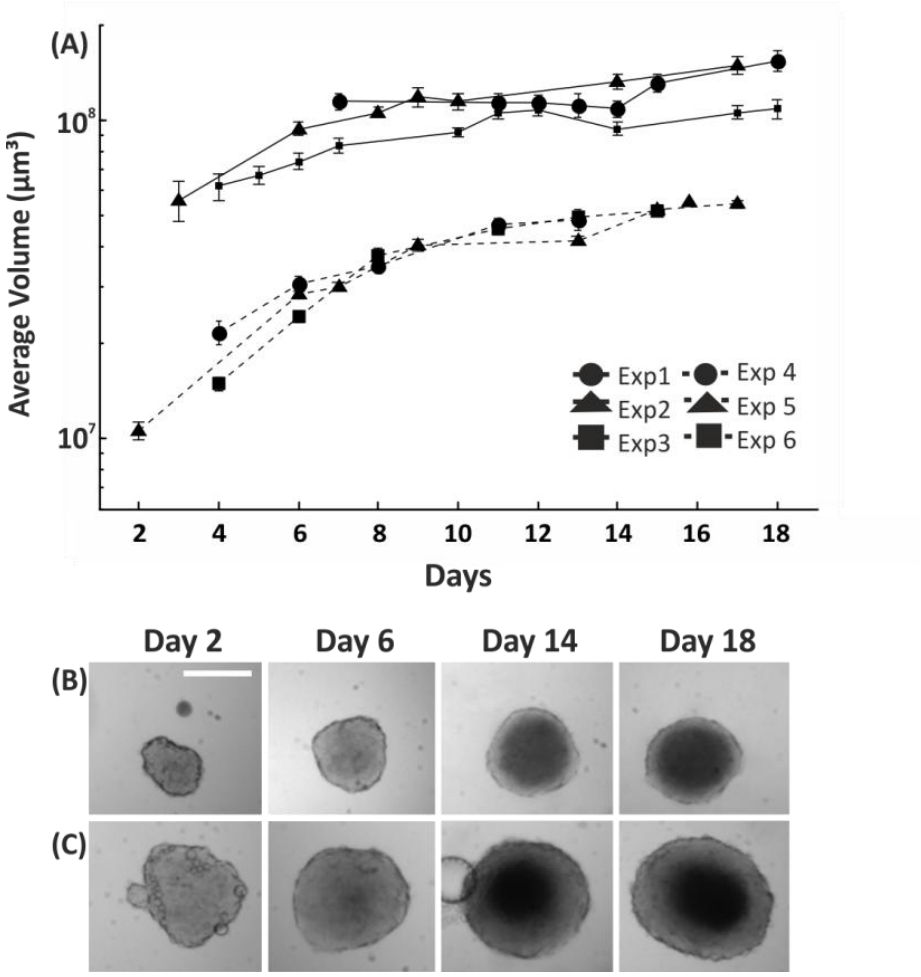

Figure 4.6: Control of Spheroid Size. The growth plot represents the average volume of spheroids over 18 days with the error bars representing the standard error of the mean and each point having an n number of 15. Experiments 1 to 3 represent spheroids with an initial spheroid diameter of 275-340 µm (small spheroids) and experiments 4 to 6 have an initial spheroid diameter of 530 to 600 µm (large spheroids). The number of spheroids per experiment (n) are as follows: exp 1(n=13), exp 2(n=15), exp 3(n=14), exp 4(n=11), exp 5(n=19) and exp 6(n=21). The brightfield images show a timelapse of spheroid growth of (B) small spheroids and (C) large spheroids. The scale bar is 350 µm. Figure taken from McMillan et al.[28].

4.5 Comparison of Spheroids formed in Emulsions versus those formed in Spinner Flasks

4.5.1 Morphology of Spheroids

To identify if there was a similarity in the morphology of spheroids formed using the droplet method to those using the spinner flask method, spheroids were sectioned and stained. Spheroids formed using the spinner flask method were initially formed within a spinner flask and on day 3 were transferred to a non-adherent plate to aid with forming spheroids of a uniform size range and analysis over time for section 4.5.2. Spheroids were sectioned so that the inside of the spheroid could be examined for differences in cell characteristics and packing between techniques and sizes. Due to the small sizes of spheroids obtained, Bio-wrap (Leica Biosystems) was used to collect and wrap the spheroids within for tissue processing (Section 4.6) so that they were not lost through the cassette during the washing stages of tissue processing. Spheroids were obtained for both techniques which included approximately 300 μm and 750 μm diameter spheroids. For the 300 μm spheroids, the ones formed using the spinner flask method did not have a smooth and compact outer rim like the ones formed using the emulsion based method (Figure 4.7). This was because the spheroid at a size of approximately 300 μm was obtained directly from a spinner flask and had not been cultured within a non-adherent plate. However, both methods formed spheroids which had cells with nuclei of a similar size throughout the section (Figure 4.7).

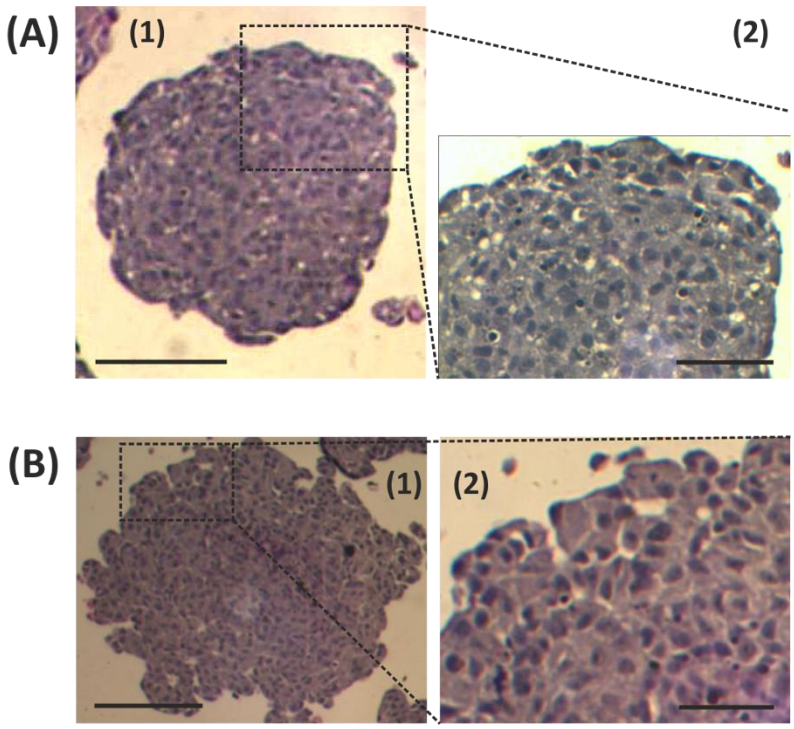

Figure 4.7: Haematoxylin and Eosin Staining of Small Spheroid Sections. Representative images of sections from a small (300 µm) spheroid grown in a droplet, (A), and derived from a spinner flask, (B). Scale bars in (A1) and (B1) are 150 µm and (A2) and (B2) are 75 µm. Figure adapted from McMillan et al.[28].

In contrast to the smaller spheroids, sections taken from larger spheroids showed a difference in the appearance of cells between those in the outer layers and those within the core (Figure 4.8). Cells in the inner layers and core were more compact and nuclei were more spherical in contrast cells on the outer layers of the sections had oblong shaped nuclei. Therefore the difference in nuclei between the cells within the inner layers and the outer layers suggests as the spheroid increased in size the cells were more tightly packed.

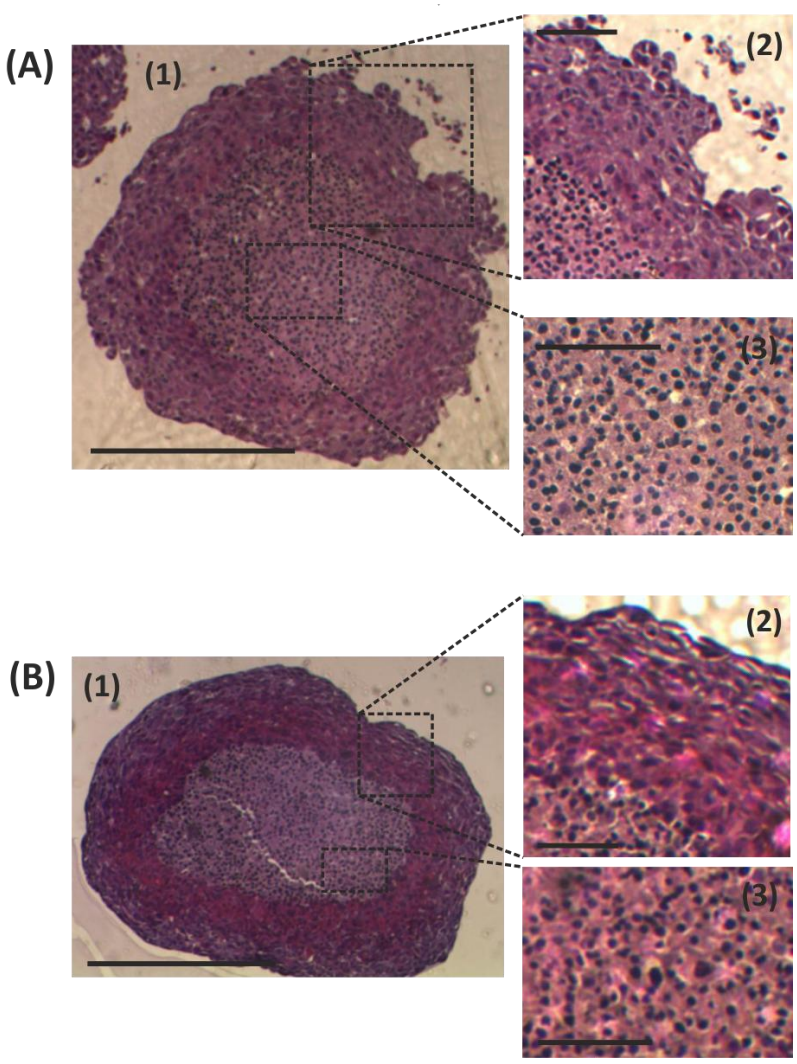

Figure 4.8: Haematoxylin and Eosin Staining of Large Spheroid Sections. Representative images of sections taken from large spheroids (approximately 700 µm) from droplet (A) and from a spinner flask and non-adherent plate (B). The scale bars in (A1) and (B1) are 400 µm and in (A2 and A3) and (B2 and B3) are 200 µm. Figure adapted from McMillan et al.[28].

4.5.2. Growth Rate of Spheroids

In addition to the morphology, the growth rate of spheroids formed within emulsion droplets were compared to those formed within a spinner flask. . For the spinner flask method, cells were seeded within a spinner flask to allow cell initial aggregation and transferred to a non-adherent plate on day 3 of spheroid culture by manually selecting the spheroids using a pipette. Transferring the spheroids to a non-adherent plate made

it easier to analyse spheroid growth over time. In addition, it reduced the variation in size between spheroids. Spheroids were formed with the aim to have them of a similar size range of approximately 450 – 500 μm for both formation techniques. This size range was chosen as it was difficult to manually collect a sample of spheroids of a uniform smaller size range of 200 – 300 μm formed via the spinner flask method. As a result of the difficulty to pick spheroids of a similar size range the initial sizes of the spheroids were significantly different between the two techniques. Overall, the growth curve obtained for spheroids formed using the same techniques was similar suggesting that the emulsion based method did not have an influence on the growth of spheroids.

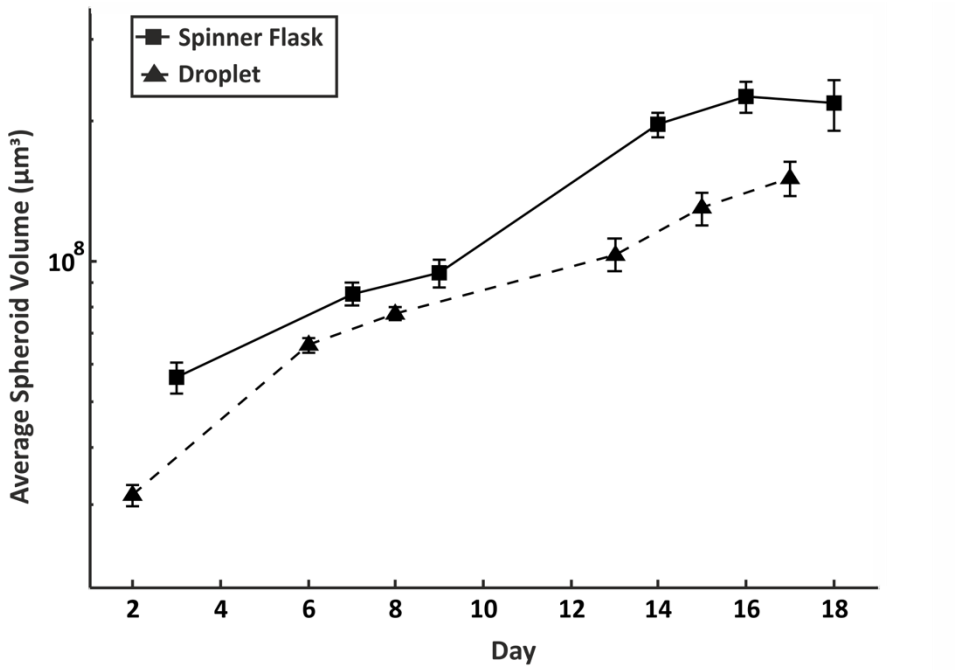

Figure 4.9: Comparison of growth of spheroids within Droplets and using the Spinner Flask Method. Growth curves showing the average spheroid volume ± standard error of the mean (error bars) over 18 days. Spheroids which were formed using spinner flasks were transferred to non-adherent plates from day 3. The number of spheroids (n) for the spinner flask experiment was n = 13 and for the droplet experiment was n = 19.

4.6 Radiotherapeutic Treatment of Spheroids

Once the conditions were characterised for the culture of spheroids within medium in oil droplets the suitability of this method to be used for the analysis of irradiation treatment on spheroid growth was examined.

4.6.1 Influence of Method on Radiotherapeutic Treatment

Spheroids were formed using an emulsion based technique and a spinner flask technique and treated on day 7 of culture with 8 Gy of X-ray irradiation. A cell seeding number of approximately 1500 cells in 100 µl was used for the emulsion method. For the spinner flask method the same cell seeding number was used as described in section 3.4. For experiments using the spinner flask method, spheroids were initially formed in spinner flasks and transferred to non-adherent plates as described in section 4.5. For both conditions, 50% medium was refreshed every second day to prevent the cells on the outer layers of the spheroid entering a dormant state to allow for spheroid growth. Even with the medium refreshment it was expected that cells within the inner layers would enter a dormant state due to the diffusive limits as the spheroid increases in size. The growth of spheroids over time and signs of cell disaggregation were monitored. The initial sizes of spheroids formed via both techniques were observed to be significantly different which could be to do with the difficulty in controlling the size of spheroids formed using the spinner flask method. In addition there is also a difficulty in collecting spheroids using a pipette by eye and making sure that they are all of a similar size range. Overall as can be observed in figure 4.10 spheroids formed using both techniques responded in a similar way with a reduction in spheroid growth observed from approximately day 13.

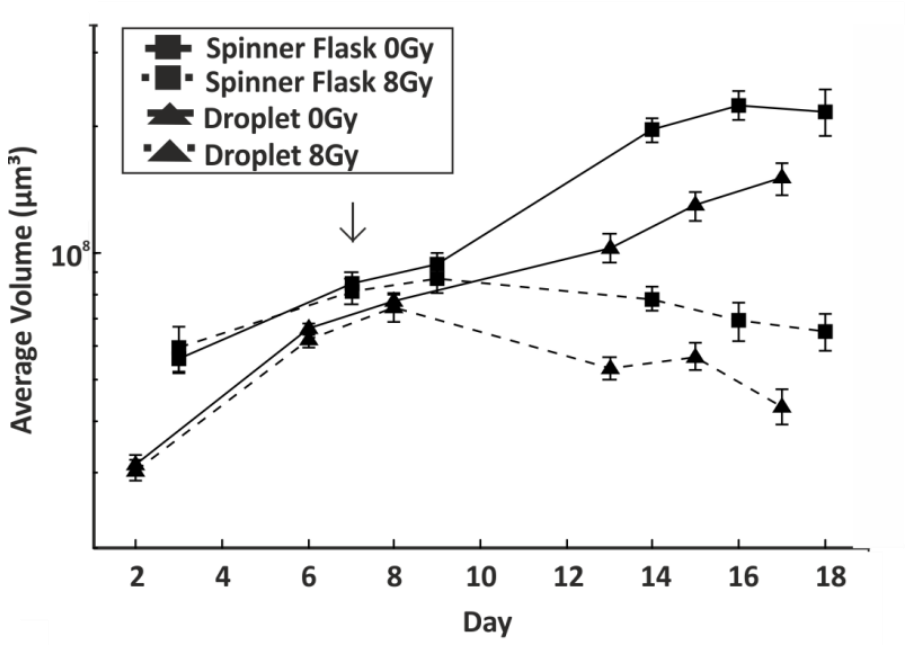

Figure 4.10: Effect of Radiation Treatment on Spheroid Growth. Line graphs showing the average volume (μm³) ± standard error of the mean over 18 days for spheroids formed in emulsion droplets and in a spinner flask. The spheroids were treated with 8 Gy on day 7 (as indicated by the arrow) with the 0 Gy spheroids representing controls. The number of spheroids per experiment (n) is as follows: spinner flask 0 Gy n=13, spinner flask 8 Gy n=10, droplet 0 Gy n=19 and droplet 8 Gy n=12. Figure adapted from McMillan et al.[28].

4.6.2 Influence of Spheroid Size on Radiotherapy Treatment

Subsequently, the effect of radiotherapy on spheroids of different sizes was investigated Small spheroids were formed at a size range of 275 to 340 μm and large spheroids at a size range of 530 to 600 μm within droplets. These size ranges were chosen as it is known at spheroids over 250 μm that quiescent cells are found within a spheroid and at over 400 μm a necrotic core forms within spheroids. Both different size ranges of spheroids were refreshed with 50% of medium every two days and were treated with either 4 or 8 Gy on day 7 of culture. For the small spheroids it was observed that a week after treatment with 4 Gy there was only a significant difference in spheroid volume in one of the experiments with a p value of less than 0.05 (Figure 4.13). In contrast treatment with 8 Gy resulted in a significant reduction in both small and large spheroids with a p value of less than 0.0001 for both sizes (Figure 4.13).

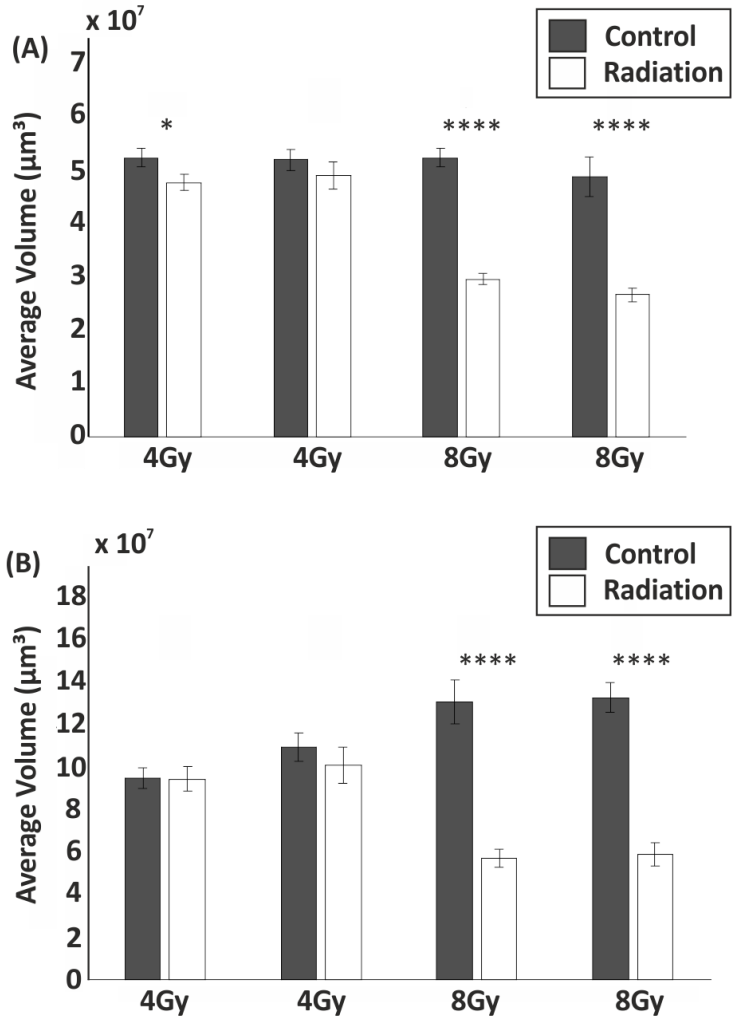

*Figure 4.11: Influence of Spheroid Size on Radiation Treatment. Bar charts showing the average volume (µm³) ± standard error of the mean of (A) small spheroids (275 – 340 µm) and (B) large spheroids (530-600 µm) one week after treatment with radiation, with each bar representing a separate experiment. The number of spheroids (n) for each experiment in (A) are 4 Gy (left) n =14 , 4 Gy (right) n = 13 , 8 Gy (left) n = 11, 8 Gy (right) n = 18 and in (B) are 4 Gy (left) n = 5 , 4 Gy (right) n =9 , 8 Gy (left) n = 13 and 8 Gy (right) n = 19. Spheroids were either treated with 4 Gy or 8 Gy of radiation on day 7 of culture within emulsion droplets. * represents a p value of ≤ 0.05 and **** represents a p value of ≤ 0.0001. Figure adapted from McMillan et al.*[28].

For both small (Figure 4.12) and large spheroids (Figure 4.13) 8 Gy resulted in a significant reduction in the growth curve in comparison to the control 2 days after treatment. The growth curve for the small spheroids did not increase in size and resulted in a slight reduction in size over time. For the large spheroids there was a

dramatic reduction in growth before the growth curve began to plateau with no further increase in size. For the small spheroids a 44% reduction in volume was observed, while for large spheroids a 55% reduction was observed when comparing to the control 7 days after treatment, respectively (Figure 4.11). Therefore this further shows that 8 Gy has a significant effect on spheroid growth for both small and large spheroids.

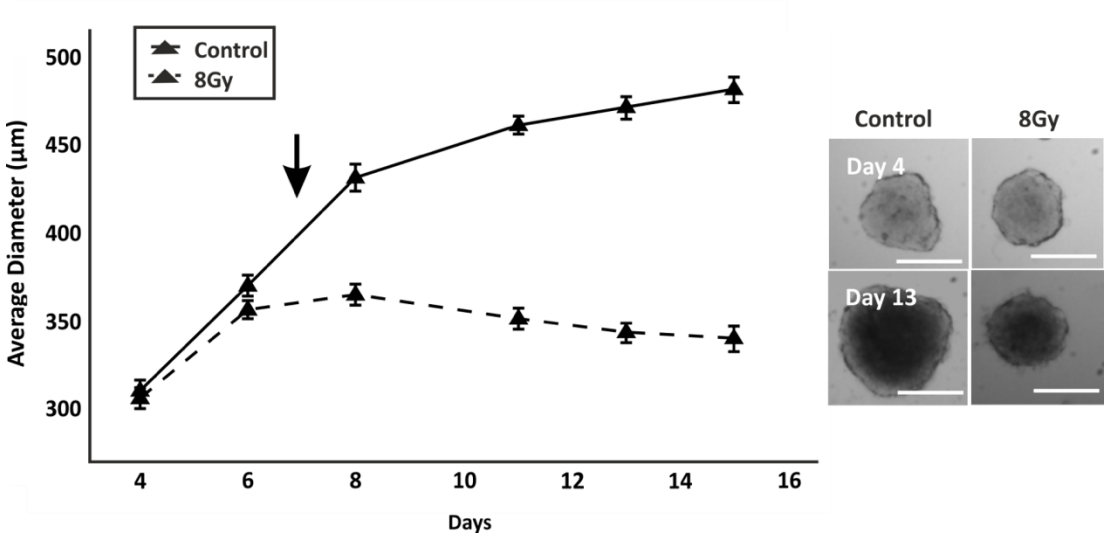

Figure 4.12: Influence of Radiotherapy on the Growth of Small Spheroids. A line graph showing the average diameter ± standard error of the mean (error bars) of small spheroids (300 – 350 µm) over 15 days with treatment of 8 Gy carried out on day 7 (the arrow indicates the day of radiation treatment). The number of spheroids (n) are for the control n=11 and for 8 Gy n=18. Brightfield images of control and spheroids treated with 8 Gy on day 4 and 13. Scale bars equal 300 µm (scale bar is relative to image cropping).

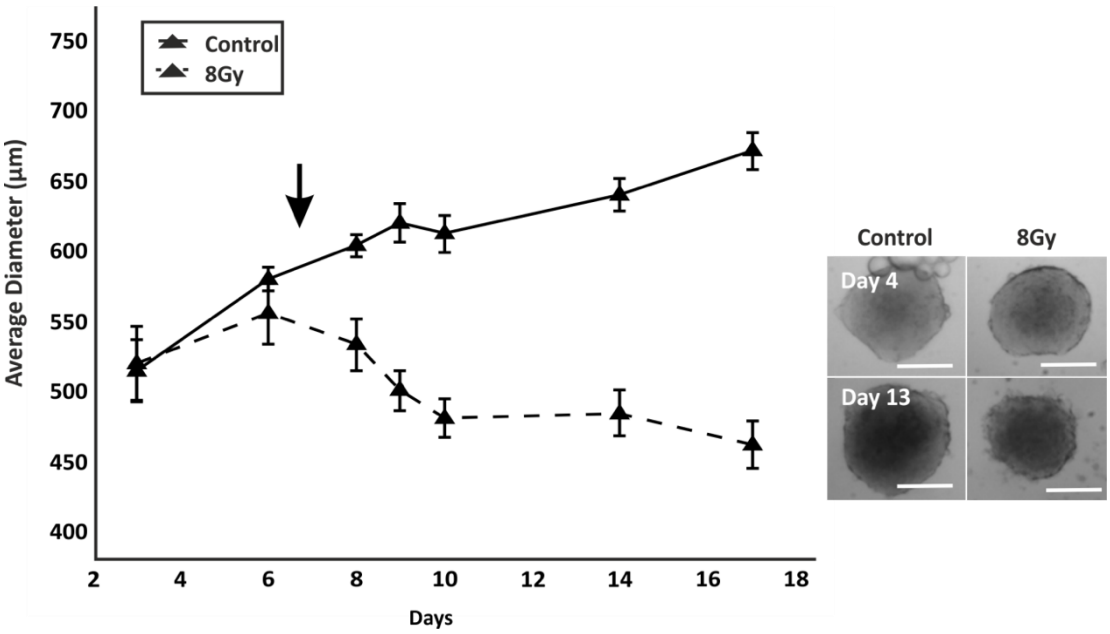

Figure 4.13: Influence of Radiotherapy on Growth of Large Spheroids. A line graph showing the average diameter ±standard error of the mean (error bars) of large spheroids (500 – 550 µm) over 17 days with treatment of 8 Gy carried out on day 7 (the arrow indicates the day of radiation treatment). The number of spheroids (n) are for the control experiment n=15 and for the 8 Gy experiments n=13. Brightfield images of control and spheroids treated with 8 Gy on day 4 and 13. Scale bars equal 250 µm (scale bars are relative to image cropping).

4.6.3 Influence of Medium Refreshment on Radiotherapy Efficacy

The next factor which was tested was whether quiescent spheroids were more radioresistant in comparison to proliferative spheroids. It is known that quiescent cells are more resistant to radiation which is suspected to be due to their enhanced ability to repair damaged cells[64]. In addition, due to the radioresistance of quiescent cells, once proliferative cells have been killed the quiescent cells are able to access fresh nutrients allowing them to proliferate[66]. Therefore this is an area of interest in developing more effective treatments which radiosensitise quiescent cells. Spheroids were cultured in droplets and not refreshed with their growth monitored to determine whether the spheroids were in a dormant state. Spheroids were treated with radiation once it was observed that spheroid growth had stopped and there were signs of cell disaggregation suggesting they were in a quiescent state. In addition spheroids were refreshed after treatment with radiation every two days to see if quiescent cells would

begin to proliferate again even after treatment. The effect of radiation on quiescent spheroids was then compared with spheroids which had been refreshed from the start of formation every two days and treated on day 7. The difference in spheroid growth was calculated as the percentage increase in spheroid volume in comparison to spheroid volume at the start of spheroid refreshment (Figure 4.14). For the refreshed spheroids this was day 6 as this was when the spheroid was considered to be formed. The non-refreshed spheroids were refreshed from day 15 as this was the day at which it was observed that the spheroids stopped increasing in size and cell disaggregation occurred thus suggesting the spheroids had entered a quiescent state.

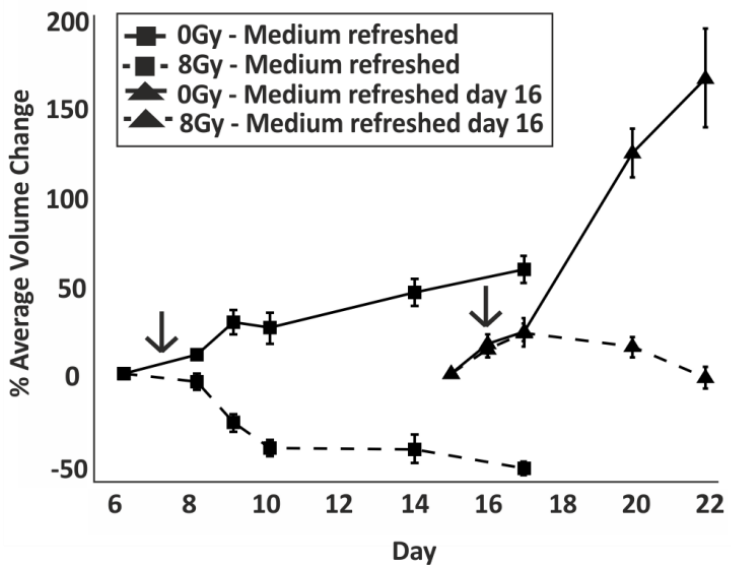

Figure 4.14: Influence of Spheroid Proliferative state on Radiation Treatment. Line graphs showing the percentage volume change ± standard error of the mean of spheroids over days. Spheroids which were refreshed every second day from the start were treated with 8 Gy of radiation on day 7 and spheroids which were deemed to be quiescent were treated on day 16 (day of treatment is indicated by the arrows). The percentage volume change refers to the percentage difference from the day after treatment from day 6 for refreshed and day 16 for spheroids refreshed on day 16. The number of spheroids (n) for medium refreshed from the start for 0 Gy was n =12 , for 8 Gy was n =14 , for medium refreshed on day 16 was n = 7 for 0 Gy and for 8 Gy was n =10 .Figure taken from McMillan et al.[28].

It was observed that in comparison to spheroids which were refreshed every two days that there was a delayed reduction in spheroid growth after irradiation in spheroids refreshed from day 16. Furthermore for the spheroids which were refreshed from the

start of culture there was a 41% reduction in volume 3 days after treatment in contrast a 14% increase in spheroid volume 4 days after treatment respectively in spheroids only refreshed from day 16. There was only a reduction in percentage volume in spheroids refreshed from day 16 of only 2% six days after treatment. Therefore this suggests for the spheroids which were not refreshed for 15 days that due to the presence of mainly quiescent cells upon exposure with radiation that they were more resistant. As a result there was a slower reduction in spheroid size by the disaggregation of cells in comparison to the spheroids refreshed every second day from the start of culture which would be mainly composed of proliferating cells on the outer rim.

4.7. Discussion of Chapter 4

In this chapter the conditions required for the formation and long term culture of multicellular tumour spheroids within medium in oil droplets have been identified. It has also been shown that it is possible to reproducibly control spheroid size through the initial cell number. Finally it was identified that the spheroids formed have a similar morphology and growth curve to those formed using traditional methods. This initial characterisation of spheroid formation within emulsion droplets is of importance when considering the development of a droplet microfluidic device to ensure that the best possible conditions are achieved for long term culture of spheroids within droplets before miniaturising via microfluidics.

4.7.1. Parameters for Spheroid Formation within Emulsions

UVW glioma cells were found to aggregate and form spheroids quickly within medium in oil droplets with the initial aggregation and formation only taking hours in comparison to days using traditional methods and alginate or matrix encapsulation methods[5],[17], [18], [20], [22]. One of the reasons for the rapid aggregation of cells was due to the non-adherent interface of the droplet. It has been previously identified in the literature that the type of fluorosurfactants used with the oil in this study produce a non-adherent interface suitable for the aggregation of cells[91], [100]. The non-adherent properties are due to the polyethylglycol head group within the chemical structure of the surfactants. The use of similar surfactants were used to form multicellular spheroids in a study by Chan *et al.*[23]. Chan et al. also found a similar

rapid spheroid formation time with human mesenchymal stem cells (hMSC). The spheroid formation times experienced in M/O droplets are similar to those observed in the hanging drop method[70]. However the hanging drop method is less stable to physical shock with droplets falling from the plate as a result of medium exchange or simply moving the plate for analysis[70]. In contrast the emulsion based method is more stable and as a result is more reliable as the duration of the assay is not affected by physical shock through moving the device from an incubator to a microscope.

Other encapsulation based methods which involve the incorporation of alginate or matrices have a longer spheroid formation time of a couple of days. Alginate or matrix based methods have longer spheroid formation times as it takes longer for cells to aggregate together due to the barriers created by alginate and matrix proteins. In contrast to the study by Chan *et al.* were they used double emulsion droplets the results presented within this chapter were for single emulsion droplets. The use of single emulsion droplets is of interest in terms of developing a microfluidic device as it reduces the complexity of droplet formation.

An important parameter which was investigated within this chapter was the volume of medium to number of cells ratio. This is of interest as one of the features of droplet microfluidics is compartmentalisation thus there is a limited volume of medium available to the cells. Therefore it is of interest to determine what the volume of medium to cell ratio is in the scenario were no medium exchange is carried out. It was found that as the volume of medium available to cells increased the duration of days for which spheroids could be cultured. In several studies involving single cells within aqueous droplets the duration of cell culture was limited to up to 4 days[12], [13], [24], [103]. Clausell-Tormos *et al.* showed the viability of Jurket cells and HEK 293T cells within droplets decreased over several days which they suggested in agreement with this chapter was due to a limited availability of nutrients and build-up of waste products[12]. Furthermore Chan *et al.* found that spheroids could only be cultured within double emulsion droplets for 4 days. A different suggestion for poor viability within droplets was made by Chen *et al.* who suggested that the cause for a reduction in viability was due to the oil and surfactant used. However, it was shown within this chapter that spheroids could remain viable for a certain period of time which was dependent on the volume of medium to number of cells ratio.

Another interesting result was that without medium refreshment spheroids entered a reversible quiescent state with proliferation occurring upon refreshment of medium. Only a few studies have investigated the influence of nutrient deprivation for controlling the proliferative state of multicellular tumour spheroids[112]–[114]. These studies did not involve the use of emulsion droplets and instead traditional methods were used for spheroid formation. In a study by Bloch *et al.,* they showed that for spheroids which were refreshed every second day the consumption of glucose increased over 20 days of culture[112]. In contrast, in spheroids which were not refreshed, their size and glucose consumption did not increase over time. Tumour cells are known to require a high concentration of glucose to produce ATP and other products required for proliferation[115]. In contrast to normal cells, which carry out oxidative phosphorylation to provide the essential products for proliferation, tumour cells undergo glycolysis. Glycolysis is a more advantageous method in comparison to oxidative phosphorylation for highly proliferative cells, such as tumour cells, as it produces a much higher proportion of glucose[116]. In addition, the breakdown of glucose is required for producing energy for the biosynthesis of products such as lipids, amino acids and nucleotides. Therefore, when there is a limited amount of glucose available to the cells, they enter a quiescent state. After this, if no nutrients are available over a set period of time the cells will undergo apoptosis[117]. Therefore through controlling the frequency of medium refreshment there is the potential to control the proliferative state of spheroids. Through this a tumour model can be created which models tumour relapse where upon re-exposure to medium previously quiescent cells begin to proliferate and the tumour increases in size. Furthermore, there is the possibility of this method being used for the testing of anticancer treatments to determine if they are efficacious towards a spheroid composed mainly of quiescent cells. As a result this could be used for the development of new treatments which aim to sensitise quiescent cells which are known to be highly radioresistant. Additionally this could be used to model when quiescent cells are reintroduced to the nutrient supply once the more sensitive proliferative cells are killed off and show how a tumour begins to grow back after treatment. Therefore this shows the importance in considering the availability of nutrients within droplets when developing a droplet microfluidic assay for spheroid culture.

A further point identified was that there was a difference in the growth rate of spheroids which had been refreshed throughout culture to those which had medium

refreshed after a period of starvation. In this chapter, a major increase in spheroid growth occurred when medium was reintroduced to quiescent spheroids, whereas in constantly refreshed spheroids they only steadily increased in size. A similar experiment was carried out by Mellor *et al.* who used a different method of using medium containing 0.1% fatty acid free BSA instead of 10% FCS to convert proliferative spheroids into quiescent ones. Mellor *et al.* found that when quiescent spheroids were re-exposed to 10% FCS medium they were able to increase in size in again. This is similar to what was observed within this chapter but instead medium was reintroduced to starved spheroids. However, Mellor *et al.* found that there was no difference in increase in growth when comparing proliferative spheroids to recently refreshed quiescent spheroids. This could be due to the fact that their "quiescent" spheroids were still slowly increasing in size whereas the spheroids in this chapter were only introduced to medium once spheroid growth had plateaued and disaggregation of cells occurred. Therefore the "quiescent" spheroids formed by Mellor *et al.* cannot be accurately defined as quiescent as they were still growing whereas the "quiescent" spheroids within this chapter can be as they had stopped growing indicating a lack of proliferating cells.

Only the conditions required for UVW glioma cells were investigated so it needs to be considered that the metabolic activity will be different for different cell types. A further important point to consider was that evaporation of the medium was observed over time when medium was not refreshed. Therefore the difference in salt concentrations could have also had an impact on the viability of the spheroids over time. The evaporation of water through PDMS is known to be an issue for cell culture within microfluidic devices even if stored within the humidified environment of an incubator[118]. The main attempt to reduce evaporation was by submerging the device in PBS while being stored in within the incubator. This did improve reducing the rate of evaporation but it is difficult to eliminate it completely with the opening and closing of the incubator door resulting in fluctuations in humidity.

4.7.2. Comparison with Spheroids Formed using Traditional Methods

Another encouraging result was that the morphology and growth rate of spheroids grown within medium in oil droplets was similar to those formed using a spinner flask

and non-adherent plates. The growth rate of spheroids was observed to change over time with the initial growth being quick and then slowing later on in the culture as described in section 4.5. The growth rate of UVW spheroids within this chapter are similar to those in a study by Neshasteh-Rizl *et al.* which were also formed in spinner flasks[119]. The change in growth rate of the spheroids is to be expected over time as when a spheroid increases in size the cells within the core of a spheroid become tightly packed together. In combination there is the development of a nutritional gradient with only cells on the outer layer able to proliferate and those within entering a quiescent state. The difference in the packing of cells between different spheroid sizes could be observed when comparing sections taken from 300 μm and 750 μm diameter spheroids. In the 750 μm spheroids, there was a visible difference in layers of cells from the outside and the inside for both methods used. Cells within the middle of the section were observed to have more compact and spherical nuclei, whereas those on the periphery had nuclei which were larger and more of an oval shape, thus suggesting those on the inside being subject to closer packing. The link between the shape of nuclei with the packing of cells within a spheroid has been previously reported by Rajcevic *et al.*[120].

4.7.3. Radiotherapeutic Treatment of Spheroids formed within Emulsion Droplets

In this chapter the potential use of the medium in oil system for the treatment of spheroids with radiotherapy has been shown. Spheroids are well regarded as excellent *in vitro* models for testing radiotherapy treatments[57], [64], [121], [122]. This is the first report of radiotherapy investigation of spheroids in emulsion[28]. The initial experiments showed that spheroids formed within emulsions did not respond differently to radiation in comparison to spheroids formed using the spinner flask method. However, there was a difference in the initial sizes for both methods due to the difficulty in controlling the spheroid size selection from with the spinner flask method in comparison to the emulsion based method as described in section 4.6.1.

The UVW glioma spheroids formed were observed to be highly radioresistant with 8 Gy required to produce a significant reduction in spheroid growth for both size ranges and 4 Gy only causing a significant reduction in small spheroids as described in section 4.6.2. The UVW glioma cell line used within this investigation is known to be highly

radioresistant, even as a monolayer, with 2 Gy required to produce a significant detrimental effect[109]. Therefore, it is to be expected that the high doses of radiation would be required within spheroids due to the enhanced radioresistance.

A useful feature of the emulsion based system was that the radiosensitivity of quiescent spheroids could be interrogated as described in section 4.6.3. In the results, it was shown in comparison to spheroids which were refreshed from the start of culture that upon treatment with 8 Gy there was a delay in the reduction in spheroid size. It is well known within the literature that quiescent cells are more radioresistant in comparison to proliferative cells[64], [65], [123]. Quiescent cells are thought to be able to repair potentially lethal damage such as that inflicted by radiation causing double stranded breaks[65]. Therefore, the ability to control the proliferative state of the spheroid opens up opportunities to test radiosensitising agents which target quiescent cells. However, one of the drawbacks of the system is that depending on their solubility, chemotherapeutic agents can partition into the oil phase if they are lipophilic[124]. The ability to use chemotherapeutic drugs using this method via droplet microfluidics has been evaluated within chapters 5 and 6. The ability to test both radiotherapy and chemotherapy on the same device is of major interest in order to develop radiosensitising agents.

5. Development of a Droplet Microfluidic Device for Spheroid Culture

5.1. Introduction

In the previous chapter the technique and conditions required for the formation and culture of spheroids within medium in oil droplets were introduced. In order to increase the throughput of data points for experiments and minimise manual procedures, the next step was to miniaturize the developed technique via droplet microfluidics. In order to do this, a suitable microfluidic device had to be developed to allow for the formation and long term culture of spheroids. In contrast to these goals, previous studies have mainly focused upon the use of droplet microfluidics for the formation of alginate beads or macrocapsules rather than aqueous droplets[16]–[20], [22]. In addition, the majority of methods involved the use of more than one microfluidic device with at least one for droplet formation and another for droplet storage. To reduce the complexity of the procedure, the focus has been upon designing a single device for droplet formation and storage. Initial investigations into the encapsulation of cells within droplets as well as the storage of droplets containing cells were additionally carried out.

5.2. Device 1 – A Single Chamber Device

5.2.1 Design of Device

The main features of the first type of devices which were designed and tested included a T-junction for droplet generation and a storage chamber for the long term storage of contacting droplets. Two different designs of storage chambers were produced, with one of the designs having a chamber with scalloped edges (highlighted by the white dashed box in Figure 5.1) to allow for the trapping of droplets, thus preventing them from moving and facilitating analysis[125]. The maximum widths of the chambers were 3.2 mm for the one without scalloped edges and 3.45 mm for the one with scalloped edges. Rectangular pillars were placed in the trapping chambers to prevent the chamber from collapsing. For both designs, two aqueous phase inlets allowed for the

addition of different substances, such as one with cells and one with only cell medium to dilute the number of cells per droplet if required. In addition, a numbered scale was included at the side of the chambers for both designs to allow for the long term tracking of a specific area of droplets. To reduce the risk of particulates entering the channels and causing blockage, a square area with pillars was added just after the inlets for both the continuous and aqueous phases. The width of the gap between the pillars was 28 μm. Both designs were fabricated on a single wafer using a single layer of SU8 3035 to create features with a thickness of 40 μm. All of the parameters of the devices are provided within the appendix.

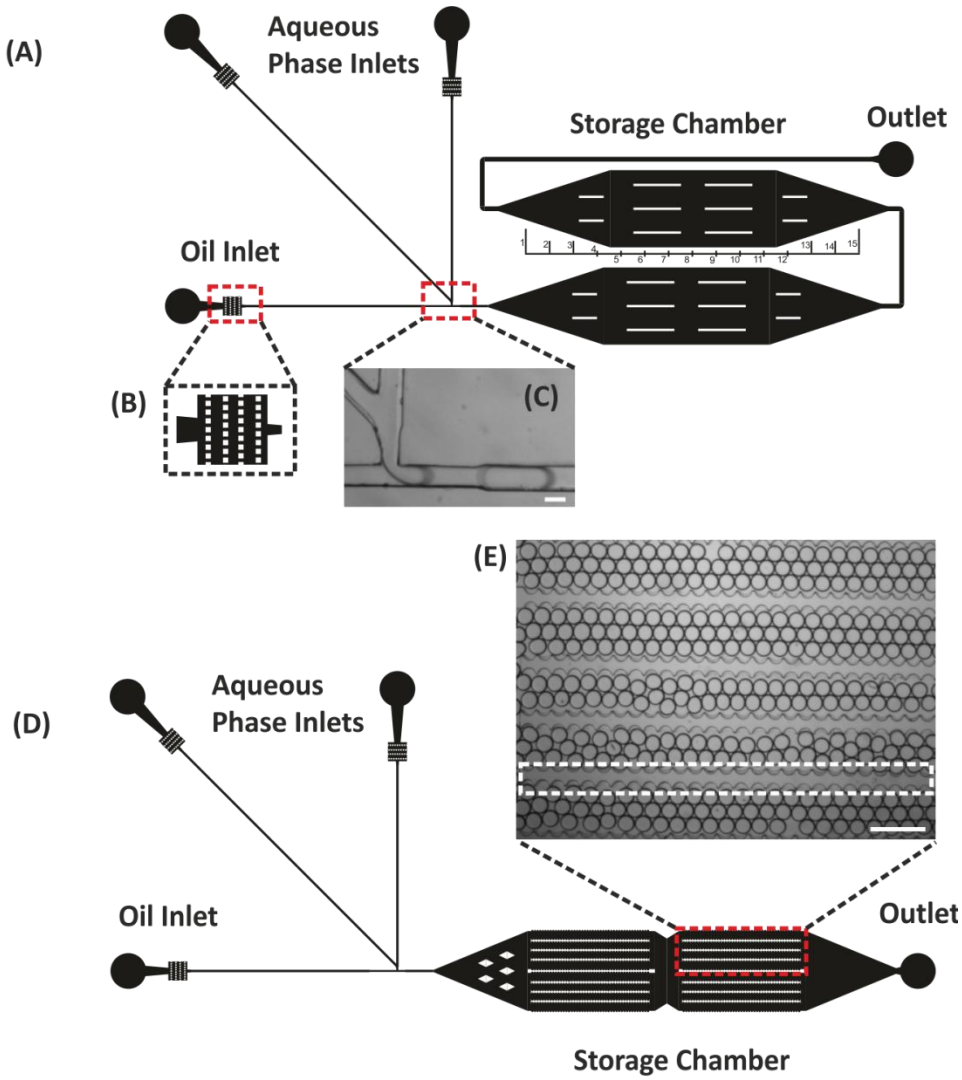

Figure 5.1: Diagram of Designs for Microfluidic Devices. (A) A microfluidic design which has two separate chambers for storage of droplets with (B) showing a magnified filter section after the inlets, (C) a brightfield image of the T-junction with droplet formation and (D) a different microfluidic design with a single chamber which has scalloped edges within the chamber to promote the trapping of droplets within the chamber; (E) the brightfield image of a section containing droplets is shown, with the scalloped edges highlighted by the white dashed box . The scale bar for (C) is 80 µm and for (E) is 350 µm.

5.2.2 Operation of Device

The initial experiments were carried out using water as the aqueous phase to identify the correct flow rates to form evenly sized droplets. The continuous phase used (FC-40 oil with 2% (w/w) fluorosurfactants) was the same as previously used for the

experiments within chapter 4. The flow rates used for both devices were 0.14 ml/hour for the continuous phase and 0.12 – 0.10 ml/hour for the aqueous phase. Once the chamber was filled with droplets the flows were stopped and the droplets remained within the chamber and did not coalesce with each other. For both designs the chambers had the potential to store over 1000 droplets. Once this was achieved, the UVW cell medium was used as the aqueous phase to determine whether the same conditions could be replicated. It was observed that once the flows of the aqueous phase and continuous phase were stopped coalescence of droplets occurred, resulting in the loss of individual compartments within as little as 10 minutes.

5.2.3. Factors influencing emulsion coalescence

To identify the causes of coalescence, an investigation was carried out with different aqueous phases used for cell culture. This investigation also included the look at further factors required for cell culture and analysis within the device. The aqueous phases tested included water, PBS, MEM without additives, MEM with individual additives and the complete cell medium used for culture of UVW cells. The additives tested in combination or individually with the MEM were penicillin/streptomycin, amphotericin (Fungizone) and FBS. Other factors, such as the movement of a device to a microscope stage for analysis and storing a device within an incubator for cell culture, were also investigated. Droplets of a similar size were formed for each condition tested and the chamber was filled. The number of droplets upon initial loading was compared to the number after a set number of minutes or after movement and calculated as the percentage coalescence (Figure 5.2):

$$\%_{Coalescence} = \frac{N_{Droplets}(t=0) - N_{Droplets}(t=x)}{N_{Droplets}(t=0)}\ x\ 100, \qquad \text{(Equation 5.1)}$$

where $N_{Droplets}(t=0)$ equals the number of droplets at the start of the experiment and $N_{Droplets}(t=x)$ equals the number of droplets after a certain period of time. The use of water as the aqueous phase did not increase the chance of coalescence until heat was added, which was similar for PBS and MEM without supplements added. In contrast, when medium was used in combination with any of the supplements, the number of coalesced droplets increased significantly, even when the device was kept stationary on the microscope over time. Furthermore, the slight physical shock produced by placing the device on a microscope stage increased the chance of coalescence by twice as much

as leaving it stationary (Figure 5.3). In addition, the use of the incubator to store the device showed that increased temperature further increased the chance of droplet coalescence. Therefore, the results showed that it was not possible to store medium droplets within a single chamber without coalescence occurring. A discussion into the possible reasons for droplet coalescence is provided in section 5.5.1 of this chapter.

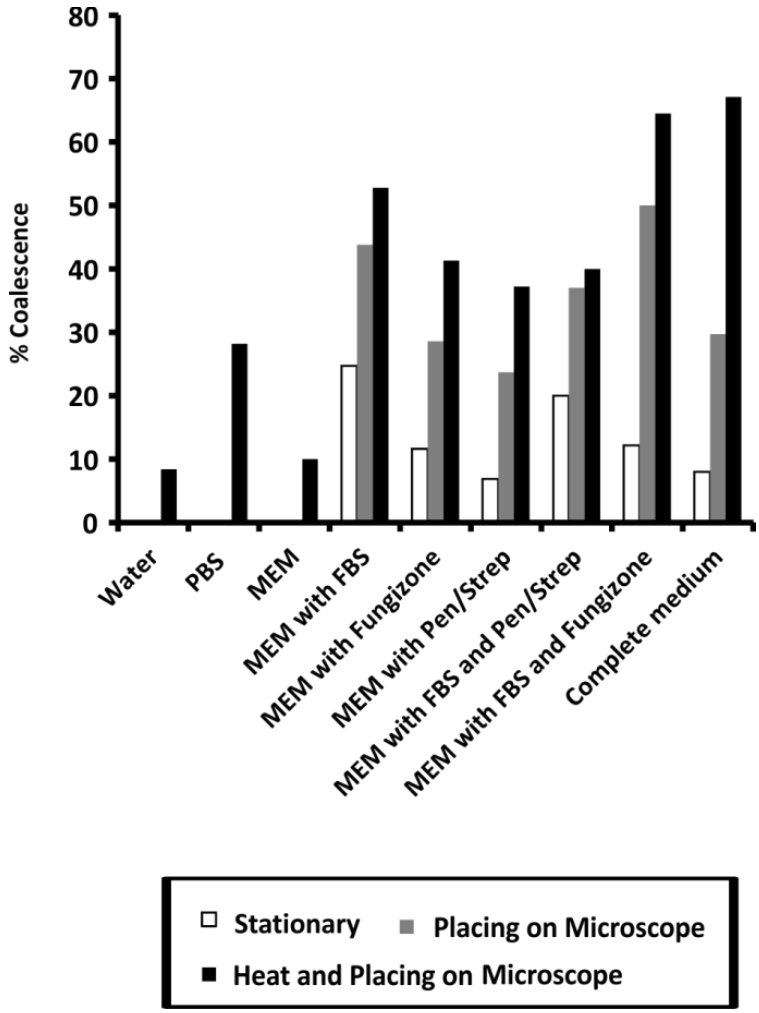

Figure 5.2: Influence of Different Aqueous Phases on Coalescence. Bar chart showing the percentage of droplets which coalesced when different aqueous phases with each aqueous phase either being kept stationary for 30 mins; placed on a microscope and transferred from an incubator to a microscope after 30 mins. Figure adapted from McMillan et al.[30].

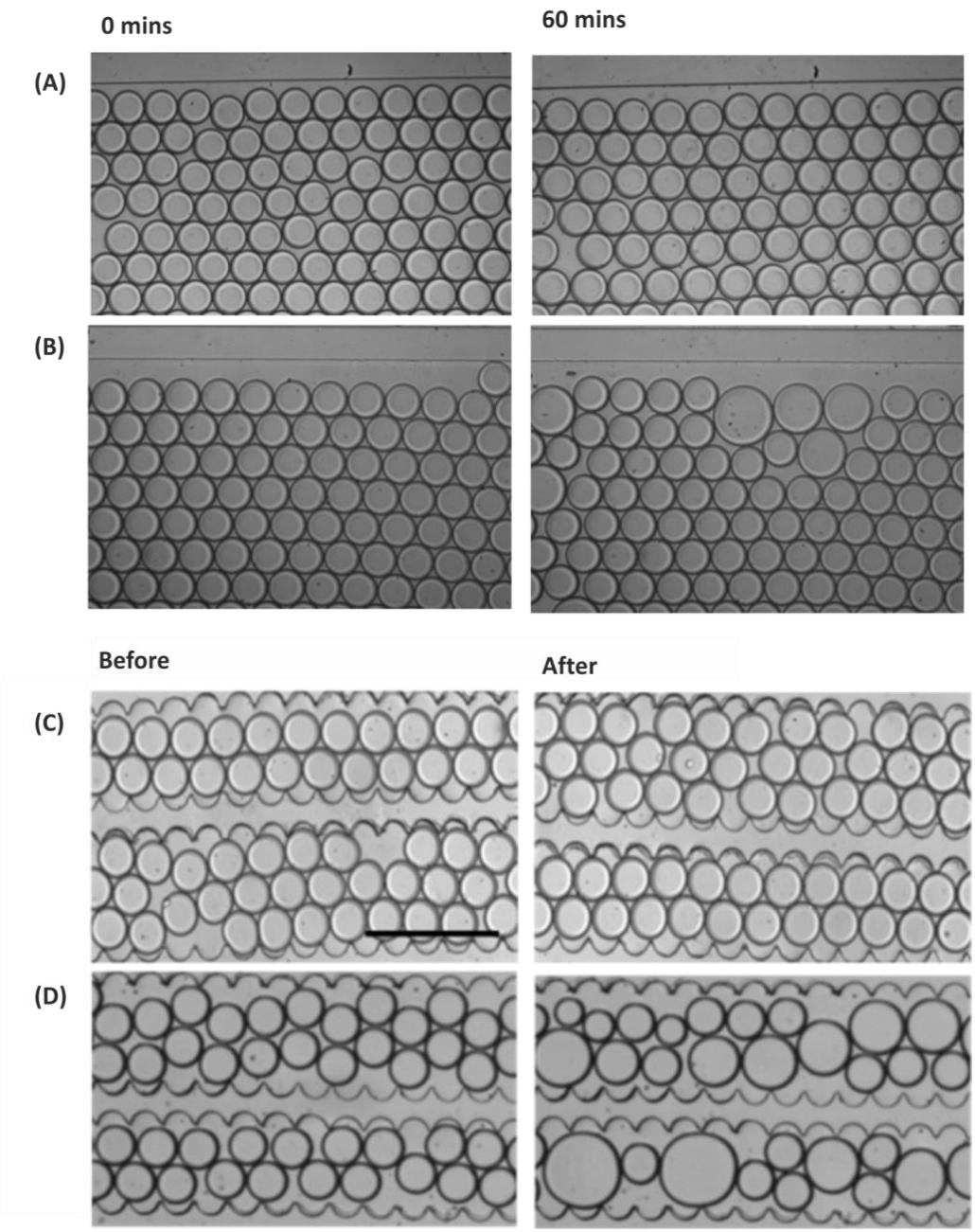

Figure 5.3: Influence of Mechanical Shock versus a Stationary Device on Droplet Coalescence. Brightfield images showing water in oil (A) and (C) and complete medium in oil (B) and (D) droplets within a single chamber device. (A) and (B) show droplets within a stationary device at 0 minutes and 60 minutes and (C) and (D) show droplets within a device before and after the device is placed on a microscope. The scale bar is 350 μm.

5.3. Device 2 – The "Dropspot" Device

5.3.1 Design of Device

As coalescence of droplets was found to be inevitable when using cell medium, the next aim was to develop a device which would store the droplets without having their interfaces in contact. The next device tested was based on the design by Schmitz *et al.*[88] who developed a configuration they named "dropspot" device. The device included a T-junction for droplet formation, a bypass channel and a droplet storage array, as shown in Figure 5.4. The device designed contained 2128 chambers within the storage array for long term storage of droplets. Two different droplet chamber diameters were produced which were 150 μm and 230 μm. Both designs were fabricated using a single layer of SU8 3035 to create features with a thickness of 40 μm for the 150 μm drop chamber device and 100 μm for the 230 μm drop chamber device. The volume of the maximum size of the droplets which could be trapped within the chambers was calculated as the volume of an ellipsoid:

$$V = \frac{4}{3}\pi\, abc\,, \qquad \text{(Equation 5.2)}$$

where the radius of the chamber was used for a and c and half the height of the features was used for b. Using Eq. 5.2 above, the maximum volume of a droplet within a 150 μm droplet chamber is 471 pl and of the 230 μm droplet chamber is 2770 pl. The width of the constrictions between the chambers was 70 μm for 150 μm droplet chamber and 100 μm for 230 μm droplet chambers. The constrictions had to be at least half the diameter of the chambers to prevent the droplets from squeezing through once they were trapped. The trapping of droplets within the chambers occurs as the interfacial tension acts to reduce the interfacial free energy by creating a droplet which is the minimum area for a given volume[126]. As the droplets remain locked within the storage array, there is little if any movement when transporting the device from the incubator to the microscope stage, which allows for long term monitoring of specific droplets. In addition, the droplets would be surrounded by a layer of oil with surfactant, which prevents the droplets from coming in contact with each other and so prevented coalescence. The bypass channel was included in the design to weaken the abrupt pressure change, which occurs once the tubing is unplugged, so that the droplets remain trapped within the storage array[88]. All of the parameters of the 150

μm chamber and 230 μm chamber "dropspot" devices are provided within the appendix.

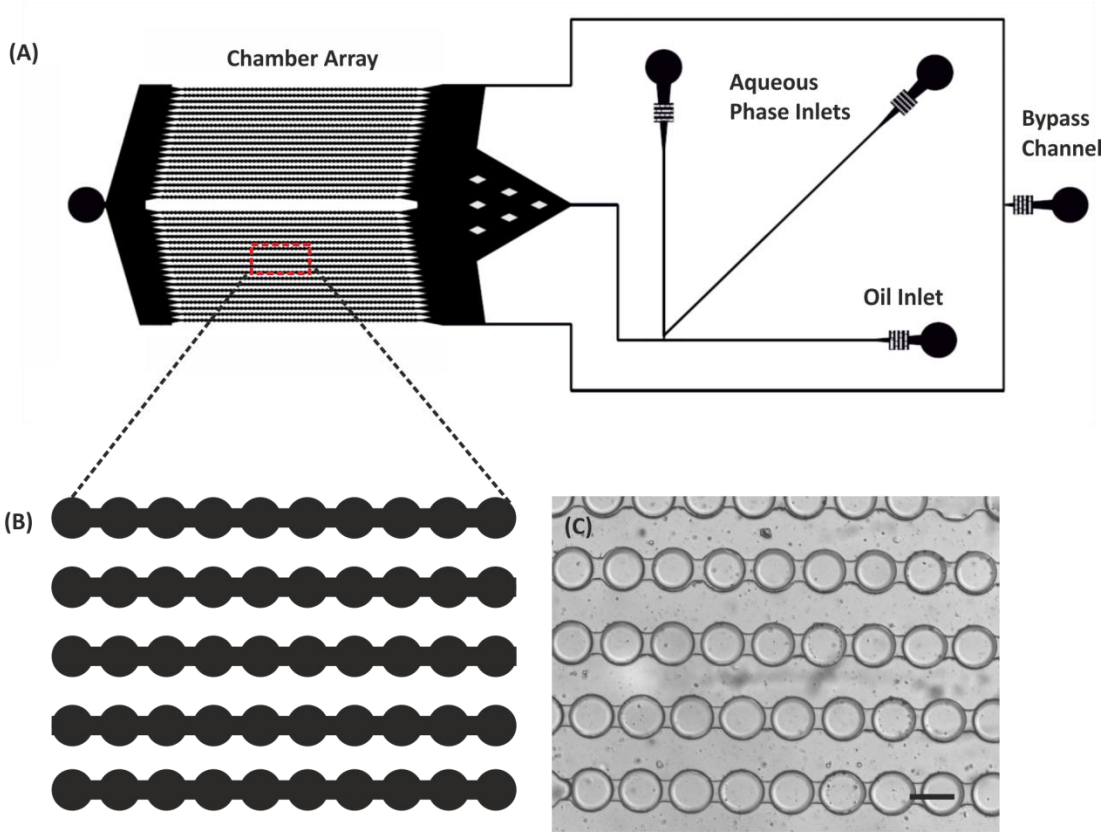

Figure 5.4: "Dropspot" Microfluidic Device Design. (A) Diagram showing the design of the "dropspot" microfluidic device and (B) shows a magnified section of the chamber array of the device. (C) A brightfield image of droplets trapped within the storage array once the flow of the continuous and aqueous phases are stopped. The scale bar represents 150 μm.

5.3.2 Operation of Device

The first parameters which had to be characterised for the "dropspot" device experiments were the flow rates required to achieve droplets of a suitable size for reliable trapping within the chamber array. The best flow rates identified for the 150 μm drop chambers were 0.14 ml/hr for the continuous phase and 0.12 ml/hr for the aqueous phase. For the 230 μm drop chambers the best flow rates were 0.12 ml/hr for the continuous phase and 0.11 ml/hr for the aqueous phase. In experiments which were carried out with droplets containing no cells, the trapping efficiency of droplets was 89%, which equates to 1893 droplets locked in position. A difference in the speed

at which droplets flowed through different scalloped channels within the chamber array was observed (Figure 5.4C). This was due to the shape of the droplet storing chamber area before the scalloped microchannels which created a higher resistance to flow for the droplets. This design feature was corrected in a second version of the device. Over time the droplets, when trapped, began to shrink in size, with them reducing to a third of their size by day 2 due to evaporation of the aqueous content through the PDMS (Figure 5.5). In order to solve this issue the device was placed within a petri dish and submerged within PBS to reduce the rate of evaporation, with little if any reduction in droplet size observed. Another drawback which was observed with this device was that air entered the inlets and outlets of the device when incubated for 2 days or more. Due to this, the droplets which were not trapped within the array and had coalesced began to push the trapped droplets within the channels, causing them to move position and coalesce. To reduce the risk of air entering the device after loading with droplets, the inlets and outlets were sealed with the end of a pipette tip using silicone glue and then filled with UVW medium. Using this method, the duration of trapping droplets without air entering into the device was increased to up to 4 days. A difference in the rates at which droplets flowed through the chamber array was noticed, which would be solved by applying pressure through the bypass channel.

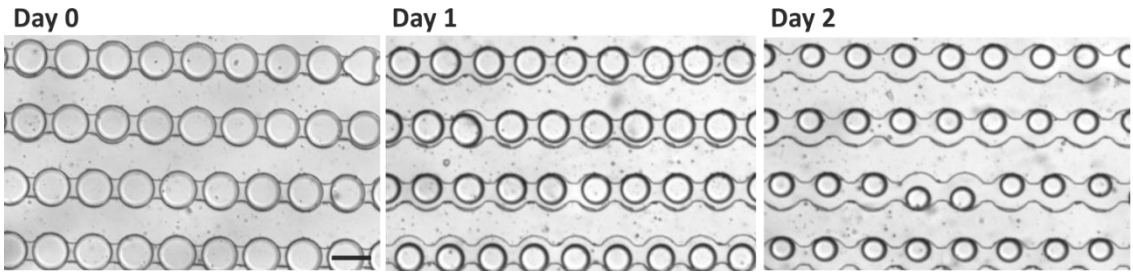

Figure 5.5. Droplet Shrinkage within the "Dropspot" Device. Brightfield images showing the reduction in size of droplets over time when stored within the chamber array and the device is not stored within PBS. The scale bar is 150 µm.

5.3.3 Cell Experiments

The next step was to identify the best cell concentration to achieve multiple cells within droplets. It is known that the encapsulation of cells is random and it follows a Poisson distribution:

$$k = \frac{\lambda^k \exp(-\lambda)}{k!} \qquad \text{(Equation 5.3)}$$

where λ is the average number of cells per droplet. Therefore, the number of cells within droplets increases with increasing the cell concentration used[127]. The initial cell concentration used in the first inlet was 3 x 10^6 cells per ml, with the second inlet containing only medium. At this cell concentration an average cell encapsulation efficiency (percentage of droplets containing cells) of 65% of the 1893 droplets trapped was achieved, with the majority of droplets containing single cells. Approximately 16% of the droplets containing single cells were observed to divide over 70 hours. When the cell concentration was increased to 5 to 6 x 10^6 cells per ml, the encapsulation efficiency increased significantly to approximately 80%, with the vast majority of droplets containing multiple cells. As observed within the medium in oil droplets in chapter 4, multiple cells within the microdroplets aggregated to form compact spheroids within 12 to 24 hours (Figure 5.6).

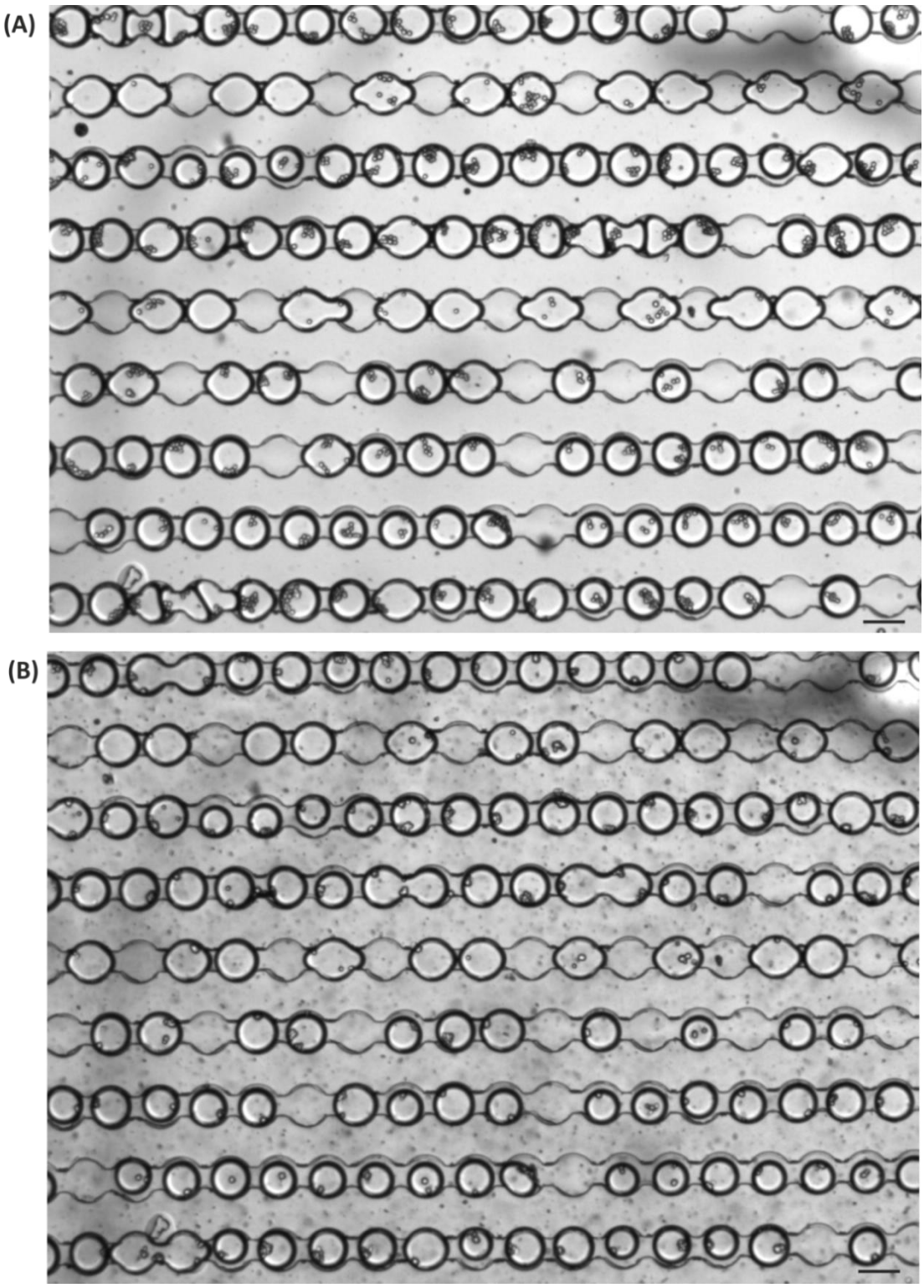

Figure 5.6: Formation of Spheroids within the "Dropspot" Device. Brightfield images of cells encapsulated within droplets and trapped within the chamber array on day 0 (A) and day 1 where they have aggregated together to form spheroids (B). The scale bar is 150 µm.

Unfortunately, due to the limited volume within a droplet, the spheroids formed only lasted for a duration of 2 to 4 days depending on the initial cell concentration within the droplet. The spheroids were considered to be dead once cells had disaggregated from the compact spheroid, as no medium could be exchanged at this point to recover the spheroids as done in Chapter 4. Three different types of spheroids/cell aggregates were formed within the droplets, which depended upon the initial cell number encapsulated within the droplets. The best case was a concentration of cells which resulted in the formation of a spheroid lasting for up to 4 days before cells began to disaggregate from the compact core of the spheroid (Figure 5.7(A)). If the concentration was too high then the cells would aggregate but not form a compact spheroid and just fall apart (Figure 5.7(C)). The third type was the formation of a compact spheroid, with the spheroid then just reducing in size without any cell disaggregation from the spheroid (Figure 5.7(B)). Overall this device showed the high-throughput potential of droplet microfluidics for the formation and storage of spheroids. However, it was not suitable for the long term culture of spheroids, as no spheroid growth was observed and spheroids could only last for a maximum of 4 days before disaggregation occurred. If we consider that the 230 μm chamber device has a maximum volume of 2770 pl (0.002770 μl) per droplet and a droplet containing 20 cells (the approximate maximum number of cells for the condition observed in Figure 5.7(A)), then the medium to cell ratio is 0.0001385 μl per cell. Therefore, at this number of cells per droplet, according to the volume of medium ratio experiments in Figure 4.2, the expected number of days for the spheroids to remain without disaggregation is around 3 to 4 days. Therefore, a different device was required which allowed for the perfusion of spheroids with medium to allow for long term culture.

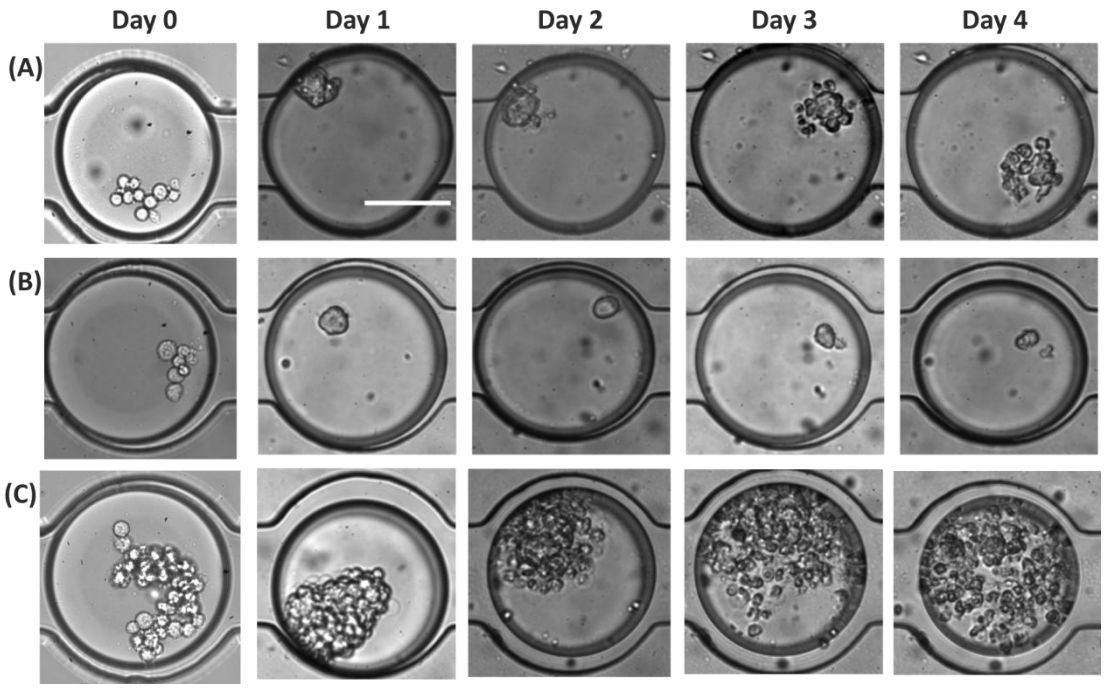

Figure 5.7: Spheroid Formation and Culture within the "Dropspot" Device. Brightfield images showing the formation of spheroids over 4 days within trapped droplets with a medium cell concentration (A), a low cell concentration (B) and a high cell concentration (C). The scale bar is 115 µm.

5.4 Device 3 - A Microfluidic Device for Perfusion

As it was identified that it was difficult to culture spheroids over a long time within microdroplets the next step was to develop a device which allowed for the refreshment of medium. With this in mind, it was deemed not essential for the droplets to remain once the spheroid had been formed. Therefore, a device had to be developed which integrated both droplet microfluidics for the initial formation of spheroids with single phase microfluidics to allow for medium exchange for long term culture. Thus the ability of the cell culture medium to reduce the stability of the emulsion droplets will be explored as a way to coalesce stored droplets.

5.4.1 Design of Device

The device used was based on the designs by Boukellal *et al.*[128] and Vanapalli *et al.*[87], [129], [130] which contains a chamber array with traps allowing for the storage of droplets and a bypass channel to allow for the flowing of droplets to the next trap or out of the device (Figure 4.7 (B)). As in the previous designs, droplets are formed via a

T-junction geometry with an extra channel added, called the air bypass channel, to aid in the removal of air from the device. In order to make sure that the droplets are trapped within the chambers, the resistance ratio between the bypass channel and chamber with restriction channel had to be in favour of the droplets trapping. Additionally, the resistance of the restriction channel has to be high enough to prevent the passing of a droplet through the channel upon the flowing of further droplets through the array. The resistance of channels within the device were calculated using the following equation[131]:

$$R = \frac{12\mu L}{wh^3}\left[1 - \frac{192}{\pi^5}\left(\frac{h}{w}\right)\right]^{-1} \qquad \text{(Equation 5.4)}$$

where μ is the dynamic viscosity; L is the length; w is the width and h is the height of the microfluidic feature. The length and width of each feature has been indicated by the black arrows (with the chamber having the same length and width) and red arrows respectively within Figure 5.8(B) and the height is determined by the thickness of the SU8 spun. The dynamic viscosity of FC-40 oil was 4.1 cP. Three different chamber diameters were designed which were 300, 400 and 500 μm. All of the parameters of the devices are provided within the appendix.

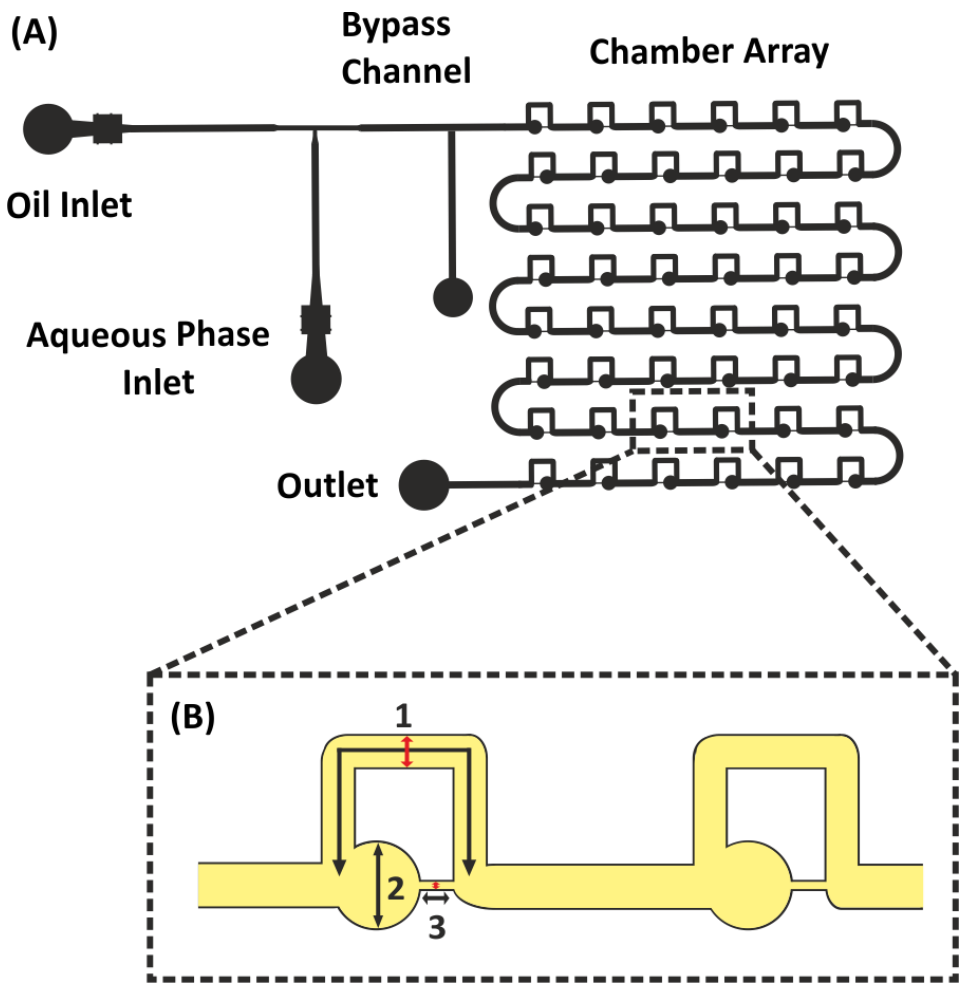

Figure 5.8: Droplet Microfluidic Device Design for Droplet Storage. (A) Droplet Microfluidic design based on previous designs with the features explained in results section 5.4.1 and (B) schematic diagram of the traps within the chamber array: 1 is the bypass channel; 2 is the chamber and 3 is the restriction channel. The black arrows indicate the lengths and the red lines indicate the widths of the bypass channel and restriction channel. The black arrow for the chamber indicate both the width and length.

For all of the chamber diameters the thickness of the features was 180 µm, which was achieved by spinning two 100 µm layers of SU8 3035 (as described in chapter 3). In cases where the width of the channel was significantly smaller than the height the value of the width would need to be switched with that of the height in the resistance equation 5.3. The dimensions, resistances and resistance ratios for the 3 different chamber designs are shown within table 5.1. The resistance ratio was calculated as the resistance of the restriction channel and the chamber divided by the resistance of the bypass channel. If the resistance ratio was less than 1, then a droplet would

preferentially trap within the chamber of the trap as the route into the chamber has a lower resistance than the bypass channel[87]. If the resistance ratio was greater than 1 then the droplets would preferably enter the bypass channel and potentially the droplet after the first would be trapped as the resistance of the bypass would be increased by the presence of the droplet. This type of trapping is referred to as indirect trapping. For this device the aim was to achieve direct trapping where the first droplet entering the storage array gets trapped within the chamber.

Table 5.1: Dimensions of the trap features and calculated resistances and resistance ratios of the storage traps within the chamber array of the microfluidic device. D is the diameter; R is the resistance; L is the length and W is the width. D, L and W are in μm and R is kg m^{-4} s^{-1}. The resistance ratio is the resistance of the chamber and restriction channel divided by the resistance of the bypass channel. The arrows within figure 5.8 (B) indicate the lengths of the bypass channel and restriction channel.

Chamber	Bypass Channel	Restriction Channel	Resistance of Restriction Channel and Chamber	Resistance Ratio
D = 300 R = 3.87×10^{11}	L = 1500 W = 100 R = 1.94×10^{12}	L = 180 W = 30 R = 2.32×10^{11}	6.19×10^{11}	0.32
D = 400 R = 5.16×10^{11}	L = 1800 W = 150 R = 2.32×10^{12}	L = 154 W = 40 R = 1.99×10^{11}	7.15×10^{11}	0.31
D = 500 R = 4.23×10^{11}	L = 2650 W = 150 R = 3.42×10^{12}	L = 435 W = 55 R = 3.68×10^{11}	7.92×10^{11}	0.35

5.4.2 Operation of Device

5.4.2.1 Trapping of Droplets within Storage Chamber

Initially, the ability to trap droplets within the device was tested. As well as the geometries of the traps, the droplet size was also a major factor in influencing the trapping of droplets within the chamber. The droplet size was controlled by changing the flow rate ratio ($Q_R = Q_o/Q_w$). If the droplet size was too large for the chamber, then part of the droplet would enter into the bypass channel of the trap. If a smaller droplet entered after the large trapped droplet the larger droplet would get squeezed, resulting in part of the droplet entering the bypass channel resulting in the displacement of the

droplet. If the droplet was too small for the chamber, it still had the potential to be trapped. However, the smaller the droplet the less medium available to the cells. Furthermore, there is the potential for a small droplet to be pushed into the restriction channel of the trap by another droplet. In order to achieve droplets of the desired size for the 300 μm drop chamber device, the continuous phase was flowed at a rate of 1 μl/min and the aqueous phase at 0.8 μl/min. For the 400 μm drop chamber device a rate of 0.9 μl/min for the continuous phase and 0.8 μl/min for the aqueous phase was selected. And for the 500 μm drop chamber device the continuous phase flow rate had to be slower than the aqueous phase in order to produce large enough droplets, so the flow rates were 0.6 μl/min for the continuous phase and 0.8 μl/min for the aqueous phase. The flow rates used above were required to produce droplets of a large enough size in order to fill the chamber entirely. The flow rates, pressure outside of the droplet and the Laplace pressure also have an influence on the preferred route taken by the droplet. In the study conducted by Boukellal *et al.,* who developed the initial design on which this device is based on, the opening of the bypass channel was suggested to act as a capillary valve[128], [132]. In order for the droplet to flow into the chamber the velocity of the droplet has to be less than the critical velocity (v_c) which can be calculated by the following equation:

$$Vc = \frac{\gamma\left(\frac{1}{w_b} - \frac{1}{w_w}\right) w_R^3}{6\mu\, L_R\ w_w}, \qquad \text{(Equation 5.5)}$$

where ϒ is the interfacial tension; w_b, w_w and w_R are the widths of the bypass channel, chamber and restriction channel respectively; μ is the dynamic viscosity and L_R is the length of the restriction channel. The interfacial tension measured for an aqueous phase with FC-40 and 2% of the fluorosurfactants used is 11 mN/m. The velocity of the droplets entering the chamber was worked out experimentally as the rate at which the droplet was flowing through the channel as it approached the chamber. If the velocity of the droplet is less than the critical velocity then the bypass channel behaves as if it is blocked and so the droplets preferably enter the chamber of the trap. For all of the different chamber diameters tested the velocity of the droplet was less than the critical velocity, allowing droplet trapping. For the 300 μm device, the velocity was 0.9 mm/s and the critical velocity was 1.5 mm/s. For the 400 μm device, the velocity of the droplet was 0.5 mm/s and the critical velocity was 1.9 mm/s. For the 500 μm device, the velocity of the droplet was 0.1 mm/s and the critical velocity was 0.26 mm/s. For

the droplets to trap using these design dimensions the interfacial tension has to be greater than 5 mN/m for the 400 μm and 500 μm designs and greater than 7 mN/m for the 300 μm design. Once the first droplet fills the first chamber, the next droplet flows through the bypass channel due to the droplet blocking the restriction channel and thus directing the flow of the second droplet through the bypass channel (Figure 5.9). A change in design had to be carried out for the 500 μm trap as the bypass channel was too close to the chamber, resulting in there not being enough space for a 500 μm droplet to fit perfectly into the chamber without part of it entering the bypass channel (Figure 5.10). As a result, in the latter configuration, droplets after the one which had been trapped would then squeeze the trapped droplet, resulting in part of it entering the bypass channel and ultimately being pushed out of the chamber (Figure 5.10). Once the chamber array was full of trapped droplets, the flow of the aqueous phase was stopped and the connector was taken slowly out of the inlet to remove any medium which could enter the device. The inlet was then blocked again with the aqueous phase to prevent the oil from flowing through the inlet, which would have less resistance in comparison to the outlet. The continuous phase was then flown through the device to remove any droplets which were not trapped. This reduces the risk of them coalescing with trapped droplets, which would increase their size and increase the risk of displacement from the trap.

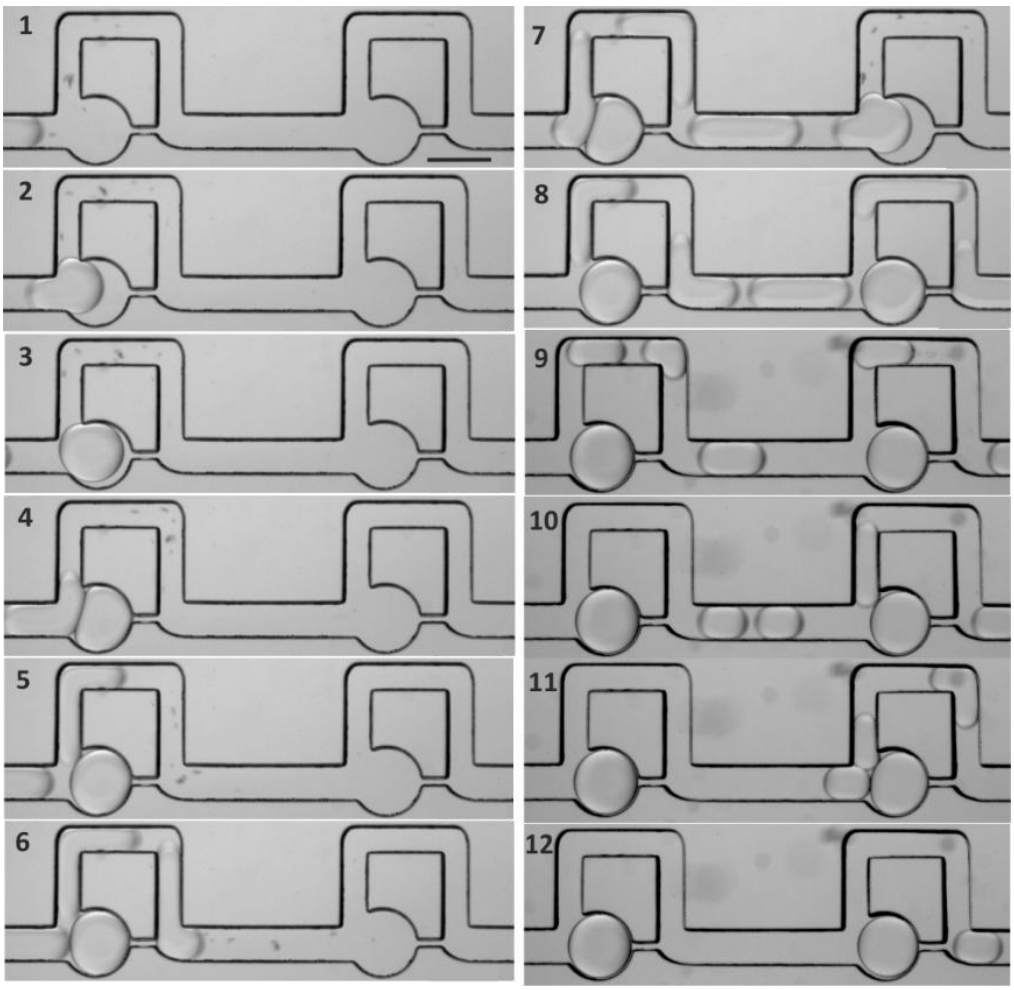

Figure 5.9: Droplet Storage, Bypassing and Clearing of Droplets within the Device. Brightfield images of the storage of droplets (1 and 2); bypassing of droplets once the first chamber is full (3 and 4); filling of the second chamber (7 and 8) and clearing of droplets from the chamber array (9 – 12). The droplets formed within the device. The scale bar equals 400 μm.

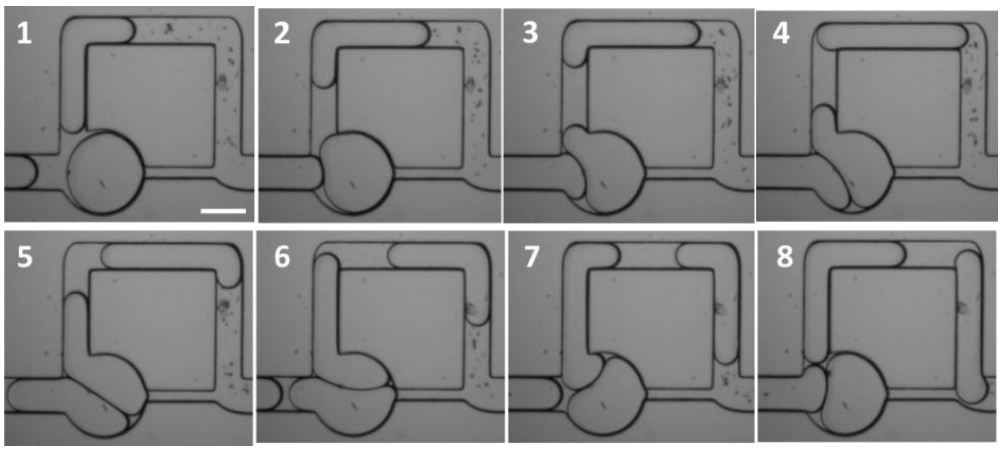

Figure 5.10: Displacement of Droplets in 500 µm Chambers. A timelapse of brightfield images showing the displacement of a trapped droplet by another in a storage array with 500 µm chamber device. The scale bar is 250 µm.

5.4.2.1 Coalescence of Droplets within Storage Chamber

The next feature of the design which was tested was the ability to coalesce the trapped droplets with medium to allow for substance exchange. It has previously been shown in section 4.2.1 that the supplements used to make up the UVW cell medium increased the risk of coalescence of droplets. Therefore, this property of the medium was tested to determine if droplet interface instability could be induced within this microfluidic device. To achieve this, a long plug of aqueous phase was formed and could be flown through the storage array to then come in contact with the trapped droplets to determine if they would coalesce (Figure 5.11). Two different aqueous phases (one as a negative control and one as a positive control) were compared, which were water and UVW cell medium with each containing 100 µM of calcein to visualise the breaking of the interface during coalescence. Prior to the long plug of calcein being flown through the chamber array the long calcein plug was flown through the two inlets to remove any air which would get into the chamber array and displace the droplets before coalescence could occur. The continuous phase inlet was blocked and the long plug of aqueous phase was flown through at a rate of 0.4 µl/min for both aqueous phases tested. As is observed in Figure 5.11, once the long plug entered it did not result in the displacement of droplets and instead remained within the bypass channel and in contact with the droplets. When water was used as the aqueous phase no coalescence of the plug with droplets was observed, even over several minutes, with the calcein

remaining within the plug. In contrast, when cell medium was used, coalescence of the droplet with the long plug was observed within seconds of the long plug being flowed into the device. This can be observed in Figure 5.11(1 to 4) where the interface between the droplet and oil remains and then breaks, and in Figure 5.11(5 & 6) where the interface has broken and calcein enters the droplet. The rupture of the interface of one droplet took approximately 25 seconds to occur, measured from the initial contact of the long plug with the droplet to the entering of the calcein into the chamber after coalescence. To make sure that the aqueous plug, now coalesced with all the droplets, did not retract from the outlet it was important to ensure that the outlet was full of medium and did not contain the oil with surfactant.

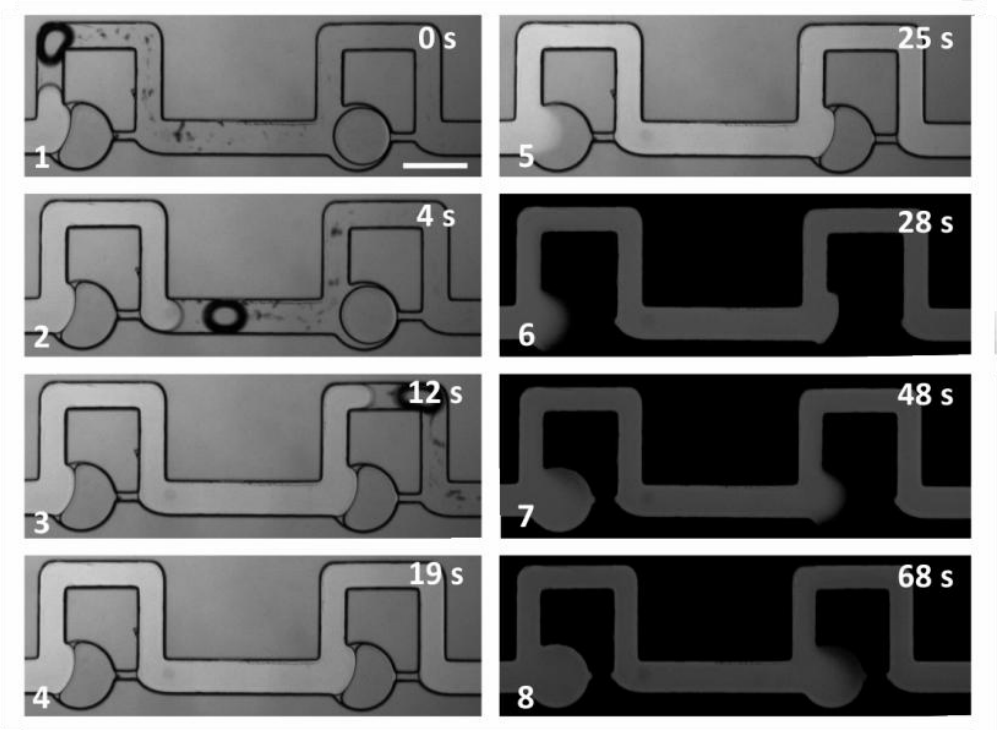

Figure 5.11: Coalescence of Droplets with a Long Plug of Medium. Brightfield (1 to 5) and fluorescent images (6 to 8) of a long plug of medium with calcein interacting with droplets with only medium and a continuous phase of FC40 +2% surfactant. Images 1 to 3 show a long plug of medium with calcein entering the chamber array and coming into contact with the droplets in the traps. Images 5 to 8 show the interface between the droplets and plug has broken, with calcein entering the droplets with the process for two traps in a row taking 68 seconds. The scale bar equals 400 µm. Figure adapted from McMillan et al.[30]

5.5. Discussion for Chapter 5

Within this chapter I have shown the development process involved in producing a droplet microfluidic device which is suitable for the storage of droplets and substance exchange. In contrast to the majority of other studies, this investigation only tested the potential of a single device to be used in contrast to multiple ones to reduce the complexity of the procedure. With a single device there is no requirement to connect devices together with further tubing or having to withdraw the droplets and place them into another device, which could further damage the droplets. Overall from the development process and results from chapter 4 it was identified that it was not possible to use only a droplet microfluidic device for long term spheroid culture. As a result a microfluidic device was developed which integrated both droplet and single phase microfluidics.

5.5.1. Influence of Cell Medium on Coalescence

The first important point that was identified with the single chamber devices was that the properties of the cell culture medium caused coalescence of droplets. As a result, the single storage chamber could not be used for the long term storage of droplets as individual droplets could not be monitored over time as they would coalesce into one large droplet. Fluorosurfactants with polyethylglycol heads, similar to the ones used within this study, have been shown to produce very stable emulsions when water is used as the aqueous phase[91]. Furthermore, the results within this chapter showed that when MEM was used by itself it had similar results to water and PBS, with coalescence only occurring once the temperature was increased. In contrast, when supplements were added to MEM such as FBS, Fungizone and penicillin/streptomycin, either alone or in combination, there was a significant increase in the percentage of coalescence which occurred even when the device was left stationary. Due to the complexity of the composition of FBS used within the medium it is difficult to identify the exact cause why FBS increases the risk of coalescence. However, one possible cause could be the albumin found within FBS as it has previously been shown that bovine serum albumin (BSA) lowers the stability of emulsions of fluorosurfactants[91]. This is thought to be due to it displacing surfactants from the interface, resulting in the droplets not being fully covered by surfactants[91]. The increased risk of coalescence

due to physical shock or increased temperature is to be expected. The chance of droplet coalescence increases with increasing temperature due to the lowering of the viscosity of the continuous phase between the droplets, resulting in the drainage of the continuous phase between the droplets. As a result the droplets are less evenly covered with oil with surfactants and so the chance of the aqueous phase droplets coming into contact and coalescing increases[133], [134]. For mechanical shock the chance of coalescence is increased as there is an increased chance of collisions between droplets in comparison to the droplets remaining stationary.

5.5.2. Spheroid Formation and Culture within Microdroplets

The next point identified using the "dropspot" device was that spheroids would form within single emulsion microdroplets. This was apparent when the "dropspot" device was tested as spheroids would form within trapped droplets within 12 hours. However, one of the major limitations was the duration of time at which the spheroids would remain intact. As observed when too high cell numbers were encapsulated within the droplet, the spheroid would break apart within days with the best case scenario being up to 4 days of culture. Furthermore, the spheroids encapsulated within the device were not observed to increase in size over time. Thus, this device would only be suitable for short term investigations, such as for single cell analysis or whether different types of cells form spheroids using this medium in oil system. In order to increase the potential duration for the culturing of spheroids, refreshment of medium is essential. As previously discussed the "dropspot" device has been used recently in a study for the formation of spheroids within alginate beads[21]. Within this study, the authors found that the device was suitable for on-chip gelation of alginates as well as spheroid formation within the beads. Furthermore, Sabhachandani *et al.* could perfuse the spheroids with medium due to the use of alginate beads to allow for long term culture. The spheroids formed within the device were only cultured for a maximum of 4 days and the spheroids formed were more similar to aggregates rather than compact spheroids. Thus even though the "dropspot" device was not suitable for spheroid culture within aqueous droplets it could be used for the formation of alginate beads. Furthermore, in the future, a potential application for this device would be to form Matrigel beads for spheroid culture as they could then be perfused like the alginate beads without the requirement for coalescence. In contrast to alginate, the use of Matrigel would provide a more accurate reflection of the extracellular matrix observed

within the tumour microenvironment due to the presence of growth factors and proteins such as laminin, collagen and enactin.

5.5.3 Development of a Droplet into Single Phase Microfluidic Device

The final device design which was tested was found to be successful for both the storage of aqueous droplets and for substance exchange via coalescence.

The trapping of the droplets was successfully achieved for the 300 μm and 400 μm devices with a change of geometry required to the 500 μm device design. A resistance ratio of between 1 and 1.5 was found to be successful for the direct trapping of droplets as described by Vanapalli *et al.* However, in their study, they observed that using a Q_w/Q_o of between 0.8 and 1 resulted in a droplet which was too large and split, which was not observed within this chapter. For the here designed device, larger droplets were required in order to fill the whole chamber. It is known that one of the factors which has an influence on the size range of droplets formed is the flow rate ratio[81], [135], [136]. If the continuous phase flow rate is increased to higher than the aqueous phase flow rate then the thinning and shearing of the aqueous phase entering the channel occurs quicker, resulting in the formation of smaller droplets. In order to create larger droplets, the continuous phase flow rate has to be reduced to be a similar flow rate as the aqueous phase or even lower, so that the thinning and ultimately the shearing of the aqueous phase plug neck does not occur as quickly. Thus this allows more of the aqueous phase plug to enter the continuous phase channel until breakage of the aqueous phase plug to form droplets occurs. Another factor which also has an influence on droplet size is the capillary number due to its effect on the deformability of droplets. However this variable was not changed in the study of the devices in this chapter[81], [135], [136]. As a result, the flow rate ratios had to be higher for the device developed in section 5.4 in order to form large enough droplets which could be trapped in the chambers.

In contrast to other studies using a similar device the surfactant concentration did not have to be reduced or removed completely due to the discovery that the medium resulted in coalescence[85], [129], [130]. In a recent study by Wen *et al.,* they encapsulated *Caenorhabditis elegans* (*C. elegans*) within droplets and found that they had to reduce the surfactant concentration to 0.001% before they managed to merge their droplets for substance exchange[85]. The low surfactant concentration was also

essential for forming the droplets containing C. elegans as Wen *et al.* would flow through a single long plug with the droplets forming due to the breakage of the plug at the trap. In a different study by Vanapalli *et al.*[130] they had no surfactant within the continuous phase to cause the merging and splitting of droplets. However, in both of those studies the surfactant was not essential to the culturing of cells to form multicellular tumour spheroids[130]. In a different study by Vanapalli *et al.*[129] they formed the droplets using a different method which involved the formation of a long plug which then split at the traps within the chamber array to form droplets. This again was carried out with no surfactant within the oil. In this study, it was preferred for the surfactant concentration to remain at 2% as chapter 4 has shown that it allows for the formation and long term culture of spheroids[28]. Furthermore, in order to carry out viability staining and drug treatment of spheroids it is preferred that the droplet is removed, to prevent the risk of a reduced initial concentration from leakage of a viability dye or drug.

Another advantage of the design used was that it did not involve the use of microvalves like in the device used by Wen *et al.* which adds to the complexity of the design and fabrication procedure. However, a limitation of the design tested within this chapter is that the traps are altogether within a serpentine, thus there is the inability to have different concentrations or drugs within a single device. By incorporating the microvalves into the device Wen *et al.* were able to have individual rows with different concentrations or solutions.

In contrast to the single chamber device and "Dropspot" device, glass syringes were used as they have been shown to be more responsive to changes in flow rate as well as produce a steadier flow in comparison to plastic syringes[137]. This was essential in the initial characterisation of the device to determine the most suitable flow rates for droplet formation and for coalescence of the trapped droplets. When considering perfusion of the device, the flow needs to be slow and steady with few fluctuations so that when spheroids are within the traps of the storage array they are not displaced by slight fluctuations in the flow.

The next challenge to be overcome with the developed microfluidic device is whether it is suitable for the formation and long term culture of spheroids. Experimental evaluation of spheroid culture within this device is provided within chapter 6, where the potential of this design to be used for radiotherapeutic and chemotherapeutic

analysis was also investigated. This has previously not been shown within a droplet microfluidic device for spheroid formation and culture. In addition, the potential of this device to be used for the culture of spheroids within alginate beads was also investigated.

Overall within this chapter a device suitable for the storage and coalescence of droplets was developed. This opens up the potential for the formation and long term culture of spheroids via substance exchange, with the results and evaluation for this shown within the final results chapter 6.

6. Characterisation of a Droplet Microfluidic Device for the Culture and Anticancer Treatment of Spheroids

6.1. Introduction

This chapter explores the potential of the devices developed within Chapter 5 for the storage of droplets and substance exchange for long term spheroid culture and drug perfusion. As previously shown in chapter 4, in order for spheroids to remain in a proliferative state, the refreshment of medium is essential. In this chapter the ability to coalesce trapped droplets containing medium was evaluated to test if this method could be used for refreshment of spheroids. Furthermore, the suitability of this method for the injection of viability stains and anticancer drugs was also investigated. A similar device to the one developed within chapter 5 has been used by Wen *et al.* for the culture of *Caenorhabditis elegans (C. elegans)* within droplets which allows for substance exchange[85]. However, substance exchange has previously not been achieved for multicellular tumour spheroids formed using droplet microfluidics within a single microfluidic device. Once the conditions were identified for the culture of spheroids, the potential of this droplet microfluidic platform for radiosensitivity and chemosensitivity assays was investigated. To conclude, the potential of this device to be used for the formation of alginate beads for the culture of spheroids within the same device, assessed. The use of alginate beads in spheroid culture is important as some cells are unable to form spheroids in non-adherent conditions due to anchorage dependence. Previous studies have focused on the development of a device or multiple devices suitable for either aqueous droplets or alginate beads/microcapsules but have not investigated the potential for a single device to be used for both applications.

6.2. Spheroid Culture within Medium in Oil Droplets in Device

6.2.1. Cell Encapsulation and Spheroid Formation

The first parameter tested using the device developed within chapter 5 section 5.4 was the trapping of droplets containing cells for the formation of spheroids. Droplets containing cells were formed in a similar method as described previously (Chapter 5)

and trapped within the storage array shown in figure 5.8. A cell concentration of 3 to 4 x 10^6 cells per ml was used to obtain multiple cells within droplets. This was lower than the single chamber devices and "dropspot" device as only one inlet for the aqueous phase was used for this device configuration. The previous designs used a second aqueous phase inlet, which acted as a medium only inlet to dilute droplets containing cells. This was deemed not essential for the design developed in this chapter, as in experiments involving cells in the previous designs the second inlet was rarely used as the range of cell numbers per droplet could be adapted through changing the cell concentration. For all cell based experiments, a 400 μm chamber device was used (Figure 6.1). During the withdrawal of cells, it was essential to mix the cell suspension to reduce the risk of cells settling at the bottom of the Eppendorf tube and subsequently forming a pellet of cells that could be withdrawn and block the tubing. It was found that, over time, blockages would form which were a result of the cells settling within the tubing and aggregating together. Due to the ability of the cells to form aggregates within the tubing, the flow rates had to be altered depending on the number of cells first entering the inlet, in order to achieve the perfect droplet size. A slight variation in droplet size formed via the T junction was observed due to differences in cell concentration whilst dispensing. Occasionally, small droplets would form at the junction after the initial connection of the tubing containing a cell suspension to the device inlets when carrying out cell based experiments (Figure 6.1). The formation of small M/O droplets was due to a blockage of the tubing with cell aggregates, resulting in a lower than expected aqueous phase flow rate. As a result the continuous phase flow rate was much greater than the aqueous phase flow rate, leading to a higher flow rate ratio and thus the formation of small droplets. The small droplets had no impact on the trapping or bypassing of droplets and would be removed during the filling of the storage array.

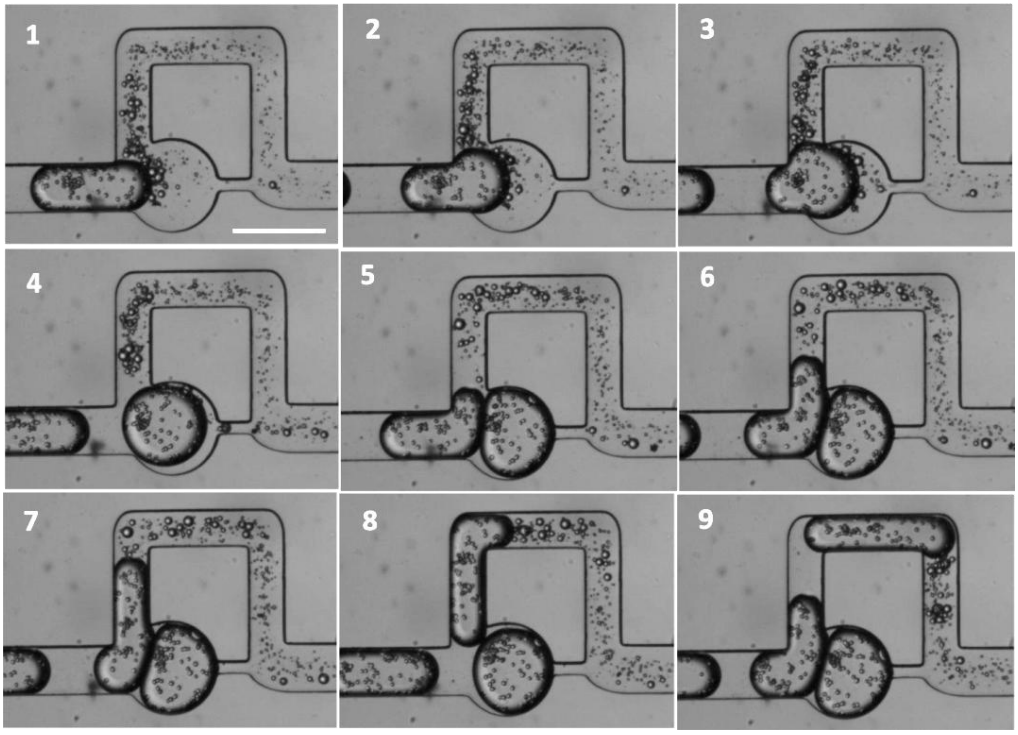

Figure 6.1: Droplets containing cells trapping and bypassing within the chamber array. Brightfield timelapse images showing the trapping of a droplet containing cells (1 – 4) and subsequent droplets bypassing to move onto the next traps (5 – 9).The smaller droplets out with the larger droplets containing cells were created before the first droplet and do not contain cells. Scale bar is 400 µm.

The number of cells encapsulated within droplets ranged from approximately 60 to 160 cells per droplet. The cells within droplets aggregated to form compact spheroids within 6 to 18 hours depending on the initial cell number (Figure 6.2). The trapping efficiency of droplets containing cells was high with nearly every trap filled in the majority of experiments (Figure 6.3). In addition, the droplets did not displace from the traps even though there was a slight shrinkage of the droplets over time due to evaporation. Spheroids formed ranged in diameter from 40 to 150 µm, depending on the initial cell number within the droplet.

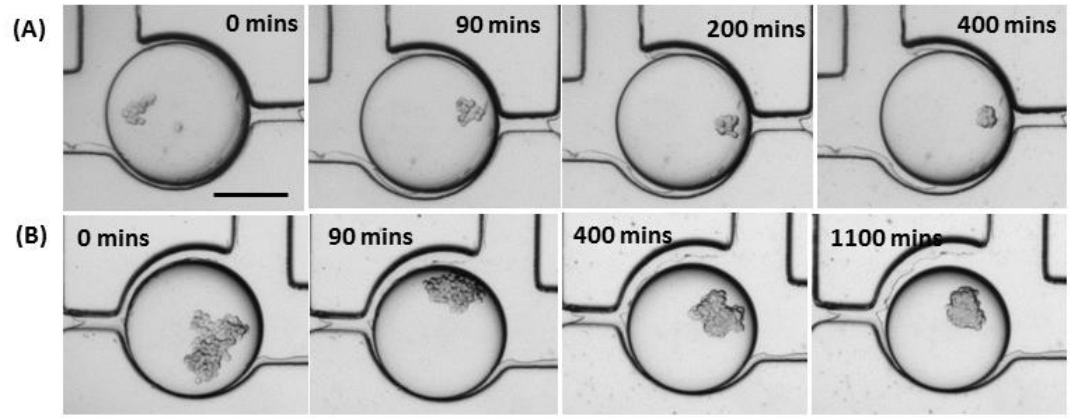

Figure 6.2: Spheroid Formation within Medium in Oil Droplets. Timelapse sequence of brightfield images of cells within droplets forming into spheroids over time with (A) a low number and (B) a high number of cells. The scale bar represents 200 µm.

6.2.2. Coalescence of Droplets for Medium Exchange

The next feature of the device tested was the ability to coalesce a long plug of medium with trapped droplets containing spheroids for medium refreshment. After 24 hours of droplet incubation within the storage array, a long plug of medium was flown through the device at a rate of 0.4 µl/min. The medium was flown through the air bypass channel (figure 5.8) to prevent any cells which remained in the aqueous phase inlet from displacing trapped droplets. Prior to creating a long plug of medium through the storage array's serpentine channel, the device was removed of air bubbles from the channels by flowing the continuous phase. Once the air was removed, the remaining inlets were blocked to allow the long plug of medium to flow through the storage array. The long plug of medium coalesced with droplets within 20 to 30 seconds of being in contact. A slight variation in time was observed between the time taken for the coalescence of droplets with the long plug, but overall all of the droplets within the storage array coalesced. Overall, the majority of spheroids were not displaced from their traps. However, a few were displaced due to the presence of air within the storage array which entered during incubation and could not be removed prior to flowing through the plug or if the droplet was too small for the trap.

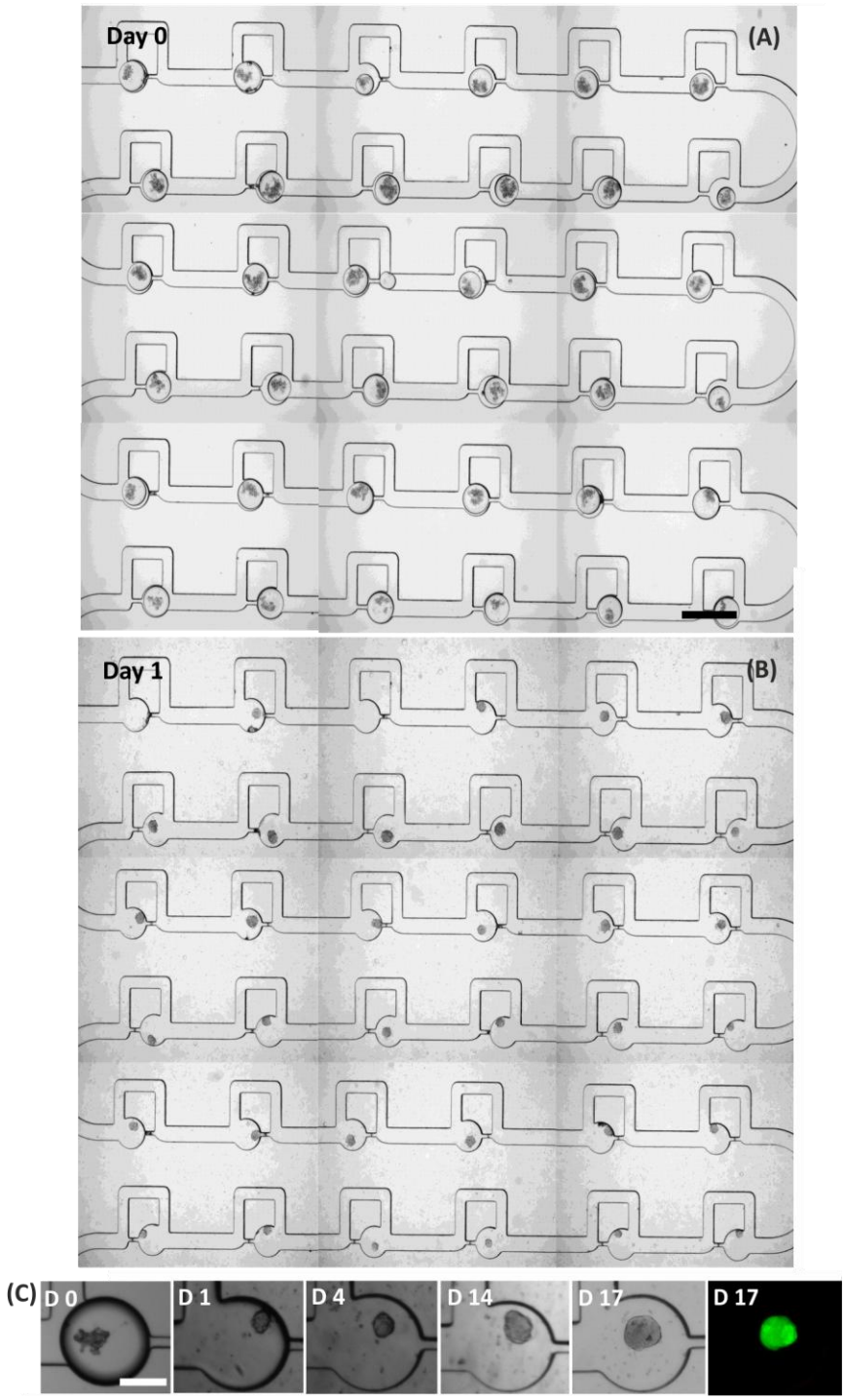

Figure 6.3: Spheroid Formation and Culture within the Device. Brightfield images of cells within droplets trapped within the array on day 0 (A) and as spheroids with the droplets coalesced with medium on day 1 (B). (C) shows a timelapse of spheroid formation after coalescence over 17 days with a spheroid stained for FDA and PI on day 17 (with D0 to D17 representing the day). The scale bar for (A) and (B) equals 400 µm and for (C) equals 200 µm.

After the droplets were coalesced, the device was perfused every 2 days with fresh medium and the growth of spheroids was monitored. If medium was only perfused for 10 minutes at 0.4 µl/min, a difference in the growth of spheroids throughout the storage array was observed (Figure 6.4). Spheroids within the first 4 rows of the serpentine increased in size whereas the bottom 4 rows either remained the same size or decreased in size. The reduction in spheroid size of those spheroids further away from the source of fresh medium (inlet), suggested that the perfusion time was not long enough. Therefore, the lower rate in spheroid growth for spheroids closer to the outlet could potentially be due to a lower amount of nutrients reaching the sites and waste products not being sufficiently washed away.

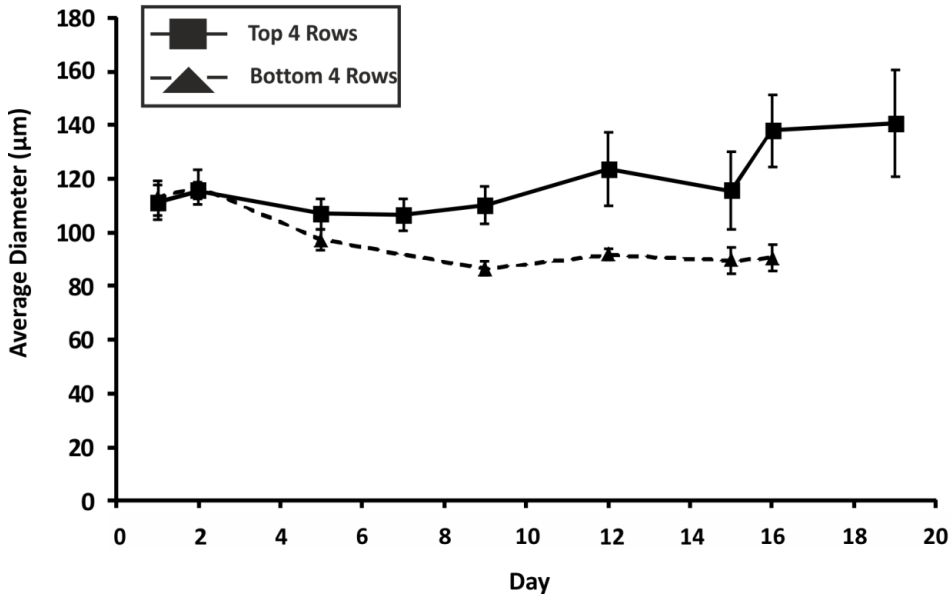

Figure 6.4: Influence of Medium Perfusion Time on Spheroid Growth. Growth curves showing the average diameter of spheroids ± standard error of the mean (error bars) over 16 to 20 days which were only perfused for 10 minutes. The solid line represents spheroids which were within the top four rows of traps of the chamber array and the dashed line represents the bottom four rows of traps of the chamber array. The number of spheroids (n) for the top 4 rows was n = 10 and for the bottom 4 rows was n = 9.

In contrast, perfusion of medium carried out at a rate of 0.4 µl/min for approximately 20 to 30 minutes resulted in a uniform growth of spheroids throughout the storage array. Spheroids remained compact and did not disaggregate or begin to adhere to the device even after perfusion with medium over 17 days. Additionally, little disaggregation of spheroids over time was observed, further demonstrating that the

spheroids were receiving adequate medium. The viability of spheroids was confirmed by carrying out live/dead staining with FDA and PI with no dead cells observed after 17 days of culture. One of the issues with the device was that due to the variability in the concentration of cells entering the device there was a variation between different experimentsof the initial cell number encapsulated within droplets (Figure 6.5). As a result there was variability in the initial spheroid sizes observed and therefore the final average diameter obtained for spheroids. However, a positive result of this observation, was that there was low variation in spheroid diameters within individual experiments for example a control device and a device to be treated with radiation. In addition the growth curves for the spheroids with different initial spheroid sizes were similar (Figure 6.5). The variation in the number of cells encapsulated within droplets from day to day could be a result of the aggregation of cells being different within tubing due to difference in timing in setting up experiments between days.

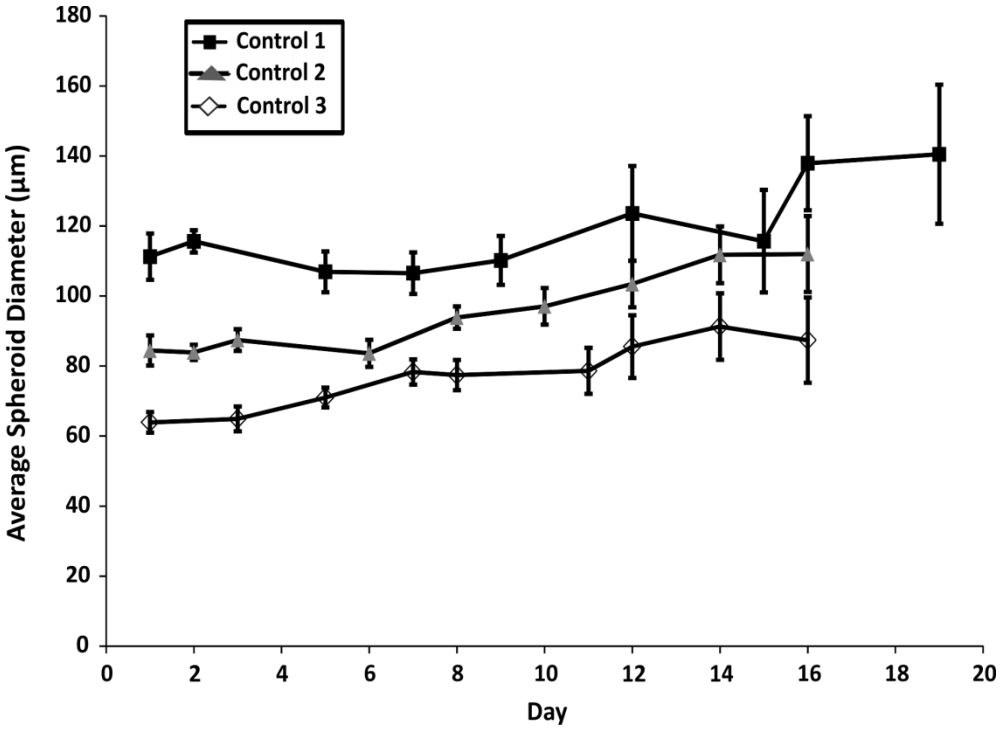

Figure 6.5: Spheroid Growth within the Device for Different Experiments. Growth curves showing the average spheroid diameter ± standard error of the mean (error bars) of spheroids over 16 to 19 days from 3 separate experiments.

6.3. Irradiation Treatment of Spheroids

To determine if the device materials were suitable for radiotherapy assays, dosimetry tests were carried out to determine if radiation was absorbed by the device before it reaches the spheroids. The materials which were tested included a glass slide, a piece of PDMS and PDMS bonded to a glass slide. An average of three measurements were taken for each material at each dose (1 Gy, 3 Gy, 6 Gy and 10 Gy). At 10 Gy the average doses measured after passing through each material were was 9.02 Gy for the glass slide, 9.25 Gy for PDMS and 8.21 Gy for PDMS bound to a glass slide. Overall it was found that the glass slide alone absorbed the most radiation in comparison to PDMS alone and PDMS bonded to the slide absorbed the most radiation with a 17% loss in the X-ray dose delivered (Figure 6.6). From these measurements the dose of radiation being received by the spheroids could be estimated.

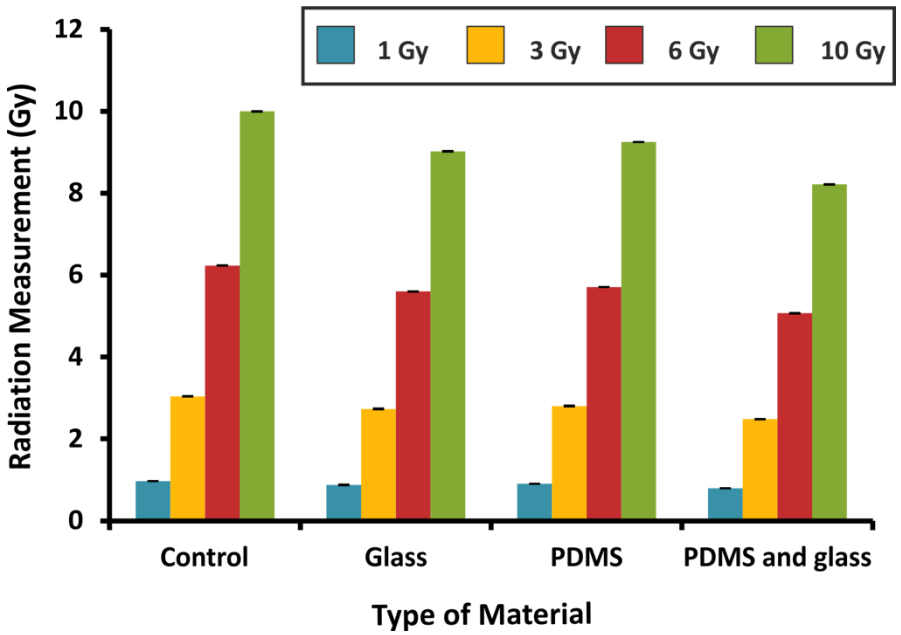

Figure 6.6: Influence of Microfluidic Device Materials on X-Ray radiation. A bar chart showing average measurement of x-ray radiation (n=3) ± standard deviation (error bars) when passed through different materials used for microfluidics which were glass, PDMS and PDMS bonded to a glass slide. The different radiation doses tested were 1, 3, 6 and 10 Gy.

As a proof of principle, an experiment was conducted with a dose of 8 Gy, which was shown to have a detrimental effect on UVW glioma spheroid viability (Chapter 4 section 4.6). Spheroids were initially formed within droplets, coalesced and perfused with medium every second day as described previously. Spheroids were treated with 8 Gy on day 7 of culture. Spheroid growth and any signs of cell death, such as disaggregated cells, were monitored and compared to a control group (0 Gy). A significant reduction in spheroid diameter was observed in comparison to the control within day 12 of culture (Figure 5.7) with a p value of less than 0.05 ($p = 4.03 \times 10^{-4}$). Furthermore, higher levels of disaggregation of cells from treated spheroids were observed, in comparison to the control group and live/dead staining confirmed that these disaggregated cells were dead. The culture was only carried out for 12 days due to the potential for washing out spheroids after the radiation treatment. After treatment the spheroid would begin to disaggregate as the cells would die from the radiotherapy this resulted in a reduction in the size of the spheroid making it easier to be washed out during perfusion either via the bypass channel. Additionally if the

spheroid fully disaggregated the spheroid would be washed out and a spheroid measurement could not be taken to assess the influence of treatment on spheroid size.

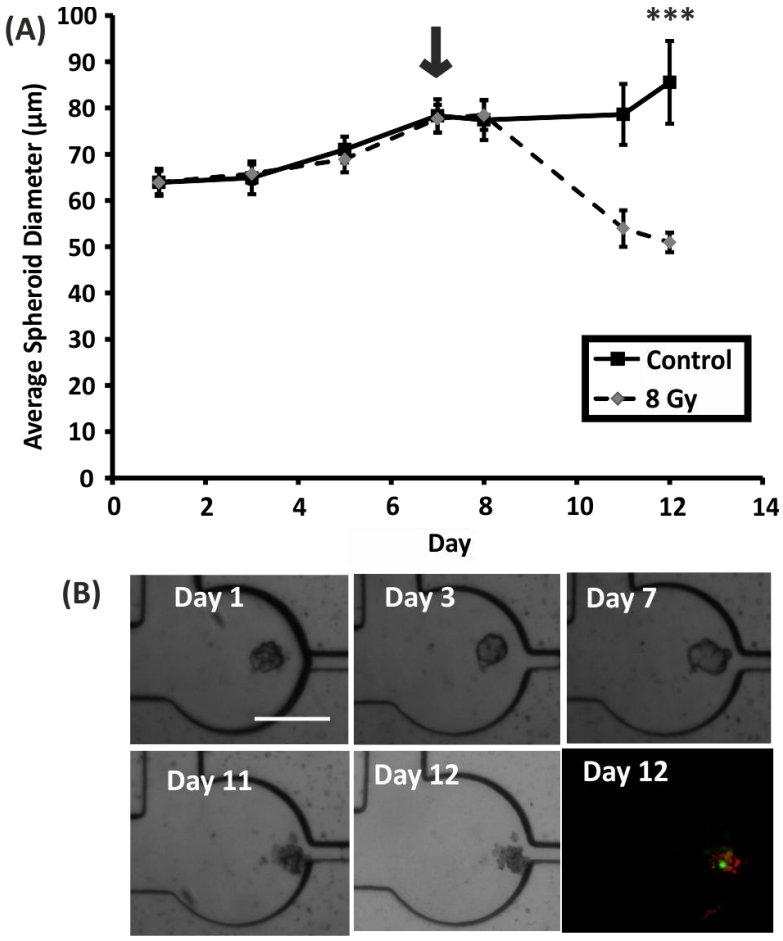

*Figure 6.7: Radiation Treatment of Spheroids. A growth curve (A) showing the average spheroid diameter (µm) over days for control and spheroids treated with 8 Gy on day 7 with the error bars representing the standard error of the mean. A timelapse of images over 12 days showing spheroids treated with 8 Gy on day 7 and a live/dead stain of a spheroid on day 12. The scale bar equals 200 µm. *** represents a p value ≤ 0.001.*

6.4. Effect of Drug Treatment on Spheroids

To test the potential of the device for performing drug treatments, the spheroids were treated with cisplatin and doxorubicin. Spheroids were formed within droplets, coalesced and perfused with medium every 2 days, as described previously in sections 6.2 and 6.3. Either cisplatin or doxorubicin was perfused through the device at a rate of 0.4 µl per min^{-1} for 30 minutes on day 7 of spheroid culture. On day 8, medium was perfused through the device to wash out cisplatin or doxorubicin from the device, thus the drug incubation time assessed was 24 hours. A significant reduction in spheroid diameter was observed in comparison to the control 7 days after treatment with a p value of less than 0.01 for both cisplatin and doxorubicin (Figure 5.8). As was observed with the irradiated spheroids, the reduction in size was caused by cells disaggregating from spheroids. The viability of the spheroids was confirmed using live dead staining with dead cells disaggregated from the compact spheroid. Thus this demonstrates that the device allowed for drug treatment and that the drug exposure time was effective for induction of cytotoxicity.

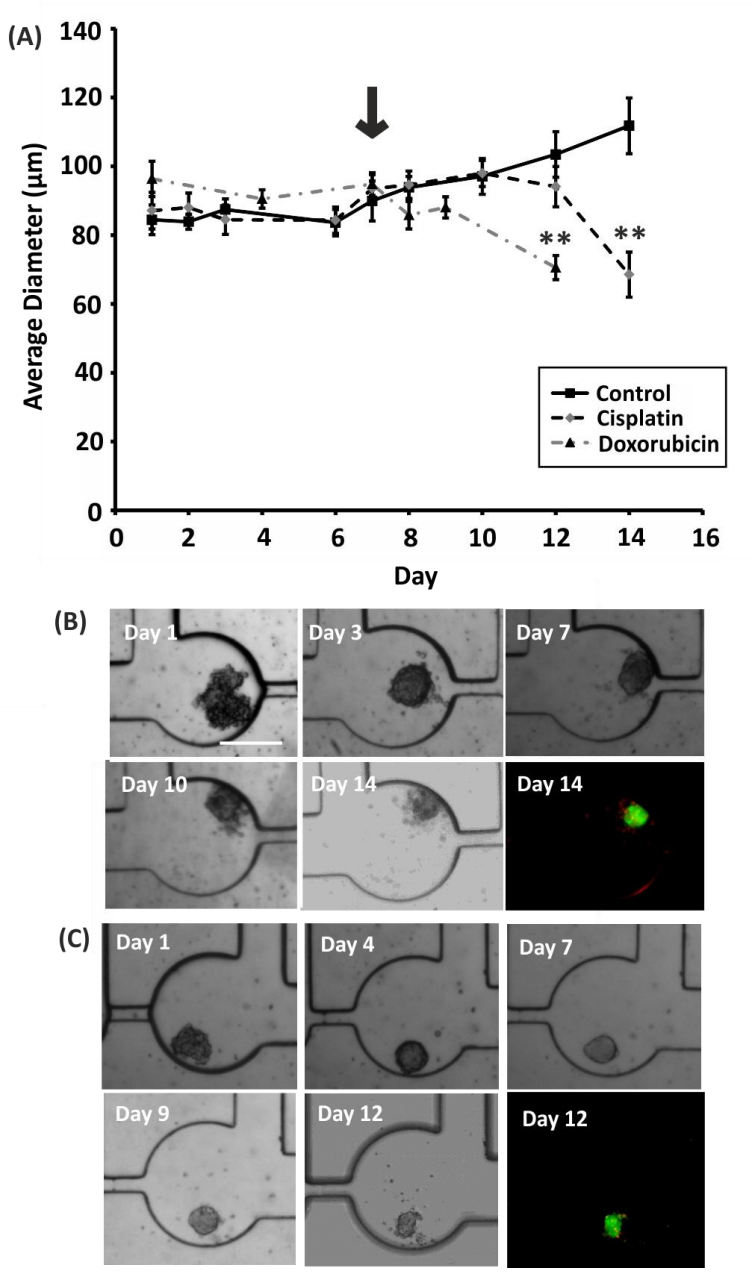

*Figure 6.8: Drug Treatment of Spheroids. A growth curve (A) of average spheroid diameter over 17 days of control and treated spheroids with 50 µm of cisplatin (black dashed line) or 4 µM of doxorubicin (grey dashed line) on day 7 which was washed off on day 8. The error bars represent the standard error of the mean. The arrow indicates the day of treatment (day 7). The n numbers for each experiment A timelapse of brightfield images of spheroids (B) treated with cisplatin over 14 days and (C) spheroids treated with doxorubicin and a FDA and PI stained image of the spheroid on day 14 for cisplatin and day 12 for doxorubicin. The scale bar equals 200 µm. ** represents a p value ≤0.01. Figure taken from McMillan et al.*[30].

6.5. Spheroid Culture within Alginate Beads

Another application which was tested was the ability to use this device for spheroid culture within alginate beads. This is of interest for developing a microfluidic assay for spheroid culture as certain cell types are anchorage dependent and thus are unable to form spheroids in non-adherent conditions, such as that found within the M/O droplets. Additionally this is of interest for 3D cell culture in other biological applications such as the culture of stem cells, as it has been shown that the cell to alginate gel contacts can have an influence on stem cell differentiation which is not observed in 2D[97]. The protocol for alginate bead formation within the device is provided as a diagram in Figure 5.9.

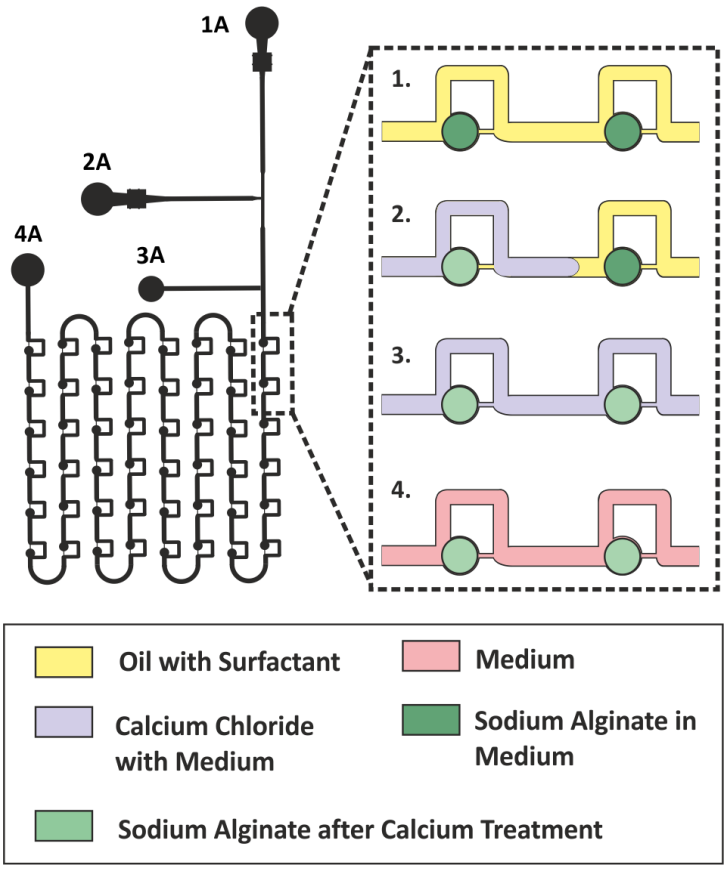

Figure 6.9: Alginate Bead formation within the Microfluidic Device. Droplet microfluidic device design with a diagram showing the process of forming alginate beads within the chamber array. The device has an inlet for oil with surfactant (1A); an inlet for the sodium alginate in medium (2A); a bypass channel used for the removal of air and the addition of calcium chloride solution (3A) and an outlet (4A). The alginate bead formation process began with the trapping of alginate in medium beads within the array (1), then a long plug of 4% calcium chloride solution was perfused through the device to form the alginate beads into hydrogels (2 and 3). Once the alginate beads had formed hydrogels medium was perfused through the device to remove the calcium chloride solution (4).

Initially, droplets containing cells in alginate medium were formed and stored within the device using the same cell concentration and procedure as before. In contrast to aqueous droplets, higher flow rates were used due to the higher viscosity of the sodium alginate in medium. For a 400 µm drop chamber device, the flow rate for the continuous phase was set at 2 µl/min and the aqueous phase at 1.6 µl/min. As was the case for the aqueous droplets, 100% of alginate droplets were trapped within the device. Once the droplets were trapped, the flow of the sodium alginate with cells was stopped and the excess droplets removed by flowing through only the continuous

phase. The continuous phase was then stopped and a 4% calcium chloride in medium solution was flown through the device for 30 minutes at a rate of 0.4 µl/min to promote the gelation of the alginate beads. The calcium chloride solution was flown through the air bypass channel to prevent the potential for the gelation of alginate, which may remain within the aqueous phase inlet. Upon addition of the calcium chloride solution to the alginate droplets, these gelled within minutes and the cells became embedded within the gel. As a result, the cells remained within the alginate and did not flow out in the calcium chloride plug. After perfusion of calcium chloride, the beads were refreshed with medium to remove the calcium chloride and to provide nutrients for the cells. The medium did not coalesce with the gelated beads and a visible interface remained between the medium plug and the alginate bead. After 24 hours, cells had aggregated together to form a cell cluster with a rough border. Some of the cells did not aggregate and remained dispersed within the alginate. The alginate beads were refreshed every second day with medium at 0.4 µl/min for 30 minutes. From day 3, the spheroids within the gelled alginate beads became smoother and more spherical.

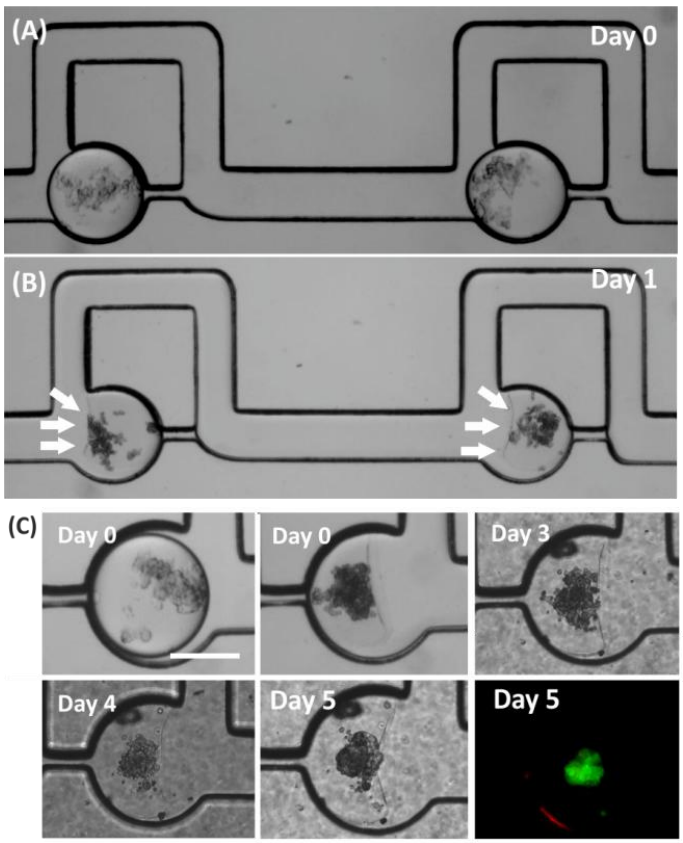

Figure 6.10: Spheroid Formation within Alginate Beads. Brightfield images of cells encapsulated within alginate droplets and trapped within the device before perfusion (A) and after perfusion with calcium chloride solution (B). (C) A timelapse of images of spheroid formation within an alginate droplet over 5 days with a spheroid stained with FDA and PI on day 5. The scale bars represent 400 μm for (A) and (B) and 200 μm for (C). Figure adapted from McMillan et al.[30].

Live/dead staining was carried out on day 5 which confirmed the spheroids were viable (Figure 6.10 (C)) and cells which had not aggregated and dispersed within the gel were dead (Figure 6.11). In addition, it was observed that alginate beads reduced in size over time (Figure 6.12). Due to this reduction in size, it was easier for the beads to be displaced from the traps upon refreshment with medium and this therefore limited the duration of the culture (Figure 6.12). The use of diffusive gelation, were the alginate beads are perfused with calcium chloride, results in a rapid gelation however as a result the resulting alginate does not have a stable structure. Therefore in the future an alternative method of gelation should be investigated to form alginate beads with a more stable structure.

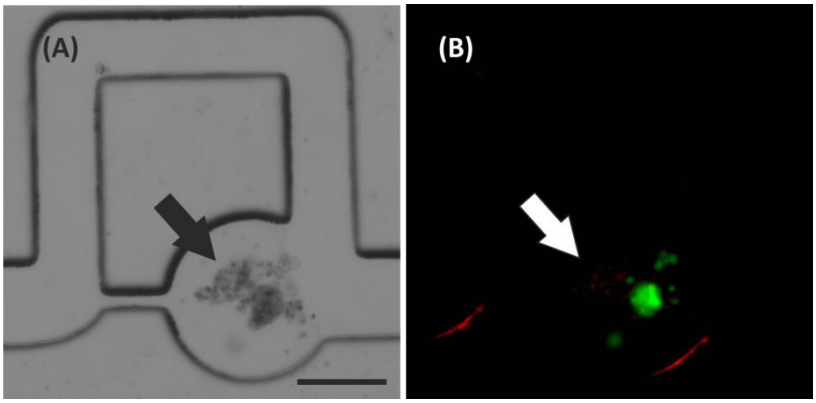

Figure 6.11: Single Cells dispersed into Alginate Bead. (A) Brightfield image and (B) fluorescence image of a spheroid stained with FDA (green) and PI (red) within an alginate bead with single cells which have dispersed into the alginate (indicated by the arrow in each picture). The scale bar is 200 µm.

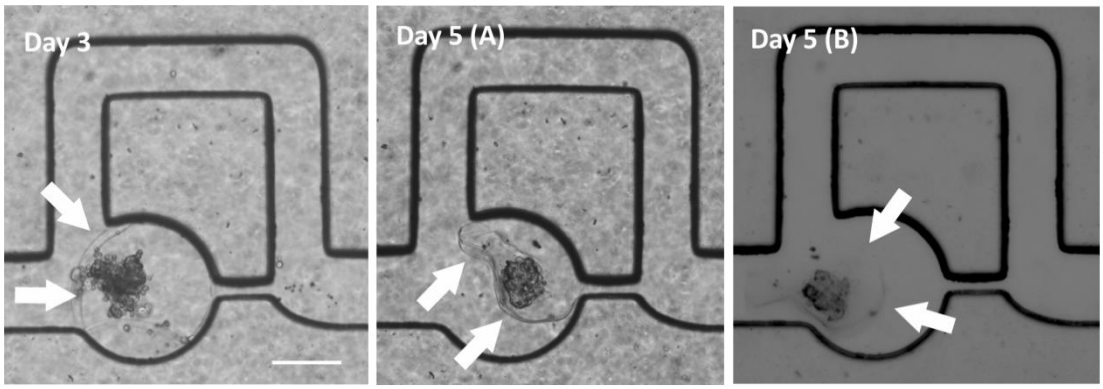

Figure 6.12: Alginate Bead Shrinkage over time. Brightfield images showing the reduction in size of alginate bead from day 3 to day 5 with the arrows indicating the interface of the alginate bead with 5(A) showing before medium perfusion and 5(B) showing after perfusion with the bead displaced from the trap. The scale bar is 200 µm.

In comparison, when alginate droplets were not perfused with calcium chloride solution, the cells aggregated to form smooth compact spheroids (Figure 6.13) which demonstrates that once gelled, it was difficult for the cells to come in contact with each other. Furthermore when the alginate beads were perfused with medium it was able to coalesce with the droplets showing that the slightly higher viscosity of the alginate did not prevent coalescence.

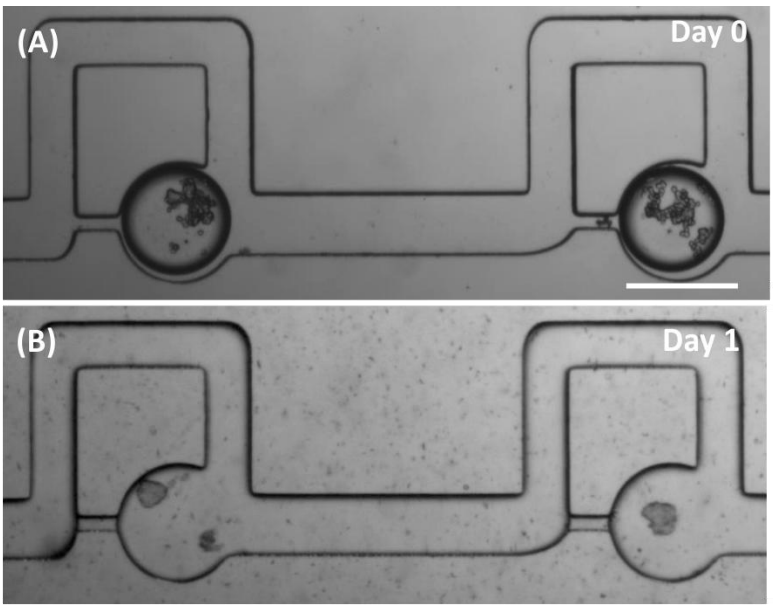

Figure 6.13: Spheroids formed within alginate beads without calcium chloride. Brightfield images showing cells encapsulated within alginate beads within the microfluidic storage array (A) and after perfusion with medium (B) with no treatment of the alginate with calcium chloride. The scale bar is 400 µm.

6.6. Discussion

In this chapter the droplet microfluidic device developed in chapter 5 has been evaluated for the formation and long term culture of multicellular spheroids. The formation of two different types of droplets for spheroid culture were evaluated: aqueous and alginate. For the aqueous droplets, the ability to coalesce medium with the droplets for medium exchange for long term culture was reliably achieved. Furthermore, the ability to carry out radiotherapeutic and chemotherapeutic treatments were investigated and live/dead staining was used to confirm the health of spheroids. For the alginate bead protocol, the device was shown to be suitable for both the gelation and storage of beads for formation and culture of spheroids.

6.6.1. Spheroid Formation and Culture within Aqueous Droplets

The device was found to be suitable for the storage of droplets for the initial aggregation of cells resulting in the formation of spheroids. Spheroids were observed to form in a similar way to those formed in macrodroplets as shown in chapter 4. The lower cell number per droplet resulted in more rapid spheroid formation in comparison to the macrodroplets. Spheroid formation within microdroplets occurred

between 6 to 18 hours, depending on the cell number. In contrast to the study conducted by Chan *et al.,* in this study spheroids were formed within single emulsion droplets which required a single device for formation of droplets and long term storage of droplets[23]. In contrast, Chan *et al.* used two devices in order to form double emulsion droplets and the spheroids were then released from the droplets to be cultured within low attachment culture plates. The long term culture of spheroids was shown to be possible within these devices, due to their ability to carry out substance exchange through coalescence. The spheroids remained intact and did not disaggregate over time suggesting that a non-adherent surface remained on the surfaces of the microchannels in the device. In addition, the majority of spheroids remained trapped within the chambers allowing for the monitoring of individual spheroids over time for up to 17 days. Spheroids would be displaced from chambers if air managed to enter the storage array prior to perfusion with medium, as the air before the medium could displace the spheroid or push it into the restriction channel of the trap. Chan *et al.* attempted to control the environment for spheroids within aqueous droplets through the use of their double emulsion system. They adopted the idea from another study by Zhang *et al.*[102] which used double emulsion droplets to allow for the diffusion of nutrients through the interface to the cells from the outer aqueous layer. However, this study found that the viability of cells reduced over time, which they suspected was due to the inability of large molecules such as growth factors to diffuse across the interface. Therefore the approach used in this chapter for the perfusion of spheroids after coalescence of droplets is superior, as the issue of large molecules such as growth factors not reaching the spheroids did not arise.

Another advantage of coalescing the droplets following the initial formation of spheroids within them was the ability to carry out live/dead staining of spheroids. Through this, it was possible to confirm the health of spheroids for long term culture, as well as after treatment with radiation and cytotoxic drugs. It was confirmed by viability staining that spheroids remained viable for up to 17 days, which is a major improvement to the results obtained by Chan *et al.* who experienced a reduction in viability over 4 days[23]. It has been shown in a study by Chen *et al.* that live and dead stains should not be encapsulated within droplets from the start as they found fluorescent probes were able to leak out of droplets over time[124]. Therefore, this would result in the production of an inaccurate fluorescent signal from the droplet. Furthermore, the majority of live and dead stains available are cytotoxic if they remain

in contact with cells over a long period of time. Thus, this also argues against the encapsulation of live and dead stains from the start of the experiment, as it would significantly reduce the duration of spheroid culturing.

One factor requiring further consideration if this device was to be used for the culture of spheroids from different cell lines or primary cells is the composition of medium. The coalescence mechanism used in this study was effective when using the standard growth medium for UVW glioma cells however different cell types may require different medium and supplements, depending on their own metabolic requirements. Therefore the influence of a different medium composition on droplet stability would need to be investigated prior to use of this system.

6.6.2. Treatment of Spheroids within Aqueous Droplets

A further achievement of the ability to coalesce droplets after spheroid formation was the ability to treat spheroids. The treatment of spheroids with anticancer drugs has previously not been achieved for spheroids formed and cultured within aqueous droplets. Encapsulation of a drug with the cells during droplet formation is not ideal as, at that point, the cells would still have to aggregate to form a spheroid. Thus it would be similar to conducting an experiment on a cell monolayer and the experiment would only be able to identify if the drug treatment would have a detrimental effect on spheroid formation. For the purpose of this project it was essential that spheroid formation occurred prior to drug treatment in order to take into consideration all of the factors in a 3D cell culture model (as mentioned in Chapter 2 Section 2.4) which can influence drug penetration and efficacy. Furthermore, drug assays which were carried out using the droplets, where separate droplets merged to create substance exchange, would limit the types of drugs which could be tested, as this process is only suitable for hydrophilic drugs. Lipophilic drugs would favourably partition out of the droplet into the continuous phase, thus potentially not produce any effect on spheroid growth or viability. As observed in Figure 6.8 (B) and (C), the cells on the outer rim of the spheroid disaggregated, leaving a viable core which suggests there was a limit to penetration of the cisplatin and doxorubicin into the spheroid. Another possible cause for the core of the spheroid being viable could be due to the presence of quiescent and hypoxic cells which are known to be more resistant to drug treatment.

A future application for this device would be to carry out combination treatments in order to investigate the use of radiosensitising agents. This is an application which has not been previously tested on spheroids formed via droplet microfluidics.

A drawback with this device for carrying out drug assays is the potential for PDMS to absorb hydrophobic molecules[138]–[140]. The absorption of drugs may be low for those which are perfused through the device for a short period of time, however, for those requiring longer incubation times diffusion into PDMS may occur. This aspect was not investigated within this study but would need to be considered in order to investigate the influence of different drug concentrations to carry out an accurate assessment. Furthermore the potential to use alternative polymers such as polystyrene may need to be considered which has been found to absorb little if any hydrophobic molecules[141].

6.6.3. Alginate Beads

A further aspect which was evaluated with this device was the ability to also form alginate beads as well as aqueous droplets. In contrast to the majority of studies involving the use of alginate beads for spheroid culture, the whole process from the formation of the alginate beads through to the storage and culture of spheroids was carried out on a single device[15], [16], [19], [21], [142], [143]. The only study which has shown the formation and culture of spheroids within alginate beads on a single device is by Sabhachandani *et al.* who used a variation of the "dropspot" device[21], [88]. In their study they encapsulated MCF-7 breast cancer cells within alginate in medium droplets that were trapped within the chamber array with a calcium chloride solution then flown through at a slow rate to promote gelation. The beads were then cultured for up to 4 days. This is similar to the duration time of spheroids cultured within alginate beads in this chapter, which were gelated using a similar method. In contrast to the spheroids formed within their alginate beads the spheroids formed in this chapter were more compact after 3 to 4 days. The spheroids presented in the Sabhachandani *et al.* were similar to aggregates, with cells remaining dispersed within the alginate and instead forming several smaller spheroids. Therefore the spheroids formed in alginate beads in this chapter are more relevant models, as the spheroids were more compact and larger and so are a more effective model for the assessment of penetration of drugs and development of a nutritional gradient.

A noticable difference in comparison to the aqueous droplets was the duration of time taken for cells to aggregate and form spheroids. It took around 3 to 4 days before the cells had aggregated to form a compact spheroid which is much slower than the 6 to 18 hours it took within an aqueous droplet. Similar spheroid formation times have been reported within alginate beads[18], [21], [22]. This is to be expected as the hydrogel network creates a barrier for cells, making it more difficult for them to come in contact with each other[18]. This was proven in the sodium alginate bead experiments which did not undergo perfusion with calcium chloride to create a hydrogel (figure 6.8). Here, the cells formed compact spheroids like those formed within aqueous droplets.

The main limiting factor identified for the culture of spheroids within alginate beads was the reduction in size over time. This limits the duration of time spheroids could be cultured within alginate beads, as they can be easily washed away as they reduce in size (figure 6.12). Furthermore, as the alginate bead reduced in size, it would no longer provide the support required for spheroid growth. The breakdown of alginate beads over time has been previously reported. One of the causes is thought to be due to the release of calcium ions into the medium, due to exchanges with cations[97]. Another cause for the degradation of alginate beads (section 6.5) is due to the method used for gelation of alginate. The perfusion of alginate with divalent cations such as Ca^{2+} ions from calcium chloride is known as diffusive gelation and is one of the most common gelation methods used[97], [144]. One of the main drawbacks of diffusive gelation is that it results in the quick gelation of alginate which cannot be well controlled. As a result the alginate hydrogel created is not strong and quickly degrades. Another method of gelation which produces a more controlled method is internal gelation. Internal gelation involves the alginate containing a gelation source, such as calcium carbonate, calcium sulphate or calcium EDTA which slowly releases calcium ions into the gel, resulting in a slower and more controlled gelation of the alginate. As a result the alginate gel produced is stronger and lasts longer. Therefore, in future experiments, this method could be assessed for the creation of alginate beads for culturing spheroids within this device. If a longer alginate bead duration could be achieved, this opens up the opportunity for testing the potential of this device for the treatment of spheroids.

6.6.4. Issues of Device for Spheroid Culture

In both aqueous and alginate droplets there was a variation in the sizes of spheroids formed which was due to the initial cell number within the droplet. Although it was previously stated in Chapter 4 that the spheroid size can be controlled using medium in oil droplets (section 4.4), this can be difficult when using droplet microfluidics due to the poisson distribution that control cell encapsulation. In addition, UVW cells can aggregate within the tubing connected to the microfluidic device, resulting in bursts of aggregated cells alternating with the flow of fewer cells. Although there is a heterogeneous range of sizes, there is the potential to investigate the differences in effect depending upon spheroid size. In addition to a variation in spheroid size within the same device, it was observed that there was a variation in the initial average spheroid diameter between experiments which were set up on different days. This was thought to be due to the variation in the withdrawal of cell concentration within the tubing resulting in variation of potential aggregates being taken up within the tubing.

7. Discussion

7.1. Introduction

Thus far this thesis has presented the advantages of multicellular tumour spheroids (MCTSs) for anticancer drug development, examined methods for the *in vitro* culture of MCTSs and the impact droplet microfluidic methods can have in anticancer screening. From the literature review carried out, the main limitations for the use of droplet microfluidics for the culture of spheroids identified were the complexities of current encapsulation based methods involving alginates and/or matrices and short cell culture times within droplets. Therefore, the main aim was to attempt to resolve these issues to develop and evaluate a microfluidic technology suitable for MCTS culture and anticancer treatment within aqueous and alginate droplets. In chapters 4, 5 and 6, the development of a device which bridges droplet microfluidics with single phase microfluidics has been presented.

Within this chapter the impact of the results obtained will be discussed with reference to the impact on *in vitro* MCTS culture and the future use of the developed microfluidics as a screening platform. . Additionally, other work which has stemmed as a result of the findings from this project will be presented.

7.2. Chapter 4 Outcomes

The first main outcome of this project was the identification of the parameters required for the formation and long term culture of MCTSs within M/O droplets. The identification of the parameters was essential for determining if it would be possible to use the emulsion system for long term culture before miniaturising it via droplet microfluidics. Within the literature, there was a gap with regards studies investigating the use of single emulsion aqueous droplets for spheroid culture. Additionally, one of the issues which had been highlighted from previous studies was the limited number of days which cells remained viable and no detailed investigation had been conducted to determine ideal conditions[11], [12], [24]. Thus, this study demonstrated that it was possible to achieve long term culture of spheroids within M/O droplets (up to 28 days) if medium was refreshed every second day. It also confirmed that spheroids could only

remain viable within a droplet for a limited period of time with little or no increase in growth happening during this period. The longest duration of spheroid culture without refreshment which could be achieved was 14 days at a cell to volume of medium ratio of 200 cells per μl. In order to extend the duration of culture, or have consistent spheroid growth, refreshment of medium was an essential factor. Therefore, determination of these parameters is important when developing a droplet microfluidic device for cell culture due to the concept of compartmentalisation, were each droplet contains a finite amount of nutrients for cells. Additionally, these aspects are useful to know when using this approach for developing a droplet microfluidic device for anticancer treatment screening, as the proliferative state can have an influence on efficacy.

The parameters required for the formation and long term culture of spheroids were only characterised using the UVW glioma cell line, with preliminary studies conducted with primary hepatocyte cells (discussed in more detail in section 7.5). Therefore, one consideration which will need to be addressed in future studies is that different cell lines or primary cells may have different growth characteristics and, as a result, require the refreshment of medium at a different frequency in order to meet their metabolic requirements for proliferation[117]. In addition, neither UVW glioma cells nor primary hepatocytes exhibit anchorage dependence and thus both cell types can form spheroids within M/O droplets or traditional non-adherent methods such as the forced floating method. Therefore, it also needs to be considered that the M/O droplet method introduced in chapter 4 will not be suitable for the formation of spheroids using cells which exhibit anchorage dependence. Anchorage dependent cells would require the inclusion of a scaffold, for example alginate or matrices, for this method to be effective.

The formation of spheroids using the M/O droplet based method is similar to the hanging drop approach[70]. The main advantage of the M/O droplet method over the hanging drop is that it is not affected by physical shock such as the movement from the incubator to microscope for analysis or by the exchange of medium[70]. This is due to the support provided by the continuous phase surrounding the medium droplet. In contrast, the droplets in the hanging drop system are not as stable and even the slight tilting of the plate or addition of extra medium is enough for a droplet to fall and potentially damage a spheroid. Therefore, the duration of an emulsion based assay is longer and more reliable than the hanging drop approach, as it is not affected by the movement of the droplets for analysis or medium exchange.

Another outcome of interest in terms of developing a droplet microfluidic device is the ability to conduct radiotherapeutic experiments. This is of major interest in terms of developing a microfluidic screening method involving spheroids as they are attractive *in vitro* models for carrying out preclinical combination therapies in order to identify potential radiosensitising agents. Within the literature this has so far not been carried out in spheroids formed within an emulsion based system, either aqueous or alginate based. Furthermore, a similar radiotherapeutic response was achieved between spheroids formed within emulsions in comparison to traditional methods, demonstrating that the emulsion method did not have an influence on the physiology of the spheroids. A future area for investigation is that of fractionated radiotherapy. Fractionated radiotherapy is where radiotherapy is delivered as smaller fractions (1.8 to 2 Gy) daily[66] instead of being delivered as a single dose. When a cancer patient is given treatment, fractionated radiotherapy reduces the risk of relapse through the treatment of cells which were in a less sensitive part of the cell cycle or quiescent cells which have recovered upon re-exposure to nutrients[66].

An interesting feature which was highlighted with this emulsion based system for spheroid culture is the ability to control the proliferative state through the frequency of medium refreshment. This has previously been shown possible through the use of non-adherent coated well plates and/or spinner flasks[112], [114],[113]. With regards to emulsion based systems, this work was the first of its kind to provide an extended investigation of cell culture in droplets[28]. This is of major interest, as it opens up the potential to miniaturise high throughput methods for testing the radiosensitivity and chemosensitivity of anticancer agents. A potential future application to further enhance the appeal of this method for testing radiosensitivity would be to investigate hypoxia.

Hypoxic cells are another area of interest as they are known to cause pro-survival signalling resulting in the resistance of cells to treatments[145]. Furthermore, radiosensitivity has been observed to decrease as the partial oxygen pressure within cells decreases, with oxygen enhancing the effectiveness of radiotherapy[146]. Thus, it has been observed that hypoxic cells require up to three times the dose of radiation in comparison to cells with normal oxygen levels[146], to achieve the same levels of cell death. The testing of the sensitivity of therapies towards hypoxic cells could be easily carried out using this method by culturing spheroids within an environmental chamber to create a low oxygen environment to create hypoxic cells. The spheroids could then be reintroduced to a normal atmosphere and fresh medium to determine whether the

spheroids would recover and continue to increase in size. Therefore, this would add another feature to the application of testing for radiosensitivity of spheroids by including the influence of hypoxic as well as quiescent cells.

Overall, chapter 4 has shown that M/O droplets are a suitable method for the formation and culture of spheroids. Additionally, it has been shown that this method is suitable for conducting radiotherapeutic treatments an area which has not previously been investigated on spheroids formed via the emulsion based approach.

7.3. Chapter 5 Outcomes

The main purpose of the investigations outlined in chapter 5 was to develop a microfluidic device which would be suitable for the formation and long term culture of multicellular spheroids. Within the literature there has not been a design presented for the formation and culture of spheroids within single emulsion M/O droplets. The majority of studies involving droplet microfluidics with single M/O droplets have focused on the study of either single cells[10]–[12], [26], [147]–[149] or organisms such as *C. elegans*[85], [150]. In terms of spheroid formation and culture, the vast majority of droplet microfluidic based approaches have involved the use of alginate[16]–[19], [21], [22] or alginate mixed with matrices[20], [99] beads and microcapsules. Within Chapter 4 it was identified that M/O droplets could be used for the formation of spheroids thus a microfluidic device was developed to accommodate the formation and storage of aqueous droplets. However, it was identified within Chapter 5 that spheroids could not be cultured for longer than 4 days within aqueous microdroplets without disaggregation occurring. Therefore, this chapter showed that a microfluidic device which involved only the storage of aqueous droplets could only be used for short term spheroid culture experiments. A study which also showed the potential of the dropspot device for spheroid formation within droplets was by Sabhachandani *et al.* and involved the incorporation of alginates[21]. The advantage of the use of alginate beads was that it only required a device for storage of droplets as the medium could be perfused through the beads due to the porous structure of the alginate (as discussed within Chapter 2 Section 2.8.1)[97]. Another useful application for the dropspot device is for single cell assays which only require short term culture prior to analysis. An example of a project in which this device was involved in alongside this project will be discussed in section 7.5.2.

A useful outcome of the initial experiments using the single storage chamber devices (section 5.2) was the identification of the increased probability of coalescence created by cell culture medium. The stability of the emulsion droplets created by the fluorosurfactants used within this study is known to be robust when water is used as the aqueous phase[91]. The only other report of an aqueous phase affecting the stability of emulsion droplets when similar fluorosurfactants were is found when 3% BSA was used as the aqueous phase[91]. This attribute of the cell culture medium was advantageous in the development of the final microfluidic device and protocols. The final device was adapted from those developed by Boukellal *et al.* and Vanapalli *et al.* which allowed for the storage of droplets which could then be coalesced for substance exchange[85], [87], [128]–[130]. In contrast to previous studies, the unique aspect of this approach was the ability to induce coalescence of droplets through the use of cell culture medium as the aqueous phase, which have otherwise been shown to be stable using this concentration of surfactants[91]. Thus, this removed the requirement for complicating the procedure by either lowering the surfactant concentration or the use of active approaches such as electrocoalescence. However, for different cell types different recipes of cell culture medium will be required with supplements which may have not been tested within this project. Therefore, other supplements added to medium for different cell types may have a different effect on the rate of coalescence of droplets.

A study which shows the competition in terms of a high-throughput assay for the formation, culture and treatment of spheroids is by Senkowski *et al.*[113] which used 384 well plates and managed to screen 1600 different drugs. To further improve upon the future potential of the microfluidic device developed in this study, a gradient generator could be connected to the inlet of several storage arrays, resulting in the ability to test a range of different concentrations of a drug. A concentration gradient can be created via microfluidics by exploiting the laminar flow experienced by liquids at the microscale[151]. Therefore, when two different streams of fluid are flown next to one another, the mixing of the liquids occurs by diffusion allowing for the precise formation of a concentration gradient[151]–[153]. Concentration gradients generated via microfluidics can provide a range of concentrations over several orders of magnitude, thus allowing for a thorough investigation of the efficacy of different drug concentrations[151], [153], [154]. The potential range of concentrations generated via microfluidics is currently unachievable using other standard methods[151].Therefore,

this would allow this device to have the potential to produce a similar if not better output to 384 well plates[113].

Overall, the study outlined in chapter 5 resulted in the development of a microfluidic device suitable for the storage of droplets and coalescence to allow for substance exchange. The use of a device which only involved droplet formation and storage was identified as not suitable for long term culture of spheroids.

An alternative device which was designed but not fabricated would have involved the use of the properties of the medium for coalescence to allow for medium exchange (Figure 7.1).

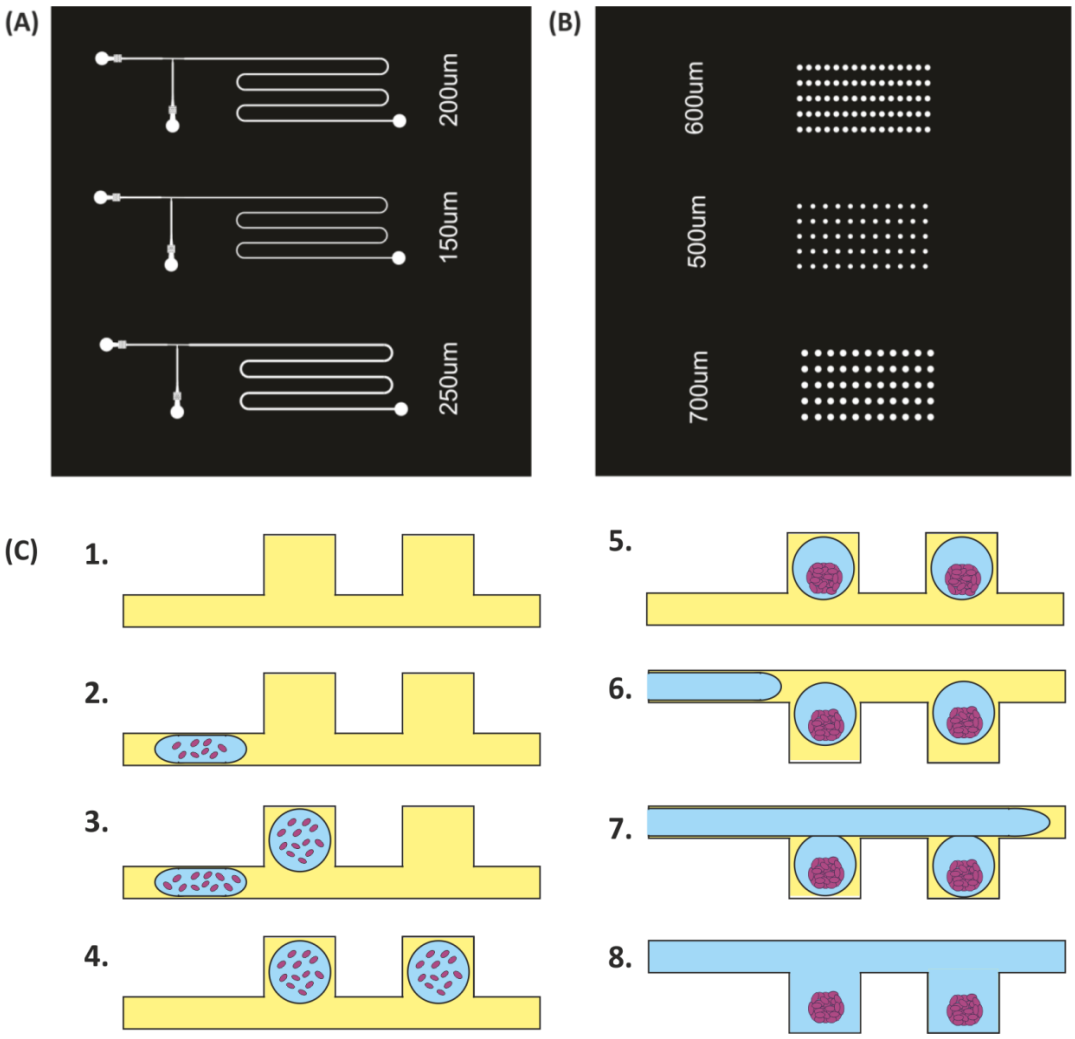

Figure 7.1: Microfluidic Device designs of two layer devices. Examples of photomasks designed for a two layer device with one layer having a serpentine channel with a T-junction which would be the bottom layer (A) and the upper layer containing wells (B). The numbers within the masks refer to the width of the serpentine channel (A) and the diameter of the wells (B) in micrometres. (C) A schematic diagram of the two layer device would in action. Steps 1 to 4 show the flow-through and trapping of droplets containing cells into the wells. Once the cells have formed spheroids at step 5 the device is inverted for the perfusion of medium through channel of the device (steps 5 to 7). Finally step 8 shows the medium coalesced with the droplets and the spheroids trapped within the wells.

The inspiration for this device came from a similar design by Shi *et al.* who used it for the culture of *C. elegans* within droplets[150]. The device involved the use of two layers with an upper layer containing wells and a lower one with a channel. The main concept behind the design that the droplets containing *C. elegans* would float to enter into the

wells due to the aqueous phase having a lower density in comparison to the continuous phase. Thus as a result, the droplets containing the *C. elegans* are stored within the wells and the channel is used to perfuse with medium. A similar approach could be tested with the device designed with spheroids. To fabricate this device a two layer fabrication process would have to be carried out with the wells aligned in rows with the channel. This device would involve firstly the formation of droplets, which would then be flown through the serpentine and trapped within the wells. Due to the higher density of the FC-40 oil in comparison to the medium it is expected that the droplets would float to become trapped within the wells. Then, as before, once the spheroids are formed the droplets would be coalesced by medium being flown through the serpentine channel.

7.4. Chapter 6 Outcomes

The final achievement of this thesis was to characterise a microfluidic device for the formation and culture of spheroids within aqueous or alginate droplets. This has previously not been achieved and resulted from the identification of the suitable conditions for spheroid culture within medium droplets in Chapter 4 and the development of a suitable microfluidic device in Chapter 5.

Other studies involving the use of droplet microfluidics have suffered from several drawbacks, such as the necessity of using more than one device or the additional use of a standard well plate in order to form and store droplets, the use of double emulsion droplets[23] and short culture times. Additionally, a droplet microfluidic device has not been previously demonstrated which is suitable for long term culture and treatment of spheroids formed within single emulsion M/O droplets. Within this thesis a device has been characterised which resolves these issues of cell culture within aqueous droplets and, in addition, allows for culture within alginate beads. Furthermore, this study has also demonstrated that it is possible to carry out either chemotherapeutic and/or radiotherapeutic assays within the same device. Overall, this is a major advancement in the development of droplet microfluidics as a method for long term culture of spheroids and treatment. In the future, there is the potential for the device to be used for testing combination therapies. As a result, it will be possible to test radiosensitising agents which target specific parameters known to cause resistance such as quiescent cells. Through the ability to control the proliferative state of spheroids within the microfluidic device this could easily be tested in the future. As shown in Chapter 4,

spheroids formed within medium in oil droplets could enter a reversible quiescent state through non-refreshment of the medium for a certain period of time. This could be achieved within this device through two different approaches; firstly by containing spheroids within droplets for a longer period of time and secondly by controlling the frequency of the medium refreshment. Due to the higher cell number to volume of medium ratio within microdroplets the latter of the two options is the most suitable.

A further advantage of this device was the ability to carry out either spheroid formation within aqueous droplets or alginate beads. The use of alginate allows for this device to be used for the formation of spheroids from cells which are anchorage dependent and which would not form spheroids within a non-adherent environment without support[74]. Furthermore, the ability to use this device for aqueous droplets also opens up its potential use in other biological applications where certain types of cells do not form spheroids in alginate. One example of this scenario is human mesenchymal stem cells (hMSC) which have the potential to be used as spheroids in tissue engineering applications[155]. Human mesenchymal stem cells cannot form spheroids in alginates but have been shown to do so within double emulsion M/O droplets[23]. With regards to the literature the ability to use aqueous droplets or alginate beads has previously not been shown with the same microfluidic device design. Furthermore, the alginate bead process is simplified using only a single device in comparison to the majority of other devices involving the use of alginates as a single device could be used without the requirement to culture the spheroids off-chip[16]–[19]. Only one previous study, by Sabhachandani *et al.,* has shown the use of a single device for the formation and culture of spheroids within alginate beads but not aqueous droplets[21]. In contrast to their spheroids the spheroids formed within the device developed within this project were more compact once the cells had aggregated and, furthermore, fewer single cells were distributed throughout the alginate. Therefore, the spheroids developed within this study were more representative of tumours *in vivo,* as the formation of large, compact spheroids results in the presence of proliferative and quiescent cells within the multicellular structure, due to close cell to cell contact creating a nutritional gradient. However, in this present study, the use of alginate beads was only assessed as a proof of principle concept. Therefore the potential for this method to be used for radiotherapeutic and chemotherapeutic assays will need to be interrogated further in future investigations.

One aspect which needs further improvement for the future use of alginate beads is the duration of time at which the alginate bead remains intact. The work presented in Chapter 6 showed that spheroid culture could only be conducted for up to five days. This was due to the alginate bead shrinking over time and being displaced from the trap upon medium refreshment. In order to improve upon the stability of the alginate beads, the gelation procedure could be altered. Diffusive gelation involving the perfusion of alginate with $CaCl_2$ is known to be a poor method for producing a strong and stable alginate structure (as discussed in more detail within Chapter 6 Section 6.6.3)[97]. An alternative method which could be used would be internal gelation through the incorporation of calcium carbonate within the alginate which slowly releases calcium ions resulting in a more controlled gelation and thus stronger alginate[144].

Another feature which could be tested using this device in the future is the formation of beads composed of matrices. In contrast to alginate, the incorporation of ECM would create an experimental environment which is more representative of the *in vivo* tumour microenvironment. The inclusion of matrices such as Matrigel would include proteins such as collagen, enactin and laminin and growth factors which influence tumour growth, cause cell differentiation and create a support for 3D cell culture[73],[6]. In addition, this method has not been investigated within a single device and previous studies have only involved the use of a device for bead or microcapsule formation and the spheroids are subsequently cultured using standard tissue culture plates[20], [99].

A further potential future application of this technology would be for the formation and culture of spheroids from cells obtained from patient biopsy samples, which are known as organoids[156]. Previously, it has been found that organoids formed from patient biopsy samples have a similar morphology to tumours found *in vivo*[157]. In addition, organoids provide a better representation of the heterogeneity of cells observed within tumours both phenotypically and genetically[157]. Therefore, this could produce one of the best possible *in vitro* 3D cancer cell culture models for use in preclinical anticancer treatment tests. As the microfluidic approach only requires a small sample of cells, it would be suitable for the testing of precious samples, such as cells extracted from a biopsy sample. As not all cells may be able to form from a biopsy sample, it may be necessary to incorporate an extracellular matrix into the droplets. This is a further advantage of this microfluidics approach over traditional methods as a method for the

formation of MCTSs which require larger quantities of cells. Furthermore it opens up the possibility to investigate personalised cancer treatments.

7.5 Collaborative Projects

As a result of the main findings of the emulsion based system and the microfluidic devices developed throughout this project there were several other projects which have been created and are ongoing.

7.5.1 Primary Hepatocyte Spheroids

Another area in which the use of three dimensional cell culture models is of interest is in hepatoxicity studies. Previously, it has been observed that hepatocytes grown in a 3D model such as a spheroid remain viable for weeks, instead of up to 4 days when grown as a monolayer. Furthermore, the hepatocyte spheroids continue to express biochemical parameters which are usually lost during monolayer culture[158]. Additionally hepatocyte spheroids have a structure which is more representative of the cuboidal structure and the formation of tight junctions observed in hepatocytes *in vivo*[159], [160],[161]. Thus the potential use of the emulsion system for the formation of 3D cell culture models using hepatocytes was investigated. Initial experiments were conducted using primary hepatocyte cells using the emulsion based system to determine if this was a suitable system for spheroid formation. The formation of liver spheroids is of additional interest as they potentially provide a more accurate *in vitro* model for drug toxicity assays. It was found that in comparison to the UVW cell line, primary hepatocyte cells initially formed aggregates with a rough border, before becoming compact from day 6 to form a spheroid approximately 300 μm in diameter. Disaggregation of the rough border was observed, suggesting that these cells were dead. In addition, the no spheroid growth was observed over time, but this was expected due to the fact that the primary hepatocytes do not proliferate. Therefore, these preliminary experiments not only demonstrated that this method could be used to form spheroids from cells other than UVW cells, it also illustrated the potential for the emulsion based system to be used for the formation of spheroids from primary cells which are less robust and more difficult to culture in comparison to cell lines.

7.5.2. Lectin Detection of Cancer Cells using Surface Enhanced Raman Spectroscopy (SERS) via Droplet Microfluidics

The "dropspot" design which was tested in Chapter 5 was used in a project which involved the use of droplet microfluidics for the encapsulation of single cells. This project was in collaboration with Dr Michele Zagnoni along with PhD student Marjorie Willner and Professor Vikesland from Virginia Tech. The main concept is that nanoparticles which bind specifically to lectins specifically located within the membrane of cancerous cells can be used to differentiate between those and normal cells[162],[163], [164]. The cells are encapsulated within droplets using droplet microfluidics in order to achieve single cell detection via the use of SERS and to achieve a high throughput of results using a low number of cells and nanoparticles. The initial testing of the microfluidic device was carried out within the lab at the University of Strathclyde in order to elucidate and standardise the fabrication of microfluidic devices, droplet microfluidics and the encapsulation of single cells for this study. This work was successfully replicated within Virginia Tech and this project is still ongoing.

7.6. Conclusions

This work outlined in this thesis has aimed to develop a methodology to improve upon current technology used for the formation of MCTSs via droplet microfluidics. The main focus was upon the use of M/O droplets for the formation and long term culture of MCTSs and the ability to carry out anticancer treatment assays within the system. Overall, this work was successful in overcoming challenges such as the short cell culture times associated with emulsion based approaches and identified the optimal parameters for the culture of MCTSs. Furthermore, a microfluidic device was successfully developed allowing for the reliable formation and long term culture of MCTSs which incorporated both droplet phase and single phase microfluidics. As a result, the device which was developed allowed for radiotherapeutic and chemotherapeutic treatment of spheroids, opening up the potential to screen combination therapies in the future. Finally, preliminary experiments were conducted showing that this device could also be used for alginate beads. Overall, this work has resulted in progress being made in the use of droplet microfluidics for spheroid assays that can improve upon the *in vitro* screening of radiotherapeutic and chemotherapeutic treatments. In the future, there is the potential for this technology to be used in the

development of personalised anticancer treatments through the incorporation of biopsy samples. Furthermore, the preliminary work conducted with hepatocytes described above shows that this emulsion based system could be implemented for other body on a chip models.

References

[1] J. Arrondeau, H. Gan, A. Rasak, X. Paoletti, and C. Tournaeu, "Development of Anti-Cancer Drugs," *Discov. Med.*, vol. 10, no. 53, pp. 355–362, 2010.

[2] A. L. Hopkins, "Network pharmacology: the next paradigm in drug discovery.," *Nat. Chem. Biol.*, vol. 4, no. 11, pp. 682–90, 2008.

[3] W. N. Hait, "Anticancer drug development: the grand challenges.," *Nat. Rev. Drug Discov.*, vol. 9, no. 4, pp. 253–4, Apr. 2010.

[4] A. C. Begg, F. a Stewart, and C. Vens, "Strategies to improve radiotherapy with targeted drugs.," *Nat. Rev. Cancer*, vol. 11, no. April, pp. 239–253, 2011.

[5] S. Breslin and L. O'Driscoll, "Three-dimensional cell culture: the missing link in drug discovery.," *Drug Discov. Today*, vol. 18, no. 5–6, pp. 240–9, Mar. 2013.

[6] W. Asghar, R. El Assal, H. Shafiee, S. Pitteri, R. Paulmurugan, and U. Demirci, "Engineering cancer microenvironments for in vitro 3-D tumor models," *Mater. Today*, vol. 18, no. 10, pp. 539–553, 2015.

[7] A. C. Luca, S. Mersch, R. Deenen, S. Schmidt, I. Messner, K. L. Schäfer, S. E. Baldus, W. Huckenbeck, R. P. Piekorz, W. T. Knoefel, A. Krieg, and N. H. Stoecklein, "Impact of the 3D Microenvironment on Phenotype, Gene Expression, and EGFR Inhibition of Colorectal Cancer Cell Lines," *PLoS One*, vol. 8, no. 3, 2013.

[8] F. Hirschhaeuser, H. Menne, C. Dittfeld, J. West, W. Mueller-Klieser, and L. a Kunz-Schughart, "Multicellular tumor spheroids: an underestimated tool is catching up again.," *J. Biotechnol.*, vol. 148, no. 1, pp. 3–15, Jul. 2010.

[9] L. A. Kunz-schughart, M. Kreutz, and R. Knuechel, "Multicellular spheroids : a three-dimensional in vitro culture system to study tumour biology," *Int. J. Exp. Pathol.*, pp. 1–23, 1998.

[10] A. B. Theberge, F. Courtois, Y. Schaerli, M. Fischlechner, C. Abell, F. Hollfelder, and W. T. S. Huck, "Microdroplets in microfluidics: an evolving platform for discoveries in chemistry and biology.," *Angew. Chem. Int. Ed. Engl.*, vol. 49, no. 34, pp. 5846–68, Aug. 2010.

[11] H. N. Joensson and H. Andersson Svahn, "Droplet microfluidics--a tool for single-

cell analysis.," *Angew. Chem. Int. Ed. Engl.*, vol. 51, no. 49, pp. 12176–92, Dec. 2012.

[12] J. Clausell-Tormos, D. Lieber, J.-C. Baret, A. El-Harrak, O. J. Miller, L. Frenz, J. Blouwolff, K. J. Humphry, S. Köster, H. Duan, C. Holtze, D. a Weitz, A. D. Griffiths, and C. a Merten, "Droplet-based microfluidic platforms for the encapsulation and screening of Mammalian cells and multicellular organisms.," *Chem. Biol.*, vol. 15, no. 5, pp. 427–37, May 2008.

[13] S. Köster, F. E. Angilè, H. Duan, J. J. Agresti, A. Wintner, C. Schmitz, A. C. Rowat, C. a Merten, D. Pisignano, A. D. Griffiths, and D. a Weitz, "Drop-based microfluidic devices for encapsulation of single cells.," *Lab Chip*, vol. 8, no. 7, pp. 1110–5, Jul. 2008.

[14] H. Hufnagel, A. Huebner, C. Gülch, K. Güse, C. Abell, and F. Hollfelder, "An integrated cell culture lab on a chip: modular microdevices for cultivation of mammalian cells and delivery into microfluidic microdroplets.," *Lab Chip*, vol. 9, no. 11, pp. 1576–82, Jun. 2009.

[15] L. Yu, M. C. W. Chen, and K. C. Cheung, "Droplet-based microfluidic system for multicellular tumor spheroid formation and anticancer drug testing.," *Lab Chip*, vol. 10, no. 18, pp. 2424–32, Sep. 2010.

[16] S. Yoon, J. A. Kim, S. H. Lee, M. Kim, and T. H. Park, "Droplet-based microfluidic system to form and separate multicellular spheroids using magnetic nanoparticles.," *Lab Chip*, vol. 13, no. 8, pp. 1522–8, Apr. 2013.

[17] L. Yu, C. Ni, S. M. Grist, C. Bayly, and K. C. Cheung, "Alginate core-shell beads for simplified three-dimensional tumor spheroid culture and drug screening.," *Biomed. Microdevices*, vol. 17, no. 2, p. 33, 2015.

[18] C. Kim, S. Chung, Y. E. Kim, K. S. Lee, S. H. Lee, K. W. Oh, and J. Y. Kang, "Generation of core-shell microcapsules with three-dimensional focusing device for efficient formation of cell spheroid.," *Lab Chip*, vol. 11, no. 2, pp. 246–52, Jan. 2011.

[19] K. Alessandri, B. R. Sarangi, V. V. Gurchenkov, B. Sinha, T. R. Kießling, L. Fetler, F. Rico, S. Scheuring, C. Lamaze, A. Simon, S. Geraldo, D. Vignjevic, H. Doméjean, L.

Rolland, A. Funfak, J. Bibette, N. Bremond, and P. Nassoy, “Cellular capsules as a tool for multicellular spheroid production and for investigating the mechanics of tumor progression in vitro.,” *Proc. Natl. Acad. Sci. U. S. A.*, vol. 110, no. 37, pp. 14843–8, Sep. 2013.

[20] Y. Wang and J. Wang, “Mixed hydrogel bead-based tumor spheroid formation and anticancer drug testing.,” *Analyst*, vol. 139, no. 10, pp. 2449–58, May 2014.

[21] P. Sabhachandani, V. Motwani, N. Cohen, S. Sarkar, V. Torchilin, and T. Konry, “Generation and Functional Assessment of 3D Multicellular Spheroids in Droplet Based Microfluidics Platform,” *Lab Chip*, vol. 16, pp. 497–505, 2015.

[22] L. Yu, M. C. W. Chen, and K. C. Cheung, “Droplet-based microfluidic system for multicellular tumor spheroid formation and anticancer drug testing.,” *Lab Chip*, vol. 10, no. 18, pp. 2424–32, Sep. 2010.

[23] H. F. Chan, Y. Zhang, Y.-P. Ho, Y.-L. Chiu, Y. Jung, and K. W. Leong, “Rapid formation of multicellular spheroids in double-emulsion droplets with controllable microenvironment.,” *Sci. Rep.*, vol. 3, p. 3462, Jan. 2013.

[24] F. Chen, Y. Zhan, T. Geng, H. Lian, P. Xu, and C. Lu, “Chemical transfection of cells in picoliter aqueous droplets in fluorocarbon oil.,” *Anal. Chem.*, vol. 83, no. 22, pp. 8816–20, Nov. 2011.

[25] S. Sugaya, M. Yamada, and M. Seki, “Manipulation of cells and cell spheroids using collagen hydrogel microbeads prepared by microfluidic devices,” *2012 Int. Symp. Micro-NanoMechatronics Hum. Sci.*, pp. 435–438, Apr. 2012.

[26] B. El, R. Utharala, I. V Balyasnikova, A. D. Griffiths, and C. A. Merten, “Functional single-cell hybridoma screening using droplet-based microfluidics,” pp. 1–6, 2012.

[27] K. M. Yamada and E. Cukierman, “Modeling tissue morphogenesis and cancer in 3D.,” *Cell*, vol. 130, no. 4, pp. 601–10, Aug. 2007.

[28] K. S. McMillan, A. G. McCluskey, A. Sorensen, M. Boyd, and M. Zagnoni, “Emulsion technologies for multicellular tumour spheroid radiation assays,” *Analyst*, vol. 141, no. 1, pp. 100–110, 2016.

[29] K. McMillan, M. Boyd, and M. Zagnoni, “Development of a Droplet Microfluidic Assay for Radiotherapy Treatment of Multicellular Spheroids,” in *MicroTAS 2014. San Diego, CA*, 2014, pp. 923–925.

[30] K. S. McMillan, M. Boyd, and M. Zagnoni, “Transitioning from multi-phase to single-phase microfluidics for long-term culture and treatment of multicellular spheroids,” *Lab Chip*, 2016.

[31] F. Bray, A. Jemal, N. Grey, J. Ferlay, and D. Forman, “Global cancer transitions according to the Human Development Index (2008-2030): a population-based study.,” *Lancet Oncol.*, vol. 13, no. 8, pp. 790–801, Aug. 2012.

[32] R. A. Weinberg, *The Biology of Cancer*. New York : Garland Science, 2007.

[33] K. Vermeulen, D. R. Van Bockstaele, and Z. N. Berneman, “The cell cycle: a review of regulation, deregulation and therapeutic targets in cancer.,” *Cell Prolif.*, vol. 36, no. 3, pp. 131–49, Jun. 2003.

[34] C. Frémin and S. Meloche, “From basic research to clinical development of MEK1/2 inhibitors for cancer therapy.,” *J. Hematol. Oncol.*, vol. 3, p. 8, Jan. 2010.

[35] D. Hanahan and R. A. Weinberg, “The hallmarks of cancer,” *Cell*, vol. 100, pp. 57–70, 2000.

[36] D. Hanahan and R. A. Weinberg, “Hallmarks of cancer: the next generation.,” *Cell*, vol. 144, no. 5, pp. 646–74, 2011.

[37] C. C. Harris, “p53 Tumor suppressor gene : from the basic research laboratory to the clinic — an abridged historical perspective,” *Carcinogenesis*, vol. 17, no. 6, pp. 1187–1198, 1996.

[38] P. Vaupel, F. Kallinowski, and P. Okunieff, “Blood flow, oxygen and nutrient supply, and metabolic microenvironment of human tumors: a review,” *Cancer Res.*, vol. 49, pp. 6449–6465, 1989.

[39] D. Fukumura and R. K. Jain, “Tumor microvasculature and microenvironment: Targets for anti- angiogenesis and normalization,” *Microvasc. Res.*, vol. 74, pp. 72 – 84, 2007.

[40] P. S. Steeg, “Tumor metastasis: mechanistic insights and clinical challenges.,” *Nat.*

Med., vol. 12, no. 8, pp. 895–904, Aug. 2006.

[41] C. L. Chaffer and R. a Weinberg, “A perspective on cancer cell metastasis.,” *Science*, vol. 331, no. March, pp. 1559–1564, 2011.

[42] F. R. Balkwill, M. Capasso, and T. Hagemann, “The tumor microenvironment at a glance,” *J. Cell Sci.*, vol. 125, no. 23, pp. 5591–5596, 2012.

[43] O. Trédan, C. M. Galmarini, K. Patel, and I. F. Tannock, “Drug resistance and the solid tumor microenvironment.,” *J. Natl. Cancer Inst.*, vol. 99, no. 19, pp. 1441–54, Oct. 2007.

[44] P. Vaupel and L. Harrison, “Tumor Hypoxia: Causative Factors, Compensatory Mechanisms, and Cellular Response,” *Oncologist*, vol. 9, no. suppl 5, pp. 4–9, 2004.

[45] A. L. Edinger and C. B. Thompson, “Death by design: Apoptosis, necrosis and autophagy,” *Curr. Opin. Cell Biol.*, vol. 16, no. 6, pp. 663–669, 2004.

[46] J. M. Brown and A. J. Giaccia, “The Unique Physiology of Solid Tumors : Opportunities (and Problems) for Cancer Therapy,” *Cancer Res.*, vol. 58, no. 9, pp. 1408–1416, 1998.

[47] H. Kobayashi, R. Watanabe, and P. L. Choyke, “Improving conventional enhanced permeability and retention (EPR) effects; what is the appropriate target?,” *Theranostics*, vol. 4, no. 1, pp. 81–9, Jan. 2013.

[48] G. Delaney, S. Jacob, C. Featherstone, and M. Barton, “The role of radiotherapy in cancer treatment: Estimating optimal utilization from a review of evidence-based clinical guidelines,” *Cancer*, vol. 104, no. August, pp. 1129–1137, 2005.

[49] R. Baskar, K. A. Lee, R. Yeo, and K.-W. Yeoh, “Cancer and radiation therapy: current advances and future directions.,” *Int. J. Med. Sci.*, vol. 9, no. 3, pp. 193–9, 2012.

[50] A. I. Kassis and S. J. Adelstein, “Radiobiologic principles in radionuclide therapy.,” *J. Nucl. Med.*, vol. 46 Suppl 1, no. 1, p. 4S–12S, 2005.

[51] C. N. Coleman and M. A. Stevenson, “Advances in Cellular and Molecular Radiation Oncology,” *Urol. Oncol. Semin. Orig. Investig.*, vol. 1439, no. 96, pp. 3–

13, 1996.

[52] O. Gallego, “Nonsurgical treatment of recurrent glioblastoma.,” *Curr. Oncol.*, vol. 22, no. 4, pp. e273–81, 2015.

[53] M. G. Castro, R. Cowen, I. K. Williamson, a David, M. J. Jimenez-Dalmaroni, X. Yuan, a Bigliari, J. C. Williams, J. Hu, and P. R. Lowenstein, “Current and future strategies for the treatment of malignant brain tumors.,” *Pharmacol. Ther.*, vol. 98, pp. 71–108, 2003.

[54] J. Kahn, P. J. Tofilon, and K. Camphausen, “Preclinical models in radiation oncology.,” *Radiat. Oncol.*, vol. 7, p. 223, 2012.

[55] J. Holtfreter, “A Study of the Mechanics of Gastrulation Part II,” *J. Exp. Zool.*, pp. 171–212, 1944.

[56] A. Moscano, “The Development in Vitro of Chimeric Aggregates of Dissociated Embryonic Chick and Mouse Cells,” *Proc. Natl. Acad. Sci. U. S. A.*, vol. 43, no. 1, pp. 184–194, 1956.

[57] R. M. Sutherland, W. R. Inch, J. A. McCredie, J. Kruuv, T. Ontario, C. Treatment, and L. Clinic, “A multi-component radiation survival curve using an in vitro tumour model.,” *Int. J. Radiat. Biol. Relat. Stud. Phys. Chem. Med.*, vol. 18, no. 5, pp. 491–495, 1970.

[58] L.-B. Weiswald, D. Bellet, and V. Dangles-Marie, “Spherical Cancer Models in Tumor Biology.,” *Neoplasia*, vol. 17, no. 1, pp. 1–15, Jan. 2015.

[59] F. Wang, V. M. Weaver, O. W. Petersen, C. a Larabell, S. Dedhar, P. Briand, R. Lupu, and M. J. Bissell, “Reciprocal interactions between beta1-integrin and epidermal growth factor receptor in three-dimensional basement membrane breast cultures: a different perspective in epithelial biology.,” *Proc. Natl. Acad. Sci. U. S. A.*, vol. 95, no. 25, pp. 14821–14826, 1998.

[60] N. S. Bryce, J. Z. Zhang, R. M. Whan, N. Yamamoto, and T. W. Hambley, “Accumulation of an anthraquinone and its platinum complexes in cancer cell spheroids: the effect of charge on drug distribution in solid tumour models.,” *Chem. Commun. (Camb).*, no. 19, pp. 2673–2675, 2009.

[61] A. J. Primeau, A. Rendon, D. Hedley, L. Lilge, and I. F. Tannock, “The distribution of the anticancer drug doxorubicin in relation to blood vessels in solid tumors,” *Clin. Cancer Res.*, vol. 11, no. 24, pp. 8782–8788, 2005.

[62] R.-Z. Lin and H.-Y. Chang, “Recent advances in three-dimensional multicellular spheroid culture for biomedical research,” *Biotechnol. J.*, vol. 3, no. 9–10, pp. 1172–1184, 2008.

[63] B. Desoize and J. Jardillier, “Multicellular resistance: a paradigm for clinical resistance?,” *Crit. Rev. Oncol. Hematol.*, vol. 36, no. 2–3, pp. 193–207, 2000.

[64] C. Dubessy, J. M. Merlin, C. Marchal, and F. Guillemin, “Spheroids in radiobiology and photodynamic therapy.,” *Crit. Rev. Oncol. Hematol.*, vol. 36, no. 2–3, pp. 179–92, 2000.

[65] A. Rodriguez, E. L. Alpen, M. Mendonca, and R. J. DeGuzman, “Recovery from potentially lethal damage and recruitment time of noncycling clonogenic cells in 9L confluent monolayers and spheroids.,” *Radiat Res*, vol. 114, no. 3, pp. 515–527, 1988.

[66] J. J. Kim and I. F. Tannock, “Repopulation of cancer cells during therapy: an important cause of treatment failure.,” *Nat. Rev. Cancer*, vol. 5, no. 7, pp. 516–25, Jul. 2005.

[67] T. J. Goodwin, J. M. Jessup, and D. A. Wolf, “Morphologic Differentiation of Colon Carcinoma Cell Lines HT-29 and HT-29KM in Rotating-Wall Vessels,” *Vitr. Cell. Dev. Biol.*, no. January, pp. 47–60, 1992.

[68] H. Song, P. D, O. David, S. Clejan, C. L. Giordano, H. Pappas-lebeau, L. I. Xu, and K. I. M. C. O. Connor, “Spatial Composition of Prostate Cancer Spheroids in Mixed and Static Cultures,” *Tissue Eng.*, vol. 10, no. 7, pp. 1266–1276, 2004.

[69] J. M. Kelm, N. E. Timmins, C. J. Brown, M. Fussenegger, and L. K. Nielsen, “Method for generation of homogeneous multicellular tumor spheroids applicable to a wide variety of cell types,” *Biotechnol. Bioeng.*, vol. 83, no. 2, pp. 173–180, 2003.

[70] Y.-C. Tung, A. Y. Hsiao, S. G. Allen, Y. Torisawa, M. Ho, and S. Takayama, “High-throughput 3D spheroid culture and drug testing using a 384 hanging drop array.,” *Analyst*, vol. 136, no. 3, pp. 473–8, Feb. 2011.

[71] S. T. A.Y. Hsiao, Y.C. Tung, C.H. Kuo, B. Mosadegh, R. Bedenis, K.J. Pienta, "Micro-Ring Structures Stabilize Microdroplets to Enable Long Term Spheroid Culture in 384 Hanging Drop Array Plates," *Biomed. Microdevices*, vol. 14, no. 2, pp. 313–323, 2012.

[72] A. Ivascu and M. Kubbies, "Rapid Generation of Single-Tumor Spheroids for High-Throughput Cell Function and Toxicity Analysis," *J. Biomol. Screen.*, vol. 11, no. 8, pp. 922–932, 2006.

[73] H. K. Kleinman and G. R. Martin, "Matrigel: Basement membrane matrix with biological activity," *Semin. Cancer Biol.*, vol. 15, no. 5 SPEC. ISS., pp. 378–386, 2005.

[74] A. M. Montgomery, R. A. Reisfeld, and D. A. Cheresh, "Integrin alpha v beta 3 rescues melanoma cells from apoptosis in three-dimensional dermal collagen.," *Proc. Natl. Acad. Sci. U. S. A.*, vol. 91, no. 19, pp. 8856–60, 1994.

[75] V. van Duinen, S. J. Trietsch, J. Joore, P. Vulto, and T. Hankemeier, "Microfluidic 3D cell culture: from tools to tissue models," *Curr. Opin. Biotechnol.*, vol. 35, pp. 118–126, 2015.

[76] D. Pappas, "Microfluidics and cancer analysis: cell separation, cell/tissue culture, cell mechanics, and integrated analysis systems," *Analyst*, pp. 525–535, 2016.

[77] T. M. Squires and S. R. Quake, "Microfluidics : Fluid physics at the nanoliter scale," *Rev. Mod. Phys.*, vol. 77, no. July, pp. 978 – 1025, 2005.

[78] E. Purcell, "Life at Low Reynolds Number," *Am. J. Phys.*, vol. 45, pp. 3–11, 1977.

[79] J. C. Mcdonald, D. C. Duffy, J. R. Anderson, and D. T. Chiu, "General Fabrication of microfluidic systems in poly (dimethylsiloxane)," *Electrophoresis*, vol. 21, pp. 27–40, 2000.

[80] S.-Y. Teh, R. Lin, L.-H. Hung, and A. P. Lee, "Droplet microfluidics.," *Lab Chip*, vol. 8, no. 2, pp. 198–220, 2008.

[81] T. Thorsen, R. W. Roberts, F. H. Arnold, and S. R. Quake, "Dynamic Pattern Formation in a Vesicle-Generating Microfluidic Device," *Phys. Rev. Lett.*, vol. 86, no. 18, pp. 4163–4166, Apr. 2001.

[82] T. P. Lagus and J. F. Edd, “A review of the theory, methods and recent applications of high-throughput single-cell droplet microfluidics,” *J. Phys. D. Appl. Phys.*, vol. 46, no. 11, p. 114005, Mar. 2013.

[83] S. L. Anna, N. Bontoux, and H. a. Stone, “Formation of dispersions using ‘flow focusing’ in microchannels,” *Appl. Phys. Lett.*, vol. 82, no. 3, p. 364, 2003.

[84] W. Shi, J. Qin, N. Ye, and B. Lin, “Droplet-based microfluidic system for individual Caenorhabditis elegans assay.,” *Lab Chip*, vol. 8, no. 9, pp. 1432–1435, 2008.

[85] H. Wen, Y. Yu, G. Zhu, L. Jiang, and J. Qin, “A droplet microchip with substance exchange capability for the developmental study of C. elegans.,” *Lab Chip*, vol. 15, no. 8, pp. 1905–11, 2015.

[86] L. Frenz, K. Blank, E. Brouzes, and A. D. Griffiths, “Reliable microfluidic on-chip incubation of droplets in delay-lines.,” *Lab Chip*, vol. 9, no. 10, pp. 1344–8, 2009.

[87] S. S. Bithi and S. a Vanapalli, “Behavior of a train of droplets in a fluidic network with hydrodynamic traps.,” *Biomicrofluidics*, vol. 4, no. 4, p. 44110, Jan. 2010.

[88] C. H. J. Schmitz, A. C. Rowat, S. Köster, and D. a Weitz, “Dropspots: a picoliter array in a microfluidic device.,” *Lab Chip*, vol. 9, no. 1, pp. 44–9, Jan. 2009.

[89] A. Huebner, D. Bratton, G. Whyte, M. Yang, A. J. DeMello, C. Abell, and F. Hollfelder, “Static microdroplet arrays: a microfluidic device for droplet trapping, incubation and release for enzymatic and cell-based assays,” *Lab Chip*, vol. 9, no. 5, pp. 692–698, 2009.

[90] J.-C. Baret, “Surfactants in droplet-based microfluidics.,” *Lab Chip*, vol. 12, no. 3, pp. 422–33, Feb. 2012.

[91] C. Holtze, a C. Rowat, J. J. Agresti, J. B. Hutchison, F. E. Angilè, C. H. J. Schmitz, S. Köster, H. Duan, K. J. Humphry, R. a Scanga, J. S. Johnson, D. Pisignano, and D. a Weitz, “Biocompatible surfactants for water-in-fluorocarbon emulsions.,” *Lab Chip*, vol. 8, no. 10, pp. 1632–9, Oct. 2008.

[92] N. Bremond, A. R. Thiam, and J. Bibette, “Decompressing emulsion droplets favors coalescence,” *Phys. Rev. Lett.*, vol. 100, no. 2, pp. 1–4, 2008.

[93] C. N. Baroud, M. R. de Saint Vincent, and J.-P. Delville, “An optical toolbox for total

control of droplet microfluidics.," *Lab Chip*, vol. 7, no. 8, pp. 1029–1033, 2007.

[94] M. Zagnoni and J. M. Cooper, "On-chip electrocoalescence of microdroplets as a function of voltage, frequency and droplet size.," *Lab Chip*, vol. 9, no. 18, pp. 2652–8, Sep. 2009.

[95] M. Zagnoni, G. Le Lain, and J. M. Cooper, "Electrocoalescence mechanisms of microdroplets using localized electric fields in microfluidic channels.," *Langmuir*, vol. 26, no. 18, pp. 14443–9, Sep. 2010.

[96] M. Chabert, K. D. Dorfman, and J. L. Viovy, "Droplet fusion by alternating current (AC) field electrocoalescence in microchannels," *Electrophoresis*, vol. 26, no. 19, pp. 3706–3715, 2005.

[97] K. Y. Lee and D. J. Mooney, "Alginate : properties and biomedical applications," *Prog. Polym. Sci.*, vol. 37, no. 1, pp. 106–126, 2012.

[98] K.-S. Huang, T.-H. Lai, and Y.-C. Lin, "Manipulating the generation of Ca-alginate microspheres using microfluidic channels as a carrier of gold nanoparticles.," *Lab Chip*, vol. 6, no. 7, pp. 954–957, 2006.

[99] L. Yu, S. M. Grist, S. S. Nasseri, E. Cheng, Y.-C. E. Hwang, C. Ni, and K. C. Cheung, "Core-shell hydrogel beads with extracellular matrix for tumor spheroid formation," *Biomicrofluidics*, vol. 9, no. 2, p. 024118, 2015.

[100] D. J. Holt, R. J. Payne, and C. Abell, "Synthesis of novel fluorous surfactants for microdroplet stabilisation in fluorous oil streams," *J. Fluor. Chem.*, vol. 131, no. 3, pp. 398–407, Mar. 2010.

[101] S. Sakai, S. Ito, H. Inagaki, K. Hirose, T. Matsuyama, M. Taya, and K. Kawakami, "Cell-enclosing gelatin-based microcapsule production for tissue engineering using a microfluidic flow-focusing system.," *Biomicrofluidics*, vol. 5, no. 1, p. 13402, Jan. 2011.

[102] Y. Zhang, Y.-P. Ho, Y.-L. Chiu, H. F. Chan, B. Chlebina, T. Schuhmann, L. You, and K. Leong, "A programmable microenvironment for cellular studies via microfluidics-generated double emulsions," *Biomaterials*, vol. 34, no. 19, pp. 4564–4572, 2013.

[103] E. Brouzes, M. Medkova, N. Savenelli, D. Marran, M. Twardowski, J. B. Hutchison, J. M. Rothberg, D. R. Link, N. Perrimon, and M. L. Samuels, "Droplet microfluidic technology for single-cell high-throughput screening.," *Proc. Natl. Acad. Sci. U. S. A.*, vol. 106, no. 34, pp. 14195–200, Aug. 2009.

[104] C. Wang, X. Tong, and F. Yang, "Bioengineered 3D Brain Tumor Model To Elucidate the Effects of Matrix Stiffness on Glioblastoma Cell Behavior Using PEG-Based Hydrogels," *Mol. Pharm.*, vol. 11, pp. 2115–2125, 2014.

[105] O. Rixe and T. Fojo, "Is cell death a critical end point for anticancer therapies or is cytostasis sufficient?," *Clin. Cancer Res.*, vol. 13, no. 24, pp. 7280–7, Dec. 2007.

[106] D. C. Duffy, J. C. McDonald, O. J. A. Schueller, and G. M. Whitesides, "Rapid prototyping of microfluidic systems in poly(dimethylsiloxane)," *Anal. Chem.*, vol. 70, no. 23, pp. 4974–4984, 1998.

[107] J. C. McDonald and G. M. Whitesides, "Poly(dimethylsiloxane) as a material for fabricating microfluidic devices," *Acc. Chem. Res.*, vol. 35, no. 7, pp. 491–499, 2002.

[108] J. Harris, H. Lee, B. Vahidi, C. Tu, D. Cribbs, C. Cotman, and N. L. Jeon, "Non-plasma bonding of PDMS for inexpensive fabrication of microfluidic devices.," *J. Vis. Exp.*, no. 9, p. 410, 2007.

[109] R. J. M. and T. E. W. M. Boyd, A. Livingstone, L. E. Wilson, E. M. Marshall, A. G. McCluskey, "Dose-response relationship for radiation-induced mutations at micro- and minisatellite loci in human somatic cells in culture.," *Int. J. Radiat. Biol.*, vol. 76, pp. 169 – 176, 2000.

[110] K. H. Jones and J. A. Senft, "An Improved Method to Determine Cell Viability by Simultaneous Staining with Fluorescein Diacetate Propidium Iodide," *J. Histochem. Cytochem.*, vol. 33, no. 1, pp. 77–79, 1985.

[111] V. T. Hamilton, M. C. Habbersett, and C. J. Herman, "Flow Microfluorometric Analysis of Cellular DNA: Critical Comparison of Mithramycin and Propidium Iodide," *J. Histochem. Cytochem.*, vol. 28, pp. 1125–1128, 1980.

[112] K. Bloch, H. Smith, V. van Hamel Parsons, D. Gavaghan, C. Kelly, A. Fletcher, P. Maini, and R. Callaghan, "Metabolic Alterations During the Growth of Tumour

Spheroids.," *Cell Biochem. Biophys.*, Sep. 2013.

[113] W. Senkowski, X. Zhang, M. H. Olofsson, R. Isacson, U. Höglund, M. Gustafsson, P. Nygren, S. Linder, R. Larsson, and M. Fryknäs, "Three-Dimensional Cell Culture-Based Screening Identifies the Anthelmintic Drug Nitazoxanide as a Candidate for Treatment of Colorectal Cancer.," *Mol. Cancer Ther.*, vol. 14, no. 6, pp. 1504–16, Jun. 2015.

[114] H. R. Mellor, D. J. P. Ferguson, and R. Callaghan, "A model of quiescent tumour microregions for evaluating multicellular resistance to chemotherapeutic drugs.," *Br. J. Cancer*, vol. 93, pp. 302–309, 2005.

[115] R. G. Jones and C. B. Thompson, "Tumor suppressors and cell metabolism : a recipe for cancer growth," *Genes Dev.*, no. 514, pp. 537–548, 2009.

[116] M. Guppy, E. Greiner, and K. Brand, "The role of the Crabtree effect and an endogenous fuel in the energy metabolism of resting and proliferating thymocytes," *Eur. J. Biochem.*, vol. 99, pp. 95–99, 1993.

[117] R. J. DeBerardinis, J. J. Lum, G. Hatzivassiliou, and C. B. Thompson, "The biology of cancer: metabolic reprogramming fuels cell growth and proliferation.," *Cell Metab.*, vol. 7, no. 1, pp. 11–20, Jan. 2008.

[118] Y. S. Heo, L. M. Cabrera, J. W. Song, N. Futai, Y.-C. Tung, G. Smith, and S. Takayama, "Characterization and Resolution of Evaporation-Mediated Osmolality Shifts that Constrain Microfluidic Cell Culture in Poly (dimethylsiloxane) Devices," *Anal. Chem.*, vol. 79, no. 3, pp. 1126–1134, 2007.

[119] a Neshasteh-Riz, W. J. Angerson, J. R. Reeves, G. Smith, R. Rampling, and R. J. Mairs, "Incorporation of iododeoxyuridine in multicellular glioma spheroids: implications for DNA-targeted radiotherapy using Auger electron emitters.," *Br. J. Cancer*, vol. 75, no. 4, pp. 493–9, Jan. 1997.

[120] U. Rajcevic, J. C. Knol, S. Piersma, S. Bougnaud, F. Fack, E. Sundlisaeter, K. Søndenaa, R. Myklebust, T. V Pham, S. P. Niclou, and C. R. Jiménez, "Colorectal cancer derived organotypic spheroids maintain essential tissue characteristics but adapt their metabolism in culture.," *Proteome Sci.*, vol. 12, p. 39, 2014.

[121] R. Sutherland, J. Carlsson, and R. Durand, "Spheroids in Cancer Research," *Cancer*

Res., vol. 41, pp. 2980–2984, 1981.

[122] P. L. Olive and R. E. Durand, "Drug and radiation resistance in spheroids: Cell contact and kinetics," *Cancer Metastasis Rev.*, vol. 13, no. 2, pp. 121–138, 1994.

[123] D. Khaitan, S. Chandna, M. B. Arya, and B. S. Dwarakanath, "Establishment and characterization of multicellular spheroids from a human glioma cell line; Implications for tumor therapy.," *J. Transl. Med.*, vol. 4, p. 12, Jan. 2006.

[124] Y. Chen, A. Wijaya Gani, and S. K. Y. Tang, "Characterization of sensitivity and specificity in leaky droplet-based assays.," *Lab Chip*, vol. 12, no. 23, pp. 5093–103, Dec. 2012.

[125] C. Martino, M. Zagnoni, M. Sandison, M. Chanasakulniyom, A. R. Pitt, and J. M. Cooper, "Intracellular protein determination using droplet-based immunoassays," *Anal. Chem.*, vol. 83, pp. 5361–5368, 2011.

[126] C. N. Baroud, F. Gallaire, and R. Dangla, "Dynamics of microfluidic droplets.," *Lab Chip*, vol. 10, no. 16, pp. 2032–45, Aug. 2010.

[127] A. R. Abate, C.-H. Chen, J. J. Agresti, and D. A. Weitz, "Beating Poisson encapsulation statistics using close-packed ordering.," *Lab Chip*, vol. 9, no. 18, pp. 2628–2631, 2009.

[128] H. Boukellal, S. Selimović, Y. Jia, G. Cristobal, and S. Fraden, "Simple, robust storage of drops and fluids in a microfluidic device.," *Lab Chip*, vol. 9, no. 2, pp. 331–8, Jan. 2009.

[129] M. Sun, S. S. Bithi, and S. a Vanapalli, "Microfluidic static droplet arrays with tuneable gradients in material composition.," *Lab Chip*, vol. 11, no. 23, pp. 3949–52, Dec. 2011.

[130] S. S. Bithi, W. S. Wang, M. Sun, J. Blawzdziewicz, and S. a Vanapalli, "Coalescing drops in microfluidic parking networks: A multifunctional platform for drop-based microfluidics.," *Biomicrofluidics*, vol. 8, no. 3, p. 034118, May 2014.

[131] W. Choi, M. Hashimoto, A. K. Ellerbee, X. Chen, K. J. M. Bishop, P. Garstecki, H. a. Stone, and G. M. Whitesides, "Bubbles navigating through networks of microchannels," *Lab Chip*, vol. 11, p. 3970, 2011.

[132] J. C. T. Eijkel and A. van den Berg, “Young 4ever--the use of capillarity for passive flow handling in lab on a chip devices.,” *Lab Chip*, vol. 6, no. 11, pp. 1405–1408, 2006.

[133] T. F. Tadros, “Emulsion Formation,Stability, and Rheology,” *Emuls. Form. Stab.*, pp. 1–76, 2013.

[134] N. Yi, B. Huang, L. Dong, X. Quan, F. Hong, P. Tao, C. Song, W. Shang, and T. Deng, “Temperature-induced coalescence of colliding binary droplets on superhydrophobic surface.,” *Sci. Rep.*, vol. 4, p. 4303, 2014.

[135] M. De Menech, P. Garstecki, F. Jousse, and H. a. Stone, “Transition from squeezing to dripping in a microfluidic T-shaped junction,” *J. Fluid Mech.*, vol. 595, pp. 141–161, 2008.

[136] P. Garstecki, M. J. Fuerstman, H. a Stone, and G. M. Whitesides, “Formation of droplets and bubbles in a microfluidic T-junction-scaling and mechanism of break-up.,” *Lab Chip*, vol. 6, no. 3, pp. 437–446, 2006.

[137] J. Zhou, K. Ren, W. Dai, Y. Zhao, D. Ryan, and H. Wu, “Pumping-induced perturbation of flow in microfluidic channels and its implications for on-chip cell culture.,” *Lab Chip*, vol. 11, no. 13, pp. 2288–2294, 2011.

[138] S. Halldórsson, E. Lucumi, R. Gómez-Sjöberg, and R. M. T. Fleming, “Advantages and challenges of microfluidic cell culture in polydimethylsiloxane devices,” *Biosens. Bioelectron.*, vol. 63, pp. 218–231, Jul. 2014.

[139] K. J. Regehr, M. Domenech, J. T. Koepsel, K. C. Carver, S. J. Ellison-Zelski, W. L. Murphy, L. A. Schuler, E. T. Alarid, and D. J. Beebe, “Biological implications of polydimethylsiloxane-based microfluidic cell culture.,” *Lab Chip*, vol. 9, no. 15, pp. 2132–9, 2009.

[140] J. D. Wang, N. J. Douville, S. Takayama, and M. Elsayed, “Quantitative analysis of molecular absorption into PDMS microfluidic channels,” *Ann. Biomed. Eng.*, vol. 40, no. 9, pp. 1862–1873, 2012.

[141] K. B. Anderson, S. T. Halpin, A. S. Johnson, R. S. Martin, and D. M. Spence, “Integration of multiple components in polystyrene-based microfluidic devices part II: cellular analysis.,” *Analyst*, vol. 138, no. 1, pp. 137–43, 2013.

[142] K. H. Lee, D. Y. No, S.-H. Kim, J. H. Ryoo, S. F. Wong, and S.-H. Lee, “Diffusion-mediated in situ alginate encapsulation of cell spheroids using microscale concave well and nanoporous membrane.,” *Lab Chip*, vol. 11, no. 6, pp. 1168–73, 2011.

[143] C. Kim, “Droplet-based microfluidics for making uniform-sized cellular spheroids in alginate beads with the regulation of encapsulated cell number,” *BioChip J.*, vol. 9, no. 2, pp. 105–113, 2015.

[144] T. Andersen, P. Auk-Emblem, and M. Dornish, “3D Cell Culture in Alginate Hydrogels,” *Microarrays*, vol. 4, no. 2, pp. 133–161, 2015.

[145] P. Vaupel, “Tumor microenvironmental physiology and its implications for radiation oncology,” *Semin. Radiat. Oncol.*, vol. 14, no. 3, pp. 198–206, 2004.

[146] L. H. GRAY, A. D. CONGER, M. EBERT, S. HORNSEY, and O. C. SCOTT, “The concentration of oxygen dissolved in tissues at the time of irradiation as a factor in radiotherapy,” *Br. J. Radiol.*, vol. 26, no. 312, pp. 638–648, 1953.

[147] J. Pan, A. L. Stephenson, E. Kazamia, W. T. S. Huck, J. S. Dennis, A. G. Smith, and C. Abell, “Quantitative tracking of the growth of individual algal cells in microdroplet compartments.,” *Integr. Biol. (Camb).*, vol. 3, no. 10, pp. 1043–51, Oct. 2011.

[148] A. Rakszewska, J. Tel, V. Chokkalingam, and W. T. Huck, “One drop at a time: toward droplet microfluidics as a versatile tool for single-cell analysis,” *NPG Asia Mater.*, vol. 6, no. 10, p. e133, Oct. 2014.

[149] J.-C. Baret, O. J. Miller, V. Taly, M. Ryckelynck, A. El-Harrak, L. Frenz, C. Rick, M. L. Samuels, J. B. Hutchison, J. J. Agresti, D. R. Link, D. A. Weitz, and A. D. Griffiths, “Fluorescence-activated droplet sorting (FADS): efficient microfluidic cell sorting based on enzymatic activity.,” *Lab Chip*, vol. 9, no. 13, pp. 1850–8, 2009.

[150] W. Shi, H. Wen, Y. Lu, Y. Shi, B. Lin, and J. Qin, “Droplet microfluidics for characterizing the neurotoxin-induced responses in individual Caenorhabditis elegans.,” *Lab Chip*, vol. 10, no. 21, pp. 2855–63, Nov. 2010.

[151] D. B. Weibel and G. M. Whitesides, “Applications of microfluidics in chemical biology.,” *Curr. Opin. Chem. Biol.*, vol. 10, no. 6, pp. 584–91, Dec. 2006.

[152] S. K. W. Dertinger, D. T. Chiu, Noo Li Jeon, and G. M. Whitesides, “Generation of gradients having complex shapes using microfluidic networks,” *Anal. Chem.*, vol. 73, no. 6, pp. 1240–1246, 2001.

[153] X. Jiang, Q. Xu, S. K. W. Dertinger, D. Stroock, T. Fu, G. M. Whitesides, and A. D. Stroock, “Article A General Method for Patterning Gradients of Biomolecules on Surfaces Using Microfluidic Networks A General Method for Patterning Gradients of Biomolecules on Surfaces Using Microfluidic Networks,” *Anal. Chem.*, vol. 77, no. 8, pp. 2338–2347, 2005.

[154] D. Irimia, D. A. Geba, and M. Toner, “Universal microfluidic gradient generator,” *Anal. Chem.*, vol. 78, no. 10, pp. 3472–3477, 2006.

[155] J. Yu, K. T. Du, Q. Fang, Y. Gu, S. S. Mihardja, R. E. Sievers, J. C. Wu, and R. J. Lee, “The use of human mesenchymal stem cells encapsulated in RGD modified alginate microspheres in the repair of myocardial infarction in the rat,” *Biomaterials*, vol. 31, no. 27, pp. 7012–7020, 2010.

[156] E. Shamir and A. Ewald, “Three-dimensional organotypic culture: experimental models of mammalian biology and disease,” *Nat. Rev. Mol. Cell Biol.*, vol. 15, no. 10, pp. 647–664, 2014.

[157] A. Fatehullah, S. H. Tan, and N. Barker, “Organoids as an in vitro model of human development and disease,” *Nat. Cell Biol.*, vol. 18, no. 3, pp. 246–254, 2016.

[158] C. Dilworth, G. A. Hamilton, E. George, and J. A. Timbrell, “The use of liver spheroids as an in vitro model for studying induction of the stress response as a marker of chemical toxicity,” *Toxicol. Vitr.*, vol. 14, no. 2, pp. 169–176, 2000.

[159] V. Rogiers, B. Blaauboer, P. Maurel, I. Phillips, and E. Shephard, “Hepatocyte-based in vitro models and their application in pharmacotoxicology. Report of an EC DGXII meeting with representatives of the European pharmaceutical industry,” *Toxicol. Vitr.*, vol. 9, no. 5, pp. 685–694, 1995.

[160] M. Juillerat, N. Marceau, S. Coeytaux, F. Sierra, E. Kolodziejczyk, and Y. Guigoz, “Expression of Organ-specific Structures and Functions in Long-term Cultures of Aggregates from Adult Rat Liver Cells,” *Toxicol. Vitr.*, vol. 11, pp. 57–69, 1997.

[161] P. Ammann and P. Maier, “Preservation and inducibility of xenobiotic

metabolism in long-term cultures of adult rat liver cell aggregates," *Toxicol. Vitr.*, vol. 11, no. 1–2, pp. 43–56, 1997.

[162] G. N. Raval, L. J. Parekh, D. D. Patel, F. P. Jha, R. N. Sainger, and P. S. Patel, "Clinical usefulness of alterations in sialic acid, sialyl transferase and sialoproteins in breast cancer.," *Indian J. Clin. Biochem.*, vol. 19, no. 2, pp. 60–71, 2004.

[163] D. Craig, S. McAughtrie, J. Simpson, C. McCraw, K. Faulds, and D. Graham, "Confocal SERS mapping of glycan expression for the identification of cancerous cells," *Anal. Chem.*, vol. 86, no. 10, pp. 4775–4782, 2014.

[164] X. Zhang, Y. Teng, Y. Fu, L. Xu, S. Zhang, B. He, C. Wang, and W. Zhang, "Lectin-based biosensor strategy for electrochemical assay of glycan expression on living cancer cells," *Anal. Chem.*, vol. 82, no. 22, pp. 9455–9460, 2010.

Appendix

Parameters of Microfluidic Devices shown in Chapter 5 and 6

Device Design 1 – Single Chamber Device (Section 5.2)

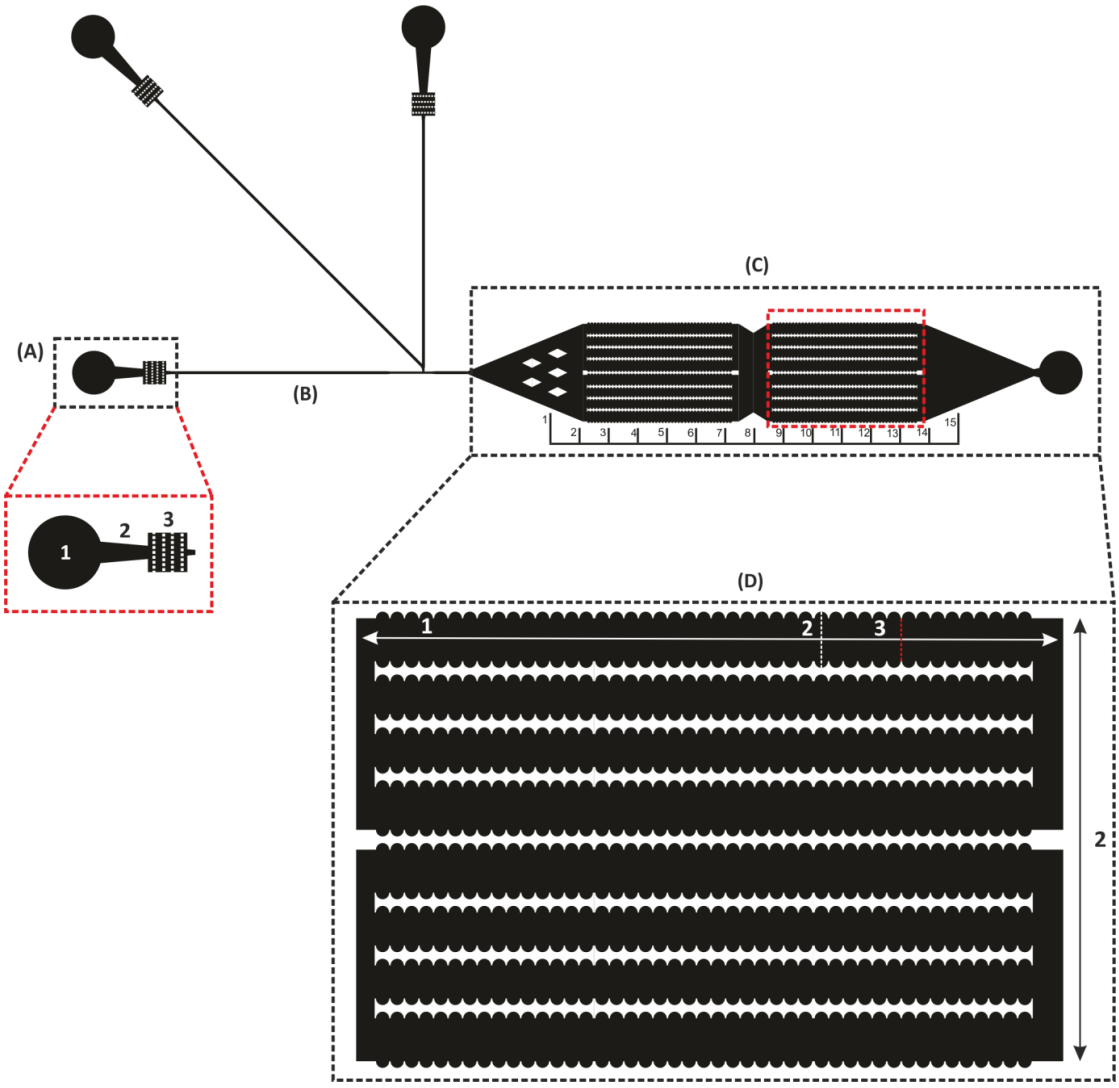

Diagram of single chamber storage device. Sections of the microfluidic design have been highlighted (A) an inlet with (1) Start of inlet (same as outlet), (2) channel connecting to filter section and (3) filter section; (B) shows a channel which makes up the T-junction; (C) storage chamber and (D) a storage chamber section with (1) Length of channel, (2) largest width of channel, (3) smallest width of channel and (4) width of chamber section.

Dimensions of the Single Chamber Device.

Device Feature	**Dimensions**
Height of Features	50 µm
(A) Inlets (1 – Start of inlet (same as outlet), 2 – channel connecting to filter section and 3 – filter section)	1 – 1.5 mm 2 – Length – 1 mm - Longest width – 400 µm - Shortest width – 200 µm 3 – Large square – 800 µm - Small squares – 60 µm
(B) T-junction Channels	Horizontal channel length – 11.07 mm Diagonal channel length – 11.07 mm Vertical channel length – 8.9 mm Width – 100 µm
(C) Storage Chamber	Length – 19.3 mm Width – 3.35 mm
(D) Storage Chamber Section (1 – Length of channel, 2 – largest width of channel, 3 – smallest width of channel and 4 – width of chamber section)	1 – 5 mm 2 – 420 µm 3 – 325 µm 4 – 3.35 mm

Device Design 2 – Chamber Device with 2 Storage Chambers (Section 5.2)

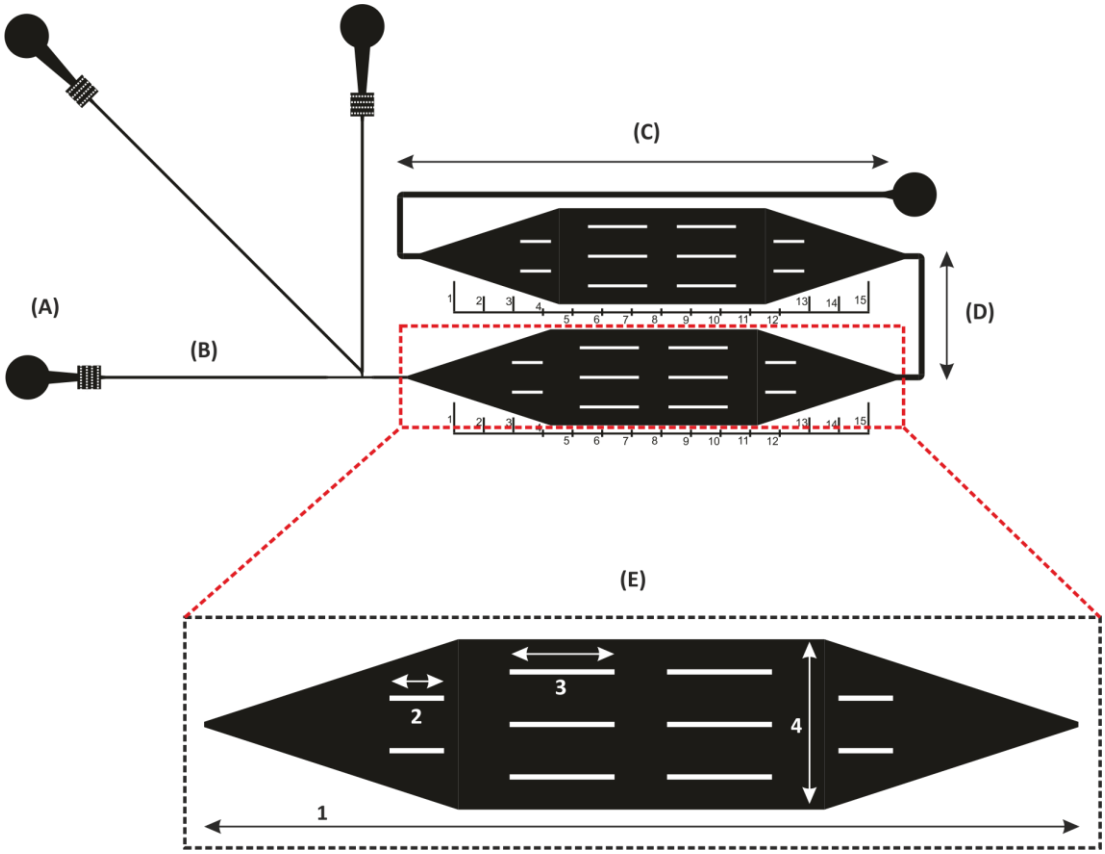

Diagram of storage device with two storage chambers. Sections of the microfluidic design have been highlighted (A) shows an inlet; (B) shows a channel which makes up the T-junction; (C) channel connecting to the outlet (D) channel connecting the two storage chambers and (E) a storage chamber with (1) Length of storage chamber, (2) short rectangular pillar, (3) long rectangular pillar and (4) width of storage chamber.

Dimensions of Storage Device with Two Chambers

Device Feature	**Dimensions**
Height of Features	50 µm
(A) Inlets	Same as device 1
(B) T-junction channels	Same as device 1
(C) Channel to outlet	Length – 18.8 mm Width – 200 µm
(D) Channel connecting storage chambers	Length – 5.5 mm Width – 200 µm
(E) Storage chamber with rectangular pillars (1 – Length of storage chamber, 2 – short rectangular pillar, 3 – long rectangular pillar and 4 – width of storage chamber)	1 – 16.4 mm 2 – Length – 1 mm - Width – 100 µm 3 – Length – 2 mm - Width – same as 2 4 – 3.2 mm

Device Design 3 – "Dropspots" Device (Section 5.3)

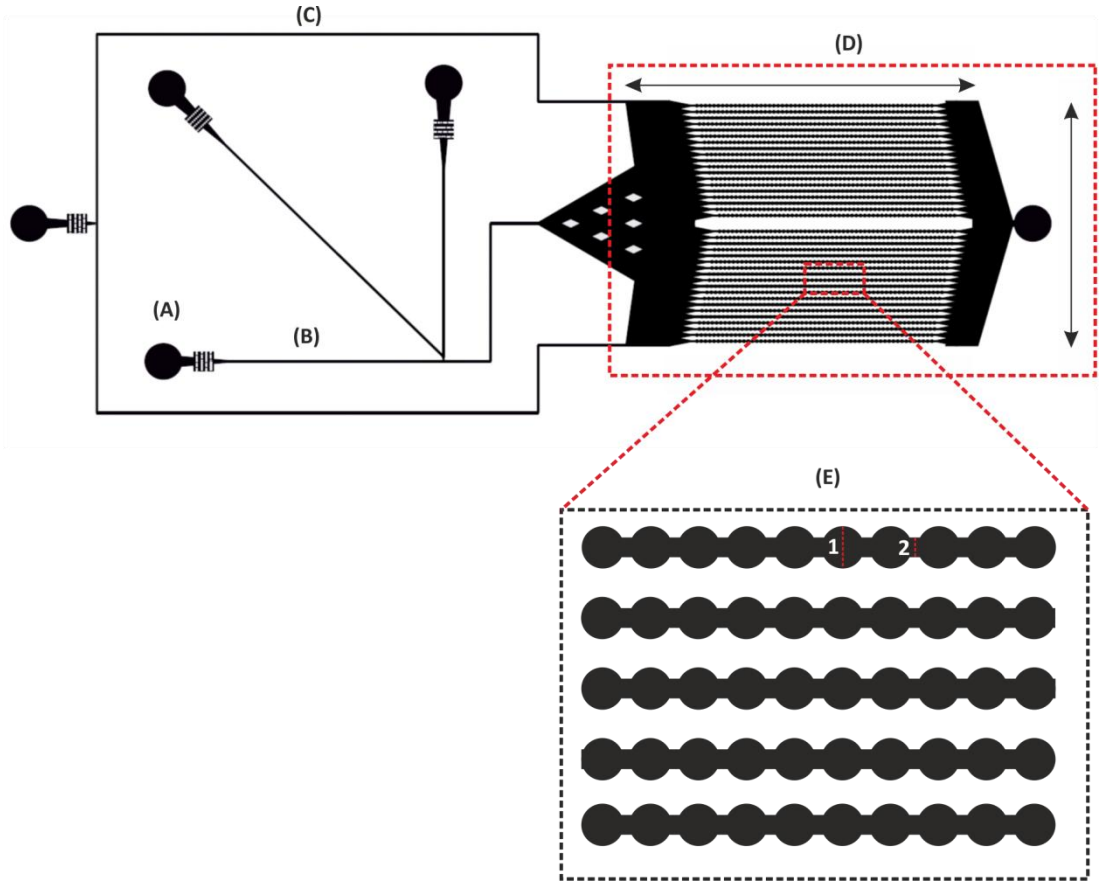

Diagram of a "Dropspots" Device. Sections of the microfluidic design have been highlighted which are as follows (A) an inlet; (B) a channel which makes up the T-junction; (C) bypass channel (D) storage chamber array and (E) a section of the storage chamber with (1) chamber and (2) a constriction between chambers.

Dimensions of a "Dropspot" Device with 150 µm Diameter Chambers

Device Feature	**Dimensions**
Height of Features	50 µm
(A) Inlets	Same as device 1
(B) T-junction channels	Same as device 1
(C) Bypass channel	Length- 50.12 mm Width – 100 µm
(C)Storage chamber array	Length – 14 mm Width – 10 mm
(D) Section of storage array (1 – chamber and 2 – constriction between chambers)	1 – 150 µm 2 – 70 µm

Dimensions of a "Dropspot" Device with 230 µm Diameter Chambers

Device Feature	**Dimensions**
Height of Features	100 µm
(A) Inlets	Same as device 1
(B) T-junction channels	Horizontal channel length – 15.6 mm Diagonal channel length – 15.6 mm Vertical channel length – 13.6 mm Width – 150 µm
(C) Bypass channel	Length – 88.49 mm Width – 150 µm
(D)Storage chamber array	Length – 21 mm Width – 15 mm
(E) Section of storage array (1 – chamber and 2 – constriction between chambers	1 – 230 µm 2 – 100 µm

Device Design 4 – A Microfluidic Device for Perfusion (Section 5.4 and Chapter 6)

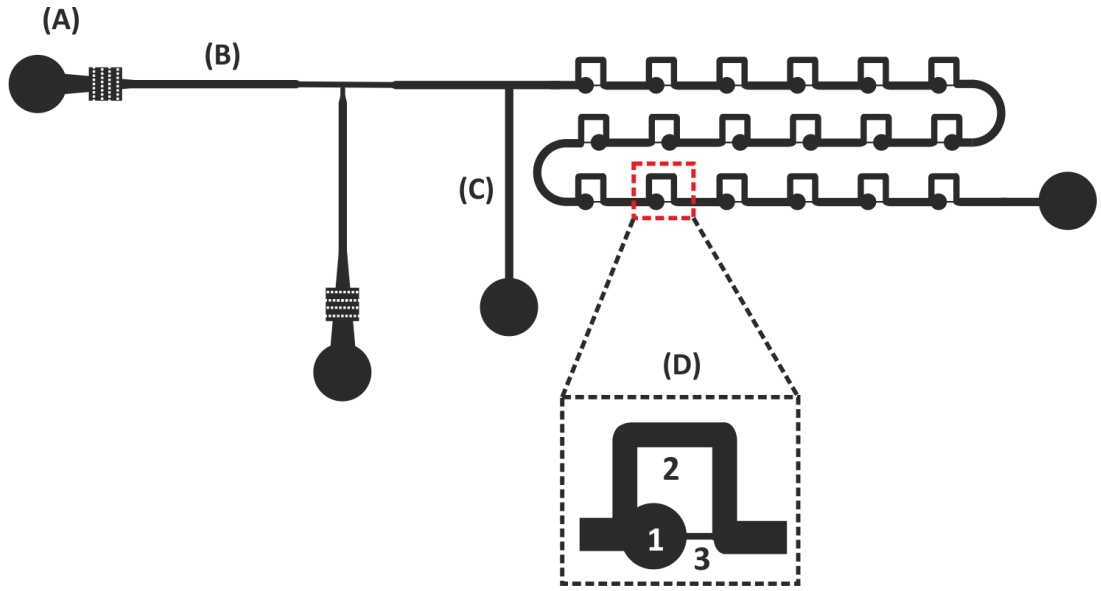

Diagram of a Microfluidic Device for Perfusion. Sections of the microfluidic design have been highlighted which are as follows (A) an inlet; (B) a channel which makes up the T-junction; (C) bypass channel (D) storage chamber array with (1) a chamber, (2) a bypass channel and (3) a restriction channel. The dimensions of the device are provided in table A.5.

Dimensions of a Microfluidic Device for Perfusion.

Device Feature	**Dimensions**
Height of Features	180 µm
(A) Inlets	Same as device 1
(B) T-junction channels	Horizontal channel – 10.6 mm Vertical channel – 4.3 mm Width – 150 µm
(C) Bypass channel	Length – 4.5 mm Width – 150 µm
(D) Storage chamber (1 – chamber, 2 – bypass channel and 3 – restriction channel)	1- 300 µm 2- Length – 1.5 mm - Width – 100 µm 3- Length – 180 µm - Width – 30 µm
	1 – 400 µm 2 – Length – 1.8 mm - Width – 150 µm 3 – Length – 154 µm - Width – 40 µm
	1 – 500 µm 2 – Length – 2.65 mm - Width – 150 µm 3 – Length – 435 µm - Width – 55 µm